

WET SPUN PCL SCAFFOLDS FOR TISSUE ENGINEERING

A THESIS SUBMITTED TO
THE GRADUATE SCHOOL OF NATURAL AND APPLIED SCIENCES
OF
MIDDLE EAST TECHNICAL UNIVERSITY

BY

ELBAY MALIKMAMMADOV

IN PARTIAL FULFILLMENT OF THE REQUIREMENTS
FOR
THE DEGREE OF MASTER OF SCIENCE
IN
MICRO AND NANOTECHNOLOGY

SEPTEMBER 2017

Approval of the thesis:

WET SPUN PCL SCAFFOLDS FOR TISSUE ENGINEERING

Submitted by **ELBAY MALIKMAMMADOV** in partial fulfilment of the requirements for the degree of **Master of Science in Micro and Nanotechnology, Middle East Technical University** by,

Prof. Dr. Gülbin Dural Ünver
Dean, Graduate School of **Natural and Applied Sciences**

Assoc. Prof. Burcu Akata Kurç
Head of Department, **Micro and Nanotechnology**

Prof. Dr. Nesrin Hasırcı
Supervisor, **Chemistry Dept., METU**

Dr. Tuğba Endoğan Tanır
Co-supervisor, **Central Laboratory, METU**

Examining Committee Members:

Prof. Dr. Kezban Ulubayram
Dept. of Pharmaceutical Basic Sciences, Hacettepe University

Prof. Dr. Nesrin Hasırcı
Dept. of Chemistry, METU

Prof. Dr. Caner Durucan
Dept. of Metallurgical and Materials Engineering, METU

Prof. Dr. Ayşen Tezcaner
Dept. of Engineering Sciences, METU

Assoc. Prof. Dr. Dilek Keskin
Dept. of Engineering Sciences, METU

Date: 11.09.2017

I hereby declare that all information in this document has been obtained and presented in accordance with academic rules and ethical conduct. I also declare that, as required by these rules and conduct, I have fully cited and referenced all material and results that are not original to this work.

Name, Last name: Elbay Malikmammadov

Signature:

ABSTRACT

WET SPUN PCL SCAFFOLDS FOR TISSUE ENGINEERING

Malikmammadov, Elbay

M.Sc., Department of Micro and Nanotechnology

Supervisor: Prof. Dr. Nesrin Hasırcı

Co-supervisor: Dr. Tuğba Endoğan Tanır

September 2017, 106 pages

Scaffolds produced for tissue engineering applications are promising alternatives to be used in healing and regeneration of injured tissues and organs. In this study, fibrous poly(ϵ -caprolactone) (PCL) scaffolds were prepared by wet spinning technique and modified by addition of β -tricalcium phosphate (β -TCP) and by immobilizing gelatin onto fibers. Meanwhile, gelatin microspheres carrying Ceftriaxone sodium (CS), a model antibiotic, were added onto the scaffolds and antimicrobial activity of CS was investigated against *Escherichia coli* (*E. coli*), chosen as a model gram-negative bacterium. β -TCP and gelatin were added to enhance mechanical properties while directing the scaffold towards osteogenic infrastructure; and to increase hydrophilicity by activating cell attachment via protein molecules, respectively. Modifications with β -TCP and gelatin enhanced compression modulus about 70%, and attachment of Saos-2 cells for 60%, respectively. Presence and release of CS demonstrated effective antimicrobial activity against *E. coli*. Bioactive scaffolds prepared in this study can be good candidates for bone tissue engineering applications.

Keywords: Bone tissue engineering, poly(ϵ -caprolactone), PCL, wet spinning, scaffold, gelatin immobilization, drug release

ÖZ

DOKU MÜHENDİSLİĞİ İÇİN ISLAK EĞRİLMİŞ PCL İSKELELER

Malikmammadov, Elbay

Y. Lisans, Mikro and Nanoteknoloji Bölümü

Tez Yöneticisi: Prof. Dr. Nesrin Hasırcı

Ortak Tez Yöneticisi: Dr. Tuğba Endoğan Tanır

Eylül 2017, 106 sayfa

Doku mühendisliği uygulamaları için üretilen iskele yapılar, zarar görmüş doku ve organların iyileşmesinde ve yenilenmesinde kullanılmak üzere umut verici alternatiflerdir. Bu çalışmada, ıslak eğirme tekniğiyle poli(ϵ -kaprolakton) (PCL) fiber iskele yapılar hazırlanmış, β -trikalsiyum fosfat (β -TCP) eklenerek ve fiberlerin yüzeyine jelatin immobilize edilerek modifiye edilmiştir. Aynı zamanda, model bir antibiyotik olarak Ceftriaxone sodium (CS) taşıyan jelatin mikroküreler de iskele üzerine eklenmiş ve CS'nin antimikrobiyal aktivitesi model bir gram negatif bakteri olarak seçilen *Escherichia coli*'ye (*E. coli*) karşı araştırılmıştır. β -TCP ve jelatin, sırasıyla, iskeleyi osteojenik altyapıya doğru yönlendirerek mekanik özellikleri güçlendirmek ve protein molekülleri aracılığıyla hidrofilitiyi ve hücre etkileşimini arttırmak için eklenmişlerdir. β -TCP ve jelatin ile yapılan modifikasyonlar, sırasıyla basma modülüs değerini %70 ve Saos-2 hücrelerinin tutunmasını %60 arttırmıştır. CS varlığı ve salımı, *E. coli*'ye karşı etkin antimikrobiyal aktivite göstermiştir. Hazırlanan biyoaktif iskele yapılar, kemik doku mühendisliği uygulamaları için uygun adaylar olabilirler.

Anahtar kelimeler: Kemik doku mühendisliği, poli(ϵ -kaprolakton), PCL, ıslak eğirme, iskele yapı, jelatin immobilizasyonu, ilaç salımı

To my family...

ACKNOWLEDGEMENTS

I would like to express my special thanks to my supervisor Prof. Dr. Nesrin Hasırcı for her continuous guidance, encouragement, motivation and support during all the stages of my thesis. I sincerely appreciate the time and effort she has spent to improve my experience during my graduate years.

I am also grateful for my co-supervisor Dr. Tuğba Endoğan Tanır and my unofficial co-supervisor Dr. Aysel Kızıltay for their comments, suggestions and help throughout my studies. I am obliged for their timeless support and guidance.

I am deeply thankful to Prof. Dr. Vasıf Hasırcı for his support, leadership and guidance in METU-BIOMAT Biomaterials and Tissue Engineering Research Group.

I am thankful for Dr. Menekşe Ermiş and Dr. Arda Büyüksungur for their support in microscopy studies and *in vitro* cell culture tests. I would like to thank Emre Ergene, Milad Feathi, Novendra Novendra, Engin Pazarçeviren and Sema Zabcı for their friendship and support throughout the thesis. I would also like to thank my labmates and all the BIOMATEN students and staff for being there and helping me.

I would like to acknowledge TUBİTAK and METU BAP for their support through 213M708 and BAP-07-02- 2014-007-507 grants, respectively.

Finally, I would like to thank my family, Akif Malikmammadov, Parvin Malikmammadova and Eldar Malikmammadov for their support, love and trust in me throughout my life.

TABLE OF CONTENTS

ABSTRACT.....	v
ÖZ.....	vi
ACKNOWLEDGEMENTS	viii
TABLE OF CONTENTS	ix
LIST OF TABLES	xi
LIST OF FIGURES.....	xii
ABBREVIATIONS.....	xiv
CHAPTERS	1
1. INTRODUCTION.....	1
1.1. Tissue Engineering	1
1.2. Bone Tissue Engineering.....	5
1.2.1. Materials Used for Scaffold Production.....	7
1.2.2. Methods Used for Scaffold Production	17
1.3. Drug Release in Bone Tissue Engineering.....	22
1.4. Aim of Thesis	26
2. MATERIALS AND METHODS	27
2.1. Materials.....	27
2.2. Preparation of Wet Spun PCL Scaffolds	28
2.3. Characterization of the Wet Spun PCL Scaffolds	29
2.3.1. SEM Imaging	29
2.3.2. Mechanical Analysis	29
2.3.3. <i>In vitro</i> Degradation Studies.....	30
2.4. Surface Modification of Wet Spun Scaffolds.....	31
2.4.1. Surface Activation with Acrylic Acid	31
2.4.2. Surface Modification with Gelatin	34
2.4.3. XPS Analysis.....	35
2.4.4. Porosity of Wet Spun Scaffolds	36

2.4.5. Preparation of Gelatin Microspheres (GM) and GM Containing Scaffolds	37
2.4.6. <i>In vitro</i> Drug Release	38
2.4.7. Antibacterial Test	39
2.5. <i>In vitro</i> Cell Culture Tests	40
2.5.1. Cell Viability	41
2.5.2. Morphological Characterization of <i>In vitro</i> Cell Culture Tests.....	43
2.6. Statistical Analysis	44
3. RESULTS and DISCUSSION	45
3.1. Optimization of Wet Spinning Process	45
3.2. Characterization of Scaffolds	45
3.2.1. Morphological Analysis	46
3.2.2. Mechanical Analysis	49
3.2.3. <i>In vitro</i> Degradation Results.....	51
3.3. Surface Modification of Wet Spun Scaffolds.....	54
3.3.1. XPS Analysis.....	54
3.4. Characterization of Activated and Modified Scaffolds	57
3.4.1. Morphological Analysis	57
3.4.2. Porosity Analysis.....	58
3.4.3. <i>In vitro</i> Drug Release and Antibacterial Efficacy	60
3.4.4. <i>In vitro</i> Cell Culture Tests	63
4. CONCLUSION	67
REFERENCES.....	71
APPENDICES.....	93
A. Optimization of Wet Spinning.....	93
B. Particle Size Analysis Results of β -TCP	97
C. Calibration curve of Toluidine Blue	99
D. Calibration curve of Ceftriaxone Sodium.....	101
E. Calibration curve of Saos-2 cells.....	103
F. Curriculum Vitae	105

LIST OF TABLES

TABLES

Table 3.1. Mechanical test results.	49
Table 3.2. Electron binding energy values (in eV) of atoms present in structure. ...	55
Table A.1. Optimization of wet spinning setup.	93

LIST OF FIGURES

FIGURES

Figure 1.1. Tissue engineering.	2
Figure 1.2. Tests and requirements for biomaterials (Billiet et al., 2012).	8
Figure 1.3. Biodegradation of PCL (Woodruff and Hutmacher, 2010).	15
Figure 1.4. Components of wet spinning method (Ucar, 2012).	20
Figure 1.5. Wet spun scaffolds.	21
Figure 1.6. Biofilm formation (Johnson & García, 2015).	24
Figure 2.1. Wet spinning setup.	28
Figure 2.2. Mechanical test setup.	30
Figure 2.3. Oxygen plasma instrument.	32
Figure 2.4. Acrylic acid grafting procedure on PCL-T ₂₀ scaffolds.	32
Figure 2.5. Acrylic acid grafting setup.	33
Figure 2.6. Gelatin immobilization.	35
Figure 2.7. Microsphere preparation, loading and adsorption on the scaffolds.	38
Figure 2.8. An example of disk diffusion result.	40
Figure 2.9. AlamarBlue® mechanism.	41
Figure 3.1. Morphology of β -TCP particles.	46
Figure 3.2. Images and elemental compositions of scaffolds.	48
Figure 3.3. Mechanical test results.	50

Figure 3.4. Degradation results.	53
Figure 3.5. Surface modification steps and XPS results.	56
Figure 3.6. SEM Images of surface modified scaffolds.	58
Figure 3.7. μ CT analysis results of the scaffolds.	59
Figure 3.8. Gelatin microspheres and release results.	62
Figure 3.9. Cell viability of PCL, PCL-T ₂₀ and PCL-T ₂₀ GM scaffolds (*p<0.05)..	63
Figure 3.10. Characterization of Saos-2 seeded scaffolds at the end of day 28.	64
Figure 3.11. Movements of cells between fibers.	65
Figure B.1. Particle size analysis of β -TCP after grinding and sieving.	97
Figure C.1. Calibration curve of Toluidine Blue (at 624 nm).	99
Figure D.1. Calibration curve of Ceftriaxone Sodium (at 270 nm).	101
Figure E.1. Calibration curve of Saos-2 cells with AlamarBlue® analysis.	103

ABBREVIATIONS

3D	Three Dimensional
AAc	Acrylic Acid
AD	Actual Density
AE	Attachment Efficiency
ALP	Alkaline Phosphatase
ANOVA	Analysis of Variance
β -TCP	β -Tricalcium Phosphate
BSA	Bovine Serum Albumin
CHCL ₃	Chloroform
CLSM	Confocal Laser Scanning Microscopy
CS	Ceftriaxone Sodium
CS ₅₀	Compressive Strength at 50% Strain
dH ₂ O	Distilled Water
DI H ₂ O	Deionized Water
DAPI	4',6-Diamidino-2-Phenylindole
DCM	Dichloromethane
DMAC	Dimethyl Acetamide
DMEM	Dulbecco's Modified Eagle Medium
DMSO	Dimethyl Sulfoxide
DRAQ5	1,5-Bis{[2-(Dimethylamino)Ethyl]Amino}-4,8-Dihydroxyanthracene-9,10-Dione
ECM	Extracellular Matrix
EDAC	1-Ethyl-3-(3-Dimethylaminopropyl)-Carbodiimide
EDTA	Ethylenediamine Tetraacetic Acid
EDX	Energy Dispersive X-Ray Spectroscopy
EtOH	Ethanol
FBS	Fetal Bovine Serum
FITC	Fluorescein Isothiocyanate
GA	Glutaraldehyde

GM	Gelatin Microvesicles
hADSC	Human Adipose Derived Stem Cell
HAp	Hydroxyapatite
HSD	Honest Significant Difference
M _E	Modulus of Elasticity
MetOH	Methanol
Micro-CT	Micro Computed Tomography
M _n	Number Average Molecular Weight
NHS	N-Hydroxysuccinimide
NS	Not Significant
PBS	Phosphate Buffer Saline
PCL	Poly(ϵ -caprolactone)
PDI	Polydispersity Index
Pen/Strep	Penicillin/Streptomycin
PFA	Paraformaldehyde
PGA	Poly(glycolic acid)
PLA	Poly(lactic acid)
PLGA	Poly(lactic-co-glycolic acid)
RT	Room Temperature
Saos-2	Human Osteosarcoma Cell Line
SBF	Simulated Body Fluid
SEM	Scanning Electron Microscope
VD	Visible Density
XPS	X-ray Photoelectron Spectroscopy

CHAPTER 1

INTRODUCTION

1.1. Tissue Engineering

Tissue engineering is a field, where scaffolds, cells and biologically active molecules are used to heal or augment a tissue. By combining porous scaffolds with different cells and active molecules, it is possible to form tissue engineered constructs for various number of applications. In the preparation of these types of constructs, various materials can be used and different methods can be applied to achieve different properties. With these structures, it is possible to mimic microenvironment of different tissues in body. Success of tissue engineered construct lies in proper integration of construct with the targeted tissue and high activity of attracting the cells in that tissue for colonizing the interior of the scaffold.

Main challenge of tissue engineering is imitating the natural environment in the body. That is crucial, since it determines whether the cells will be populated in the scaffold and that the scaffold will be integrated into tissue. A tissue engineered construct should be able to do three functions, 1) form the required three-dimensional (3D) structure, 2) integrate cells into the structure and 3) integrate itself into the live tissue. Upon completing these three properties, the construct can be called as tissue engineered construct (Figure 1.1).

Cells used in tissue engineering can be obtained from three different sources: autogenic (from the patient), allogeneic (from another human) and xenogeneic (from different species). These three cell sources have different characteristics as described below.

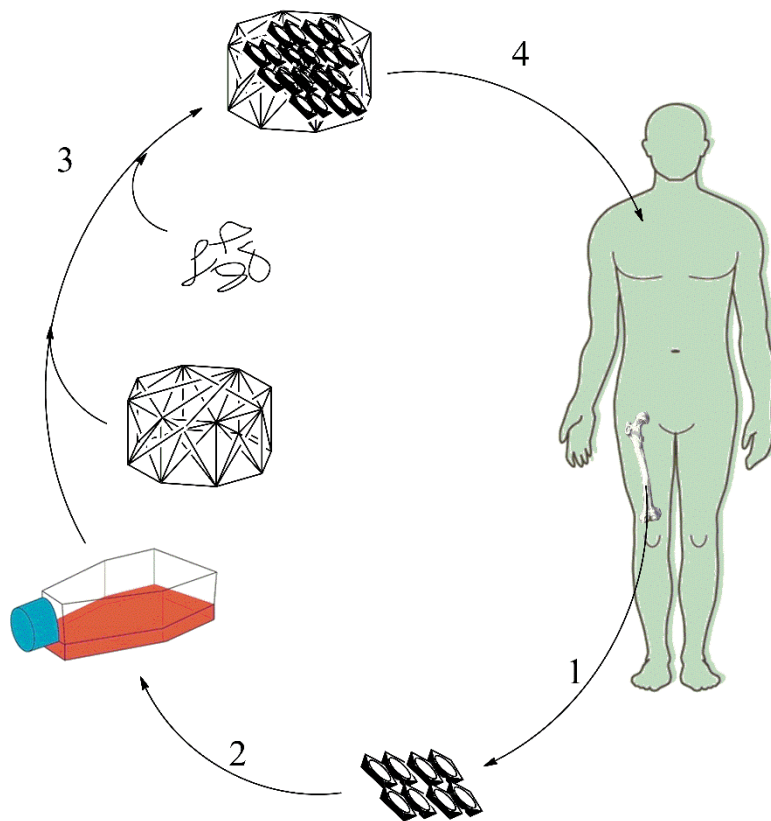


Figure 1.1. Tissue engineering. (1) Cells are taken from patient, (2) grown in tissue culture flasks, (3) cells and bioactive molecules are put into tissue engineering construct, (4) cells are allowed to grow and populate the construct and (5) construct with cells is introduced back to patient.

- Autogenic: These cells are taken directly from the patient. They provide the highest acceptance by patient's immune system. But they are scarce. Most commonly used autogenic cells are stem cells, which are mostly bone marrow stem cells and obtained from long bones (such as femur) using invasive surgical entrance into bones. This may not comply with the ill or older patient. Other procedures for stem cell extraction are also present, as taking them from urine (urine derived stem cells (Zhang et al., 2014)), fat tissue (adipose derived stem cells (Frese et al., 2016))
- Allogenic: These cells are taken from other humans. They have lower acceptance by patient's immune system but they are more abundant than

autogenic cells. There are also many successful end products made of allogenic cells; examples are Apligraf® and Transcyte®, both skin tissue engineered end products (Lanza et al., 2007)

- Xenogenic: These are the cells taken from other species. They are more abundant than other two cell sources but provide lowest acceptance by immune system.

The source of the cells, which is going to be applied to the patient, is very important. Because if the cells other than autogenic are used, then, a dosage of immune suppressant is required to suppress the rejection of cells by the host body. In general, cells used in tissue engineering studies are cancer cell lines or undifferentiated cells. Cancer cell lines are actively reproducing and stop only when the environment is unfavorable. Undifferentiated cells are cells that have not reached their lineage. They are also actively reproducing, but the rate of proliferation decreases when they finally start to differentiate to their cell lineage. Different undifferentiated cell types are present in body, including hematopoietic stem cells, bone marrow stem cells etc. However, for medical applications, cancer cells cannot be used. Thus, the cell types used in medical applications are stem cells or progenitor cells (Tevlin et al., 2016). Stem cells are totipotent, which means they can differentiate into any cell type; whereas progenitor cells are pluripotent, which means they have a limited number of cell types they can differentiate. Examples of progenitor cells used in tissue engineering are human fetal osteoblast cells, endothelial progenitor cells etc.

There has been an important development for increasing the amount of cells that can be captured from patient (Takahashi and Yamanaka, 2006). The autogenic pluripotent stem cells were produced by reprogramming the differentiated cells. Differentiated cells are the stromal cells (e.g. skin cells), where only a small part of their genetic code are actively used, to perform the functions of cell lineage to which they have differentiated into (contraction for muscle cells, protection for skin cells etc.). The part of the genes that is not used by these differentiated cells is being disabled. By reprogramming the genetic code, and re-enabling the inactive genes, it is possible to

reprogram a differentiated cell into an undifferentiated cell. Such cells produced by reprogramming, are called induced pluripotent stem cells (iPSCs). Undifferentiated cells can give rise to many different cells, depending on environment (nearby cells, chemical signals and tissue properties), like stem cells. Possibility of forming iPSCs from these differentiated stromal cells gives hope for usage of high number of autogenic cells in tissue engineering applications.

Preseeding cells into construct provides some advantages:

- 1- Preseeded cells produce extracellular matrix and form a construct required by cells of tissue to attach and populate.
- 2- Preseeding provides easier integration of construct into live tissue of the patient.
- 3- Preseeding direct the differentiation lineage of patient's cells.

3D constructs produced for tissue engineering applications should be compatible for cells to colonize and heal/regenerate tissues. These constructs should have the following major properties:

- Interconnected porosity – for cells to migrate inside the constructs and for deeper fluid & gas exchange; mostly a porosity value of higher than 50% is required.
- Microenvironment – to mimic the *in vivo* environment of cells; including soluble molecules, extracellular matrix and the required physical forces for the cells.
- Mechanical properties – to be compatible with the tissue; where some tissues require elasticity and some require toughness.

3D construct has the integrity to hold and provide environment for regeneration/repair of the tissue. Different methods and materials can be used for the preparation of tissue engineered 3D constructs. The shape, surface topography and chemistry of the scaffolds are decisive factors for their application to different tissues.

Another important element of tissue engineering is usage of bioactive molecules. They can be as simple as minerals (β -tricalcium phosphate (Li et al., 2017a), hydroxyapatite (HAp) (Lee et al., 2016) and etc.), or complex as hormones (thyroid/parathyroid hormones (Gentile et al., 2015)), proteins (bone morphogenic proteins (Yilgor et al., 2009; Mitsak et al., 2011), etc.) or drugs (antibacterial (Sezer et al., 2013; Ashbaugh et al., 2016)). Their choice depends on the requirements of the host tissue. Bioactive molecules can be integrated within the scaffold (as HAp) or can be immobilized on the surface of the scaffold (as proteins) or can be loaded in nano or microparticles and released from the surface of construct (Ucar et al., 2016) or from vesicles/spheres incorporated in structure (Ossa et al., 2012; Sezer et al., 2014b). Adjusting the release behavior and selecting a molecule assists the work of 3D construct and improves its function.

The last step is integration of construct into target tissues. At this step, the physical, chemical and biological properties are very important to be similar to the integrated host organ/tissue. Inability to do so, may end up with forming a barrier/grain between live tissue and the construct, leading to delayed regeneration and repair of the tissue. After the preparation of a proper tissue engineered construct, it is essential to examine its integration into live system. This step is generally achieved on animal subjects. In this stage, it is known whether the construct is being accepted by the living system or not. If it is not compatible and not accepted, it can lead to “foreign body response”, which means that the construct will be enclosed in a collagen sack to keep it away from the other parts of body (Murdock and Badylak, 2017). Success in animal studies leads to human trials (clinical trials). All these studies are evaluated by presented value systems, for their immune response, inflammatory response, integration into tissue etc.

1.2. Bone Tissue Engineering

Bone tissue engineering has received a significant attraction due to increased traffic accidents, active lifestyle and expended lifespan, which causes diseases, damages and malfunctions in bone tissue. The importance of bone tissue engineering is in the

belated healing of the damages in bone tissue, due to its relative rigidity and less complexity with respect to other tissues. Due to rigid property and presence of small numbers of blood vessels, the cell and tissue fluid movement is slower in bones. This brings the need for constructs to fill the void in the bone caused by damage. Bone tissue engineering applications are supported by scaffolds, which ensure the integration of cells, provide interconnected porosity for nutrients and waste flow and enhance the healing of bone tissue.

Requirements of a functioning bone tissue engineering construct are:

- Around 70% interconnected porosity (Polo-Corrales et al., 2014)
- Modulus of elasticity in at least 100-500 kPa range (Murphy et al., 2013)
- Slow degradation (Yildirimer and Seifalian, 2014)
- Providing osseointegration, osteogenesis, osteoconduction and osteoinduction (Albrektsson and Johansson, 2001)

Interconnected porosity is required for cells to be able to infiltrate to inner parts and colonize scaffolds. It is also vital to have the nutrient, metabolic waste and gas flow in and out of the scaffold. Porosity of 70% is reported to be sufficient for bone tissue integration and regeneration (Ghanaati et al., 2010; Tang et al., 2016). This value is also good to keep the mechanical properties of scaffold high enough to be used in bone tissue. Mechanical properties of scaffolds have to be at least in 100-500 kPa range to have the bone tissue integration. This value is also important to provide mechanical differentiation cue towards bone tissue by mechanosensing mechanism, which works by interaction of cells' with substrate and sensing its stiffness (Plant et al., 2009; Lange and Fabry, 2013; Smith et al., 2017). Degradation is an important property for the materials used in the preparation of scaffolds. In tissue engineering it is expected that the rate of degradation of the material should be similar to the tissue regeneration rate. If degradation is slower than the tissue regeneration rate, it hinders the growth of tissue and if it is faster, then leads to loss of connection between the

tissue and the scaffold and delay the healing process (Yildirimer and Seifalian, 2014). Degradation of scaffolds should be at similar rate as the formation of new tissue.

Bone tissue regeneration is a slow process due to its rigidity, thus the scaffold aimed to be used in bone tissue engineering application should also have slow degradation rate to keep up with the pace of bone regeneration. Integration of scaffold into the bone tissue is called as osseointegration. This is an important phenomenon, since it defines the success of regeneration. If poor integration is present, it will affect the integrity of bone and will cause fragmentation, which will lead to weak link in mechanical durability. Presence and levels of osteogenesis and osteoinduction, which are formation of new bone tissue and driving osteogenic differentiation for stem cells nearby, respectively, affects the success of construct in bone tissue engineering applications (Albrektsson and Johansson, 2001).

1.2.1. Materials Used for Scaffold Production

Any material, which is aimed to be used in scaffold production, should be a biomaterial, which means it has to comply with the biocompatibility rules. In most body parts, to be biocompatible is enough, whereas for tissues having blood circulation and have high blood contact, hemocompatibility is also required. The requirements of biomaterials are listed in Figure 1.2 given below:

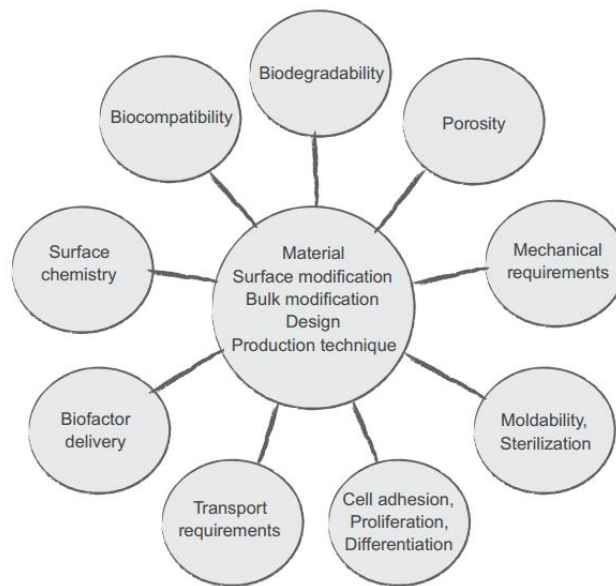


Figure 1.2. Tests and requirements for biomaterials (Billiet et al., 2012).

Biocompatibility requires that, a material:

- Should not elicit an acute systemic toxicity.
- Should not be cytotoxic (killing cells).
- Should not be mutagenic (generate genetic mutations).
- Should not produce any toxic material when it is degraded and degradation products should not be toxic either.
- Should not be pyrogenic (inducing fever).
- Should not elicit sensitization (progressive amplification of a response after repeated administrations).

Different materials, like bioceramics, natural/synthetic polymers, metals and composites have been used in scaffold production. Each material has its own advantages and disadvantages. The tissue of interest has a big impact on decision of material to be used. Scaffolds should have similar biological, chemical and physical properties with the tissues they are going to be applied. It is important for scaffolds

to integrate to tissue as easily as possible and accelerate the healing process. Properties and examples of different biomaterial groups are listed below:

Bioceramics – Advantages: inert materials; have superior mechanical (compressive) properties.

Disadvantages: have high density (stress concentrating region); are very brittle.

Examples: tricalcium phosphate, hydroxyapatite, etc.

Synthetic Polymers – Advantages: easy processing; low batch-to batch variation; easy modification.

Disadvantages: can initialize immune/inflammatory reactions; cannot resist harsh processing steps.

Examples: poly(ϵ -caprolactone), poly(lactic acid), etc.

Natural Polymers – Advantages: similar properties with living tissues; presence of cell attractant residues; low cost; abundance in nature.

Disadvantages: can initialize immune/inflammatory reactions; cannot resist harsh processing steps.

Examples: gelatin, collagen, chitin, chitosan, cellulose, etc.

As we can observe above, many advantages and disadvantages are present for different material types. By using different materials from different groups together as a composite, it is possible to overcome some disadvantages. For example, by using bioceramics with soft polymers, it is possible to overcome low mechanical strength of soft polymers whilst reducing brittleness and high density of bioceramics.

1.2.1.1. Bioceramics

The most commonly used minerals in bone tissue engineering are bioceramics. Due to the ions present in their structure, they can mimic the bone tissue environment and with the property of inertness, it is possible to integrate bioceramics into every structure. They have been used in tissue engineering applications for osteogenesis (Albrektsson and Johansson, 2001) or improving mechanical properties (Sharma et al., 2016; Tong et al., 2016).

1.2.1.1.1. Calcium Phosphates

Calcium phosphates are minerals present in hard tissues to enhance mechanical properties of the tissue. There are many different forms of calcium phosphates, ranging from tricalcium phosphates (with three calcium ions) to hydroxyapatites (that occurs naturally in bone tissue, with ten calcium ions). Their presence does not only enhance mechanical properties, but also provide environment for differentiation of stem cells to bone cells. Bioceramics have been used as additives into the scaffolds in order to enhance both of these properties in bone tissue engineering.

Calcium phosphates have been used either as is, or in addition to polymers to help to treat bone damages and help bone regeneration. Cobalt-doped hydroxyapatite was prepared by wet chemical precipitation method for production of bone tissue engineering scaffold, where cobalt provided pro-angiogenesis and hydroxyapatite provided osteogenesis (Kulanthaivel et al., 2016). Poly(ϵ -caprolactone) (PCL) and poly(ethylene glycol) (PEG) crosslinked scaffolds with addition of hydroxyapatite were prepared by using thermal polymerization method (Koupaei et al., 2015). Incorporation of hydroxyapatite increased porosity and compressive mechanical strength and decreased degradation rate of the scaffolds. Addition of hydroxyapatite also increased ALP activity in osteosarcoma cell line. In another study, electrospun PCL/hydroxyapatite scaffolds were prepared to be used in bone tissue (Derakhshan et al., 2015). Methacrylated chondroitin sulfate was blended with hydroxyapatite to

form photocrosslinkable cell encapsulating gels. Inclusion of hydroxyapatite into gels vastly increased osteogenesis in adipose derived stem cells. The increased hydroxyapatite percentage lead to formation of calcium phosphate droplets in mats and increased mechanical properties. Fayyazbakhsh et al prepared gelatin-hydroxyapatite blend solution, crosslinked with glutaraldehyde and freeze dried for bone tissue engineering purposes, where addition of hydroxyapatite increased porosity but also made the scaffolds brittle (Fayyazbakhsh et al., 2017). Aragon et al prepared core/shell PCL/PCL and PCL/poly(vinyl acetate) scaffolds by electrospinning with or without hydroxyapatite addition for bone tissue engineering applications (Aragon et al., 2017). In another study, foaming technology was used for formation of chitosan-gelatin-alginate-hydroxyapatite scaffolds, which were crosslinked with glutaraldehyde and applied for bone tissue engineering (Sharma et al., 2016). In all these studies, mechanical superiority of hydroxyapatite containing scaffolds was reported, including high cell attachment to the scaffolds and fast healing in the treatment of bone defects in *in vivo* experiments.

One of the frequently used bioceramics in bone tissue engineering is β -tricalcium phosphate (β -TCP), which has the chemical formula of $\text{Ca}_3(\text{PO}_4)_2$. It has been used as osteogenic material and to increase the mechanical properties of scaffolds. By using electrodeposition method, β -TCP was deposited onto reduced graphene oxide nanosheets with a needle-like appearance in acidic environment, and immersion into simulated body fluid resulted in high mineralization of particles (Metoki et al., 2016). Such construct showing high biomineralization was effective in bone tissue engineering due to its osteogenic activity. Effects of scaffolds present in market as Genderm® was studied for the treatment of critical size bone defects either with β -TCP, or magnesium doped β -TCP and compared to control group of Genderm® (Costa et al., 2016). *In vivo* study lasting for 6 months lead to 4-5 fold increase in bone regeneration for β -TCP and β -TCP-Mg group, where β -TCP-Mg group could filled both the sides and the central region of defect, reaching closer to whole regeneration of bone tissue. In another study, PCL was mixed with gentamicin loaded β -TCP/gelatin microspheres were added into PCL to form freeze dried scaffolds for

bone tissue engineering (Sezer et al., 2013). Addition of β -TCP containing microspheres significantly decreased degradation rate of scaffolds in lipase containing environment (Sezer et al., 2014b) and significantly increased both post-implantation push-out mechanical results and post implantation histological scores (Sezer et al., 2014a). Injectable β -TCP microspheres were prepared for healing of irregular bone defects and the presence of microspheres proved to be osteogenic, and *in vivo* studies showed the microspheres can gather osteoblasts and enhance regeneration of bone tissue (Li et al., 2017a).

1.2.1.2. Synthetic Polymers

High number of synthetic polymers were used in bone tissue engineering studies up to this time. Their advantage of easy processing and toleration to harsh chemicals makes them preferable materials because it is easier to provide additional properties on to these materials. Meanwhile, it is also easy to produce same properties from different batches of synthetic polymers rather than the natural polymers.

Synthetic polymers have been used for their ease of control over mechanical properties (Patrício et al., 2013; Narayanan et al., 2015; Felfel et al., 2016; Vashaghian et al., 2016; Yao et al., 2016), degradation (Dong et al., 2005; Lam et al., 2009; Díaz et al., 2014; Gleadall et al., 2014a, 2014b; Sabbatier et al., 2015; Felfel et al., 2016) and surface chemistry (Ozcan et al., 2008; Xu et al., 2010; Al Meslmani et al., 2014; Kara et al., 2014; Kim et al., 2014; Chi et al., 2016; Petisco-Ferrero et al., 2016). Synthetic polymers can be used with strong chemicals (Chandy et al., 2002; Sabzi and Boushehri, 2005; Shalumon et al., 2010; Bajpai et al., 2015; Prabhakar et al., 2016) and in harsh environments (Seyednejad et al., 2011; Lou et al., 2014; Cañas et al., 2016). These properties provide ease of manipulation of polymer properties for modification with respect to requirements.

Cui et al prepared melt spun poly(L-lactide-co-glycolide) (PLGA) scaffolds with addition of hydroxyapatite into polymer solution (Cui et al., 2015). Supercritical CO₂ treatment was done to pressurize and mold the scaffolds. ALP activity *in vitro* studies and bone markers *in vivo* studies showed that the setup was successful for usage in bone tissue engineering. In another study, electrospun PLGA:PCL mat was prepared for coating implants used in bone tissue engineering to escape bacterial infections (Ashbaugh et al., 2016). Drugs were added into polymer solution and release was observed *in vitro* on the implants and *in vivo* in tissue. Effective zone of inhibition of bacterial growth was observed even after storage in freezer. Lou et al combined two methods, thermally induced phase separation and salt leaching for preparation of PLLA- β -TCP scaffolds (Lou et al., 2014). The scaffolds prepared by combination of these two methods were porous, had increasing compressive properties with increasing β -TCP percentage and had higher cell affinity with incorporation of β -TCP into polymer solution. In another study, β -TCP scaffold was prepared by solvent evaporation and sintering, which was then coated with PLLA solution by dipping the scaffold into polymer solution and dry in room temperature (Arahira et al., 2015). Pores in scaffold were homogeneous and the prepared scaffolds had increasing compressive modulus with increasing PLLA content.

1.2.1.2.1. PCL

Poly(ϵ -caprolactone) (PCL) is a material that is frequently used in tissue engineering and other biomedical applications. PCL can be degraded by hydrolytic, enzymatic, or intracellular mechanisms under physiological conditions. However, PCL degrades at a much slower rate than poly(lactic acid) (PLA), poly(glycolic acid) (PGA), and poly(lactic-co-glycolic acid) (PLGA), which makes PCL less attractive for soft tissue engineering applications but more attractive for bone tissue engineering, long-term implants and drug-delivery systems (Guo and Ma, 2014).

PCL is one of the non-hazardous polyesters obtained by ring-opening polymerization of ϵ -caprolactone monomers, which can proceed via anionic, cationic, coordination

or radical polymerization mechanisms (Hoskins and Grayson, 2009). Different methods were described for the polymerization of caprolactones; which used different catalysts as stannous octoate (Woodruff and Hutmacher, 2010; Azimi et al., 2014) or aluminum alkoxides (Alexandru, 2011). These reactions were performed under different conditions such as polymerization temperature and duration, presence, type and concentration of catalysts, monomer to solvent ratio, etc. By changing one or more of these variables, it was possible to produce PCLs having different number average molecular weights (M_n) and polydispersity indices (PDI) (Huang et al., 2016), which in turn led to differences in the degradation behavior and mechanical strength. Solubility of PCL is high in benzene, carbon tetrachloride, chloroform, cyclohexanone, dichloromethane, toluene, and 2-nitropropane. Its solubility is lower in acetone, acetonitrile, 2-butanone, dimethylformamide, ethyl acetate, and it is insoluble in water, ethyl alcohol, diethyl ether and petroleum ether (Sabzi and Boushehri, 2005; Woodruff and Hutmacher, 2010; Ossa et al., 2012; Sezer et al., 2013, 2014a, 2014b; Azimi et al., 2014; Tong et al., 2016).

PCL is semicrystalline at room and human body temperatures. Its glass transition temperature (T_g) is about $-60\text{ }^\circ\text{C}$ and melting temperature (T_m) is about $60\text{ }^\circ\text{C}$ (Huang et al., 2002; Murphy, 2011; Schäler et al., 2013; Feng et al., 2015). At ambient temperatures amorphous chains are in rubbery state which gives PCL chains free movement at the body temperature, and thus increases its permeability for the body metabolites when replaced into the body (Herman, 2007).

PCL is biodegradable but more stable compared to polylactides because it has less frequent ester bonds per monomer, and therefore, degradation takes longer for PCL chain fragments to be enzymatically hydrolysed in the body. Degradation depends on the molecular weight, shape, residual monomer content, autocatalysis in addition to other factors. In general, complete degradation of PCL occurs in 2-3 years in the biological media having a constantly changing interstitial fluid (Abedalwafa et al., 2013; Díaz et al., 2014; Gleadall et al., 2014a, 2014b). Enzymatic degradation takes place by the action of lipase enzyme (Martins et al., 2009; Murphy, 2011). The

enzyme is present in the interstitial fluid secreted by cells, and function by cleaving the ester bonds of PCL (Tietz and Shuey, 1993). The pH of the medium is influential on the degradation rate. In the alkaline environment degradation of PCL is faster than in the acidic environment (Hernández et al., 2013). The degradation product of this step is 6-hydroxycaproic acid which is released into the medium (Edlund and Albertsson, 2002). This molecule can be taken up by cells and undergo 2- β oxidations to form 3-acetyl CoA molecules, that are further metabolized in the citric acid cycle (Buchanan, 2008; Migonney, 2014) as shown in Figure 1.3, and get cleared by renal excretion (Díaz et al., 2014). The degradation products do not accumulate in the body.

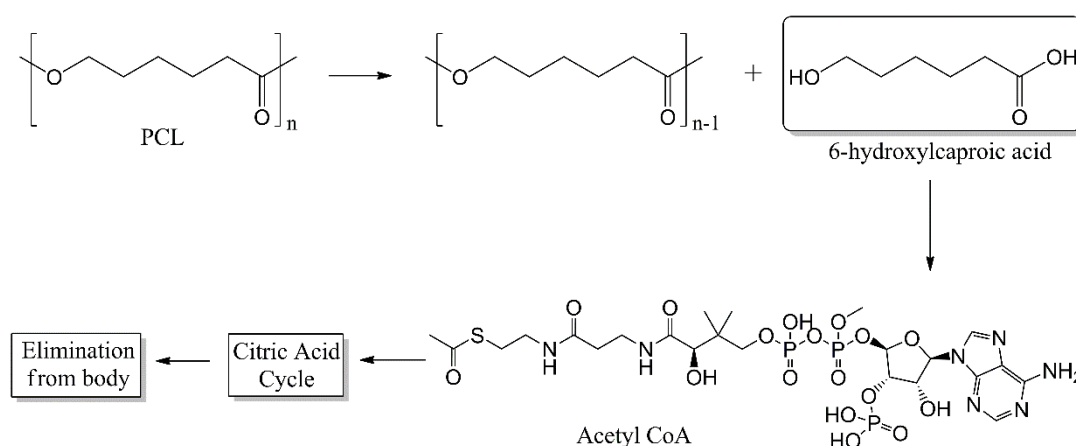


Figure 1.3. Biodegradation of PCL (Woodruff and Hutmacher, 2010).

PCL has many good qualities for being considered as a biomaterial. Although its biocompatibility is very low, its rubbery property, adjustable biodegradability, ease of forming blends, composites and copolymers make it a desirable material for use as supporting device especially for hard tissue, a good scaffold material to be used in tissue engineering, and a desirable material for surgical sutures and micro and nano drug delivery vesicles (Woodruff and Hutmacher, 2010; Abedalwafa et al., 2013; Azimi et al., 2014). Also its tailorability of surface roughness and hydrophilicity provides preferable surfaces and interfacial characteristics for cell attachment (Shah and Amiji, 2006; Xu et al., 2010). Some of the devices composed of PCL have already

been approved by the Food and Drug Administration (FDA) to be used in human. For example “Monocryl” sutures (Paulson, 1996), prepared by copolymerizing glycolide and ϵ -caprolactone to form a monofilament absorbable surgical suture (trademarked by Ethicon), “Capronor” (Maquet et al., 2006), consisting of PCL rods that releases a progestin-like hormone for birth control purposes, and “SynBiosys” drug release spheres made of multi-block copolymers of ϵ -caprolactone lactide and ethyl glycol (Hissink et al., 2005) are examples for the FDA approved PCL containing medical systems.

1.2.1.3. Natural Polymers

Natural polymers are either taken directly from the natural environment (as cellulose, chitin, collagen, etc.) or modified afterwards (like gelatin, fibroin, chitosan, etc.). Natural polymers should be handled and processed under mild conditions, since they are not as durable and resistant to harsh chemical and physical environments as synthetic polymers. However, natural polymers create compatible environment and provide the increased cell interaction, which helps to the integration of the constructs into the living tissue. Natural polymers have different effects on chemical, physical and biological environments. Chitosan, for example, is used for its mechanical integrity (Yilgor et al., 2009; Cooper et al., 2011; Hong and Kim, 2011; Isikli and Hasirci, 2012; Cañas et al., 2016; Khan et al., 2017), as is collagen (Fuse et al., 2015; Wu et al., 2017; Zhang et al., 2017) and silk fibroin (Lee and Kim, 2010; Bhattacharjee et al., 2015; Zhang et al., 2015; Li et al., 2017b). Other natural polymers like starch (Tuzlakoglu et al., 2010; Phromsopha and Baimark, 2014) are used as plasticizer.

1.2.1.3.1. Gelatin

Gelatin is the natural polymer formed by heat denaturation of triple-helix collagen and forming random coils in the structure. Collagen is one of the main constituents of extracellular matrix that contains cell-binding domains, which are composed of

three amino acid chains, known as RGD sequence. Attachment proteins called integrins on the cell surface, bind to the RGD sequence on collagen for the movement and integration of the cells into structure. Gelatin, which is polymer of amino acids, also has these domains and can provide similar binding residues. Gelatin is a polymer of amino acids (i.e. a protein). It has been used both as a backbone and as an add-on in many tissue engineering constructs. A solution of chitosan-gelatin blend was fed with PLGA microparticles loaded with simvastatin and freeze dried for scaffold formation (Gentile et al., 2016). Cell proliferation results showed high biocompatibility of scaffolds, while mechanical test results were lower than synthetic polymers due to natural polymer backbone. Another chitosan-gelatin blend was prepared by freeze drying (Cañas et al., 2016). In this study, highly porous (90-95%) structures demonstrated higher compressive moduli with increasing amounts of chitosan and more cell viability with increasing amounts of gelatin.

Electrospun PLGA scaffolds showed significantly lower water contact angle and mean fiber diameter after blending with gelatin (Mehrasa et al., 2015). This shows the hydrophilicity of gelatin residues that changes the surface chemistry of constructs. Gelatin-hydroxyapatite blend solution which was crosslinked with glutaraldehyde and freeze dried for bone tissue engineering purposes, showed that presence of gelatin significantly increased cell number and osteogenesis (Fayyazbakhsh et al., 2017). Increase in cell proliferation is due to presence of cell-binding RGD residues on gelatin. This sequence enhances cell binding and proliferation. Foaming technology was used for formation of chitosan-gelatin-alginate-hydroxyapatite scaffolds for bone tissue engineering and it was reported that presence of gelatin led to increase in hydrophilicity and increase in swelling ratio (Sharma et al., 2016). These properties of gelatin make it so attractive and frequently used in tissue engineering studies.

1.2.2. Methods Used for Scaffold Production

Scaffolds are man-made environments for cells to divide, grow and differentiate in tissue engineering applications. The main principle of scaffolds is to provide an

environment inside body that would help to the cells to proliferate so that it would lead to healing or replacing and/or forming an organ or tissue. Scaffolds are the imitations of living tissues. Different methods that use various properties of materials are employed for scaffold production. Non-fibrous polymers are produced by freeze drying, particulate leaching and phase separation methods. Freeze drying has been adapted for bone tissue engineering for its simplicity and compliance with large number of different natural and synthetic polymers (Algul et al., 2015; Frydrych et al., 2015; Serra et al., 2015), since it requires a soluble polymer and volatile solvent. A more sophisticated method is salt leaching, which requires an extra sacrificial substituent, that produces pores as it leaves the structure (Hou et al., 2003; Lou et al., 2014; Cui et al., 2015).

Another technique of non-fibrous scaffold production is phase separation. It uses the interaction of solvent/non-solvent for production of hardened polymer chains. In general, these methods were studied separately, but sometimes were used in combination for production of more complex units for tissue engineering. Fibrous scaffolds on the other hand, have been produced mainly by electrospinning, additive manufacturing or wet spinning. Electrospinning relies on voltage difference between two plates, which drives the movement of polymers from the solution either into a metal wall or a rolling drum (Rajzer et al., 2014; Liao et al., 2015; Mehrasa et al., 2015; Chaudhuri et al., 2016; Yao et al., 2016; Correia et al., 2016; Gozutok et al., 2016; Münchow et al., 2016; Russo et al., 2016; Aragon et al., 2017; Wu et al., 2017; Savelyeva et al., 2017). Additive manufacturing is achieved by extrusion of melt polymer solution based on CAD drawing (Mondrinos et al., 2006; Yilgor et al., 2008; Elomaa et al., 2013; Kim and Kim, 2014; Hsieh et al., 2015; Kiziltay et al., 2015; Goyanes et al., 2016; Qu et al., 2016; Yi et al., 2016). Another example of fibrous scaffold production method is wet spinning.

1.2.2.1. Wet Spinning

This process is based on the idea that if a solvent of polymer will be extruded into a non-solvent of the polymer, the polymers in the solution would try to escape from the non-solvent by decreasing their surface area (as in pouring a hydrophobic solution into water), thereby forming fibrous structures. The extrusion has to be precisely controlled for fine-tuning of fiber diameter and homogeneity. In addition, to evade the sticking of concurrent fibers onto each other, the non-solvent bath should be rotated periodically. There are many wet spinning setups discussed and prepared in the literature (Tuzlakoglu et al., 2010; Ucar et al., 2013, 2016; Puppi and Chiellini, 2017). Basic wet spinning setup is composed of following components as shown in Figure 1.4 (Ucar, 2012):

- Extruder – A device that functions as a reservoir of polymer solution and can inject its content through a needle.
- Pump System – A machine that can press the plunger top of the extruder in the given velocity invariably.
- Polymer Solution – A solution of polymer(s) prepared for extrusion.
- Needle – A thin metal injector for extrusion of polymer solution, to give it a finite radius.
- Coagulant (Non-solvent Solution) – A solution that is repellent to polymers for them to form coagulant structures.

The fiber formation setup is as explained above. However, for scaffold formation, these extruded fibers should be molded to give a desired shape and form. A basic setup is to form a meshwork by randomly mixing fibers onto each other. Examples of traditionally wet spun scaffolds are shown in Figure 1.5.a,b (Puppi, Dinucci, Bartoli, Mota, & Migone, 2011), where such random mixing can be observed. For the scaffolds produced with computer-aided wet spinning setup this action is not required (Figure 1.5.c-e) (Puppi et al., 2012, 2016; Dini et al., 2015).

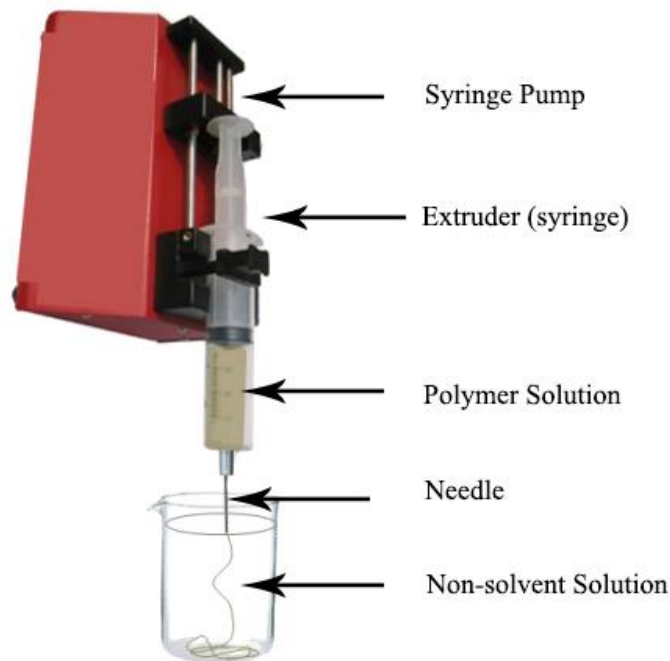


Figure 1.4. Components of wet spinning method (Ucar, 2012).

Li et al. obtained elastic chitosan wet spun fibers by introducing different reaction temperatures (Li et al., 2016). Formed fibers had smooth surfaces and increasing elongation at break with higher temperature. In another study, wet spun chitosan scaffolds were fabricated with biomineralization on their surface (Ucar et al., 2013, 2016). After wet spinning, immersion into simulated body fluid attached calcium phosphate minerals onto chitosan fibers. The inorganic coat was also loaded with an antibiotic. Cell viability and apoptosis assays showed that the scaffolds could perform as functional tissue engineering constructs and function as local antibiotic release systems. By using wet spinning methods, it is possible to decrease the fiber diameters from millimeters down to $\sim 8 \mu\text{m}$ by adjusting the setup characteristics (Zhang, Wang, Zhu, Wang, & Xiao, 2014). Wet spun PCL scaffold was fabricated using this setup for muscle tissue. For that case, a different setup has been provided, where a spinning rod reduces the produced fibers' diameters by stretching motion. This makes the formed fibers very thin. It is also possible to automate wet spinning by making the spinning motion and direction being controlled by a computer. A setup like that for

wet spinning was made for PCL and hydroxyapatite blend solution, where not only feeding rate, but X-Y motion of needle is also controlled (Puppi et al., 2012). This setup provided scaffolds that were mechanically durable and osteogenic with MC3T3-E1 cell line. Wet spinning of PCL was conducted for regeneration of annulus fibrosus (Xu et al., 2015). Circumferential rotation of microfibers resulted in a cylindrical scaffold that was seeded with cells. *In vivo* tests showed high expression of marker genes and superior compressive properties after day 21.

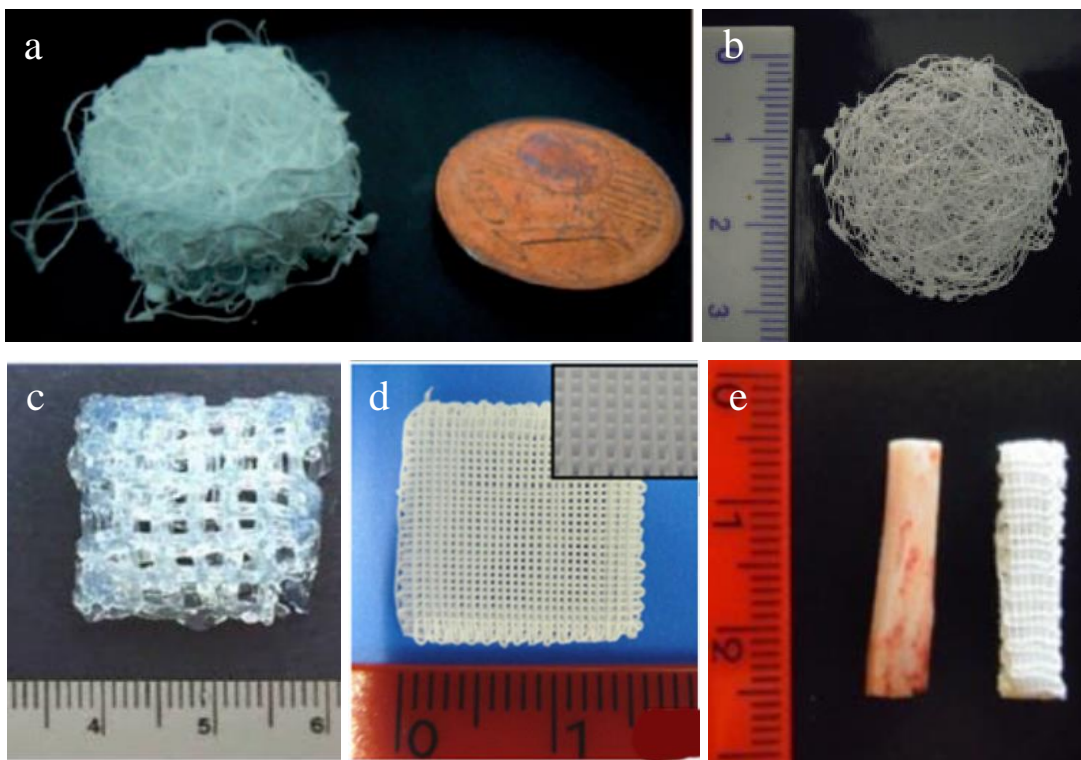


Figure 1.5. Wet spun scaffolds. Using traditional wet spinning setup a) (Puppi et al., 2011a), b) (Puppi et al., 2011b); using computer aided wet spinning setup c) (Puppi et al., 2016), d) (Puppi et al., 2012), e) (Dini et al., 2015).

Microfluidic systems are also used for the preparation of wet spun constructs where input of more than two solutions are required simultaneously. Alginate, calcium chloride and gelatin were introduced into a microfluidic channel (Hiramatsu et al.,

2016). The wet spinning of alginate was achieved by mixing it in calcium chloride solution, which ends up in gelled alginate fibers, containing gelatin. A step of glutaraldehyde immersion was administered to crosslink gelatin inside the alginate. Lastly, alginate layer was removed using alginate lyase enzyme to retrieve the fibers composed of crosslinked gelatin. Another study conducted for preparation of wet spun vertebra disc scaffold was carried out by using polysaccharide and silk fibroin (Zhang et al., 2015). Silk fibroin moieties formed globular structures when introduced into non-solvent solution of ethanol, which affected the morphology of fibers. The lowest concentration of introduced silk fibroin (1% w/v) provided highest stress resistance in this study. To modulate the degradation profile, alginate fibers were formed by submerging it into solution with calcium chloride in either distilled water or isopropyl alcohol (Mun et al., 2016). Spinning into isopropyl alcohol resulted in denser, more compact and aligned fibers, due to entrapment of more calcium ions into alginate fibers. Fibers spun into isopropyl alcohol showed less swelling and slower degradation profile too, in addition to showing a higher cell proliferation with respect to fibers spun into distilled water.

1.3. Drug Release in Bone Tissue Engineering

Release of biologically active molecules into bone tissue can be applied to (a) provide antibiotic effect, (b) provide cell differentiation cue, (c) provide cue for anabolism/catabolism of bone tissue constituents, etc. The idea behind release systems is to provide a prolonged release rather than having only initial burst release.

Prolonged release of:

- (a) Antibiotics – will eliminate any present germs in the region of interest, or any germs that may come from outside of region of interest (e.g. from neighboring tissues) (Diaz and Newman, 2015).
- (b) Cell differentiation cue – will drive the differentiation of stem cells nearby towards osteogenic lineage (e.g. BMP-2, BMP-7, etc.).
- (c) Provide cue for anabolism/catabolism – will help regeneration by presence of hormonal cues (i.e. thyroid/ parathyroid hormones, etc.).

Type of the released agent is as important as the release kinetics. There are different kinetic approaches for different requirements; zero order, first order, sustained release and burst release. Drugs that should not be introduced in large quantity (i.e. growth hormones) should be kept at low release rate with zero order release. The difference in kinetics of zero order and first order is that the zero order is expressed by drug quantity per time interval, whereas first order release is expressed as drug percent/ratio per time interval. In real life cases, generally zero order release occurs after an initial first order release. As an example, a drug reservoir of 100 mg, will start the release with first order kinetics (i.e. releasing 2% drug per min). This is done until the drug concentration has met the saturation/equilibrium. After the equilibrium is met, the drug release will be continued, but with zero order kinetics (i.e. releasing 1 mg drug per min). Sustained release has a slightly relaxed zero order kinetics, with less control over continuous steady drug release. Whereas burst release is release of high quantity of drug in the first seconds or minutes and then continued with less amount of released drug for following time points. Burst release is mostly used for drugs that can be administered in high quantity and do not have adverse effects.

Because of being a hard tissue with stiff structure, bone tissue remodeling and repair takes longer than other tissues. Even though it has a much expanded vessel network, the evading infection or fighting with it requires some remodeling in the occurring tissue. Antibiotics are drugs that are administered to fight infection. Bacterial infection can result in many different scenarios, where it ends in biofilm formation as shown in Figure 1.6 (Johnson and García, 2015).

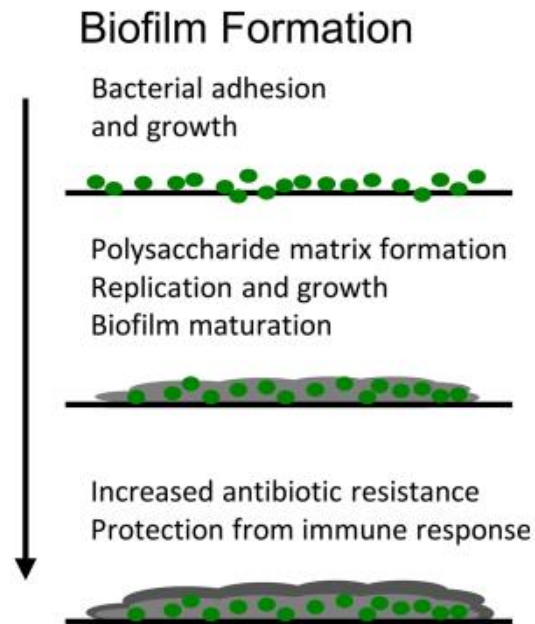


Figure 1.6. Biofilm formation (Johnson & García, 2015).

The formed biofilm protects itself from the environmental conditions and grows to infect more sites. For bone tissue, this is a threatening situation, since growth of biofilm on bone tissue would end up in weakening of bone structure. As numbers represent, 2-5% of implant procedures may end up with infection (Darouiche, 2004) and presence of open fractures will bring this number up to 30% (Trampuz and Widmer, 2006). Germs coming from neighboring tissues can manifest a surgical site infection, too (Diaz and Newman, 2015). Thus, it is important to provide an antibacterial regimen to the bone tissue that has been damaged or could be infected.

Microspheres are good delivery systems due to their high capacity carriage and high surface area to volume ratio. Gelatin microspheres have been used for their natural origin, swelling ability and controllable degradation kinetics by adjusting their crosslinking degree. Gelatin microspheres have already been tested *in situ*, *in vitro* and *in vivo*, previously (Sezer et al., 2013, 2014a, 2014b). Release kinetics of gelatin

microspheres depend on many factors, like chemistry and size of particles, types and amounts of the drugs and the crosslinkers:

(a) Kinetics of release from gelatin microspheres is faster if there is direct interaction of microspheres with release medium, rather than if the microspheres are entrapped inside a matrix material (Sezer et al., 2013),

(b) Smaller microspheres result in shorter release duration than larger microspheres (Ulubayram et al., 2005),

(c) Crosslinkers that hold the gelatin structure tighter (like genipin) result in longer release duration (García Cruz et al., 2013; Phromsopha and Baimark, 2014),

(d) Kinetics of release is directly proportional to the hydrophilicity of the drug used (Ulubayram et al., 2005).

1.4. Aim of Thesis

In this study, PCL-TCP wet spun scaffolds were prepared and modified by immobilizing gelatin and by adding antibiotic loaded gelatin microspheres onto the scaffolds, so that enhancement of cell attachment and prevention of bacterial invasion would be provided. Although there are some studies reported about wet spun PCL and HAp containing scaffolds (Puppi et al., 2011b, 2012), to best of our knowledge there is no PCL-TCP system modified with gelatin immobilization and with gelatin microspheres carrying an antibiotic. The scaffolds prepared were characterized for their morphology using scanning electron microscopy (SEM) imaging; mechanical properties using compressive force; chemistry using X-ray photoelectron spectroscopy (XPS); drug release abilities using UV-visible spectrophotometer and antimicrobial efficacies against *Escherichia coli* (*E. coli*), using disk diffusion test. Enhanced attachment of Saos-2 cells (human osteosarcoma cell line) and effective antimicrobial efficacy of these multifunctional scaffolds were expected in order to prove their suitability in bone tissue engineering and possible translation to *in vivo* applications.

CHAPTER 2

MATERIALS AND METHODS

2.1. Materials

Poly(ϵ -caprolactone) (PCL, $M_n=80.000$) (Aldrich, UK) and β -tricalcium phosphate (β -TCP) (Riedel-de Haen, Germany) were used in the preparation of scaffolds. β -TCP was ground, sieved and stored in a desiccator. Acrylic acid (AAc) (Fluka, Belgium), gelatin (Scharlau, Spain), N-hydroxysuccinimide (NHS) (Merck, Germany) and N-(3-dimethylaminopropyl)-N-ethylcarbodiimide hydrochloride (EDAC) (Sigma Aldrich, USA) were used for surface modification processes. Glutaraldehyde (GA) (Sigma, USA) was used as crosslinking agent. For *in vitro* degradation studies, lipase enzyme (Sigma, Switzerland) was used. As a model antibiotic, Ceftriaxone sodium (CS) (Nobel Kimya, Turkey) was used. Human osteosarcoma cell line (Saos-2) (ATCC, HTB-85), cultivated in McCoy's 5A medium (Lonza, Belgium), penicillin-streptomycin solution (pen/strep) (Hyclone, USA) and fetal calf serum (Hyclone, USA) were used for *in vitro* analysis. For storage and retrieval of cells, trypsin-ethylenediaminetetraacetic acid (Trypsin-EDTA) (Lonza, Sweden) and dimethyl sulfoxide (DMSO; Sigma Aldrich, USA) were used. *In vitro* characterization of biological samples were carried out by using cacodylic acid (Sigma, USA), para-formaldehyde (PFA) (Sigma Aldrich, USA), DAPI (Sigma, USA), Alexa 532 - Phalloidin and DRAQ5 (Sigma Aldrich, USA), Triton-X (AppliChem, USA) and Bovine Serum Albumin (BSA; Sigma, USA). For cell counting assays, Nucleocounter was used with its reagent A and reagent B (Chemometec, Denmark). Cell attachment and proliferation tests were carried out by AlamarBlue® (Invitrogen, USA) assay.

2.2. Preparation of Wet Spun PCL Scaffolds

In the preparation of PCL wet spun scaffolds, PCL solutions (20% w/v in acetone) were used (optimization of wet spinning setup can be found in Table A.1). For composite scaffolds, PCL solutions of same concentration (20% w/v in acetone) were mixed with β -TCP (10% or 20% w/w with respect to PCL) particles. The average size of β -TCP particles were found from particle size analysis (Malvern Mastersizer 2000, UK) (Appendix B) and SEM image analysis (FEI Quanta 400F; Holland).

Polymer solutions (PCL or β -TCP containing PCL) were degassed for 5-10 min in ultrasonic bath prior to wet spinning process, then spun with a syringe pump (New Era Pump Systems NE-300, USA) using glass syringe (Birgi, Turkey) and metal needles (gauge number of 23) (Hamilton, Switzerland). Wet-spinning system was prepared by placing the pump system in a vertical position in an elevated site as shown in Figure 2.1.



Figure 2.1. Wet spinning setup. Spinning of fiber (a) overall view, (b) zoomed side view and (c) zoomed top view.

Polymer solution was extruded into the coagulation bath (ethanol at 4 °C). For this process, the tip of the needle was placed in to the coagulation bath so that the tip was inside the solution ~3 mm. Flow rate of the polymer solution was adjusted to 0.8 mL/h and needle diameter was selected as 12.02 mm in syringe pump. The wet spinning process was preceded by rotating the beaker holding the coagulant solution of 80 mL to gather up the polymer poured through syringe needle. Volume of extruded polymer was detected by “dispensed volume” mark on the syringe pump. The produced fibrous meshes were placed in Teflon molds having two different heights (4 mm or 6 mm) with diameter of 10 mm. Produced scaffolds were kept in ethanol overnight at –20 °C and then dried under vacuum. After removing the remains of ethanol and acetone from the scaffolds, they were kept in a vacuum desiccator till further usage. Pure PCL scaffolds and the ones having 10% or 20% β -TCP particles were labelled as PCL, PCL-T₁₀ and PCL-T₂₀, respectively, and pure PCL scaffolds were used as control group in all experiments. Mechanical analysis were carried out using scaffolds having 6 mm height. All the other tests were achieved by using scaffolds having 4 mm height.

2.3. Characterization of the Wet Spun PCL Scaffolds

2.3.1. SEM Imaging

The microstructures and chemical structure of scaffolds were studied by Scanning Electron Microscope (SEM, FEI Quanta 400F; Holland) and Energy dispersive X-ray spectroscopy (EDX), respectively. To examine and quantify fiber thickness (n=40) and microsphere diameters (n=200), ImageJ software program (NIH, USA) was used.

2.3.2. Mechanical Analysis

Compression tests were performed on the scaffolds (h:6 mm; d:10 mm) using LLOYD® LRX 5K testing machine (LLOYD Instruments Limited, UK) with a cell load

of 100 N by the help of computer interface program of WindapR. Compression tests were applied with a speed of 1 mm/min. At least 5 samples were tested per each group. After each test, load (N) versus displacement (mm) graphs were obtained from which compressive strength at 50% strain (CS_{50}) and modulus of elasticity (M_E) values were calculated. Mechanical testing setup is shown below (Figure 2.2).

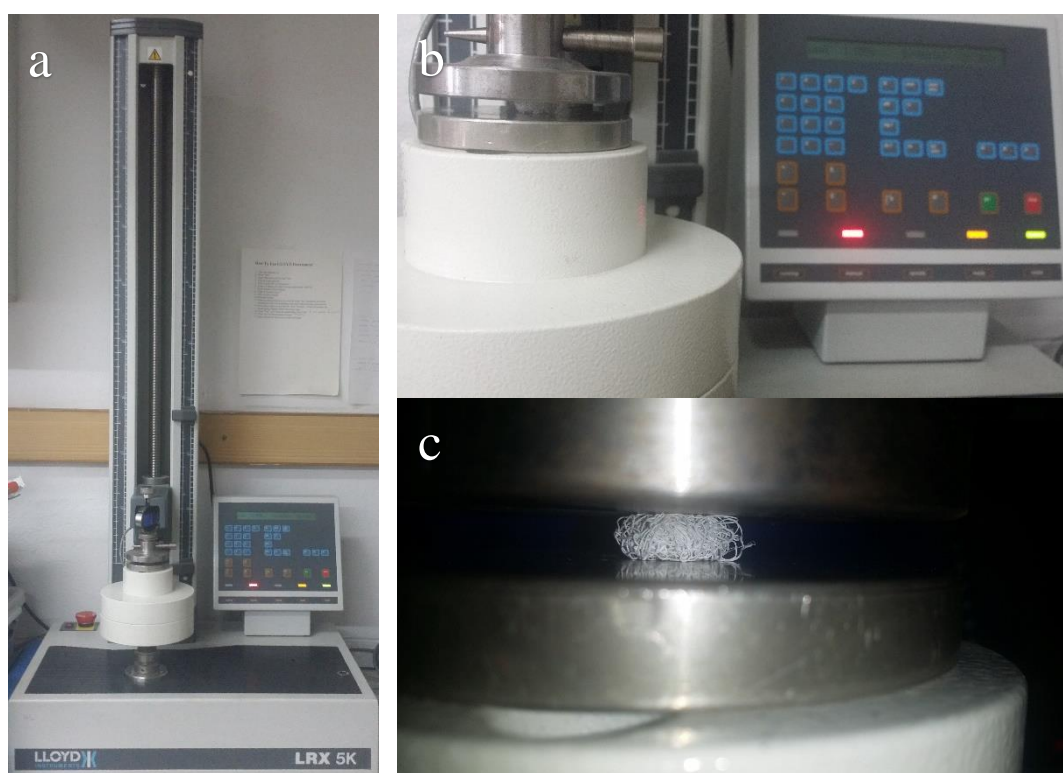


Figure 2.2. Mechanical test setup. (a) Mechanical tester, (b) sample holder and control panel, and (c) sample in compression test.

2.3.3. *In vitro* Degradation Studies

Enzymatic degradation of the scaffolds was investigated in lipase solution (0.18 U/mL) prepared in PBS (0.01 M, pH=7.4) according to ASTM standard no.F1635.5246 (Martins et al., 2009). Sodium azide (0.02% w/v) was added into the medium to inhibit any bacterial growth. The scaffolds (h=4 mm; d=10 mm) were incubated in 5 mL of this solution (having 0.18 U/mL lipase and 0.02% w/v sodium

azide) at 37 °C in a shaking water bath. The average weights of the samples were 32.5 ± 2.5 mg. At certain time points, the scaffolds were removed from the solution, frozen, lyophilized and weighed. Percent weight loss was calculated from the gravimetric measurements, using equation 1:

$$\text{Weight loss (\%)} = \frac{W_0 - W_1}{W_0} \times 100 \dots \dots \dots [1]$$

Where W_0 = Initial weight; and W_1 = Weight after degradation

Degradation analyses were performed with 4 samples for each group. Meanwhile, the samples were examined with SEM at the end of 30 days of lipase treatment.

2.4. Surface Modification of Wet Spun Scaffolds

The scaffolds were activated with acrylic acid (AAc) to link gelatin covalently on the surfaces of the fibers. After the immobilization of gelatin on the surface of the fibers, gelatin microspheres loaded with drug were attached on the scaffolds.

2.4.1. Surface Activation with Acrylic Acid

Surface activation with AAc and further gelatin immobilization was applied only to PCL-T₂₀ scaffolds. These samples were activated with oxygen plasma by applying 100 W power for 5 min with a flow supplying 50 mTorr inside pressure (Advanced Plasma Systems Inc. SerenR300, 13.56 MHz RF Power Generator, USA) as described previously (Yildirim et al., 2005; Endogan et al., 2012). The plasma reactor is a cylindrical parallel plate chamber with a 15 cm distance between two electrodes (Figure 2.3).



Figure 2.3. Oxygen plasma instrument.

Samples were placed inside the reactor, vacuum was applied till the inside pressure drops to 50 mTorr and then glow discharge was applied having 100W power. After 5 min, the power was turned off and samples were kept inside the chamber subjected to O₂ environment for 15 more minutes. Then, the samples were immersed in acrylic acid (AAc) solution (prepared in methanol:dH₂O:AAc = 7:28:15 v/v) for 1 h while nitrogen gas was purged through the solution. The scaffolds were left overnight in this solution at 37 °C, then washed with distilled water and dried at room temperature (RT) (Gupta et al., 2012). The scaffolds treated with AAc were labelled as PCL-T₂₀A. Schematic view of grafting steps are shown in Figure 2.4 and the setup in Figure 2.5.

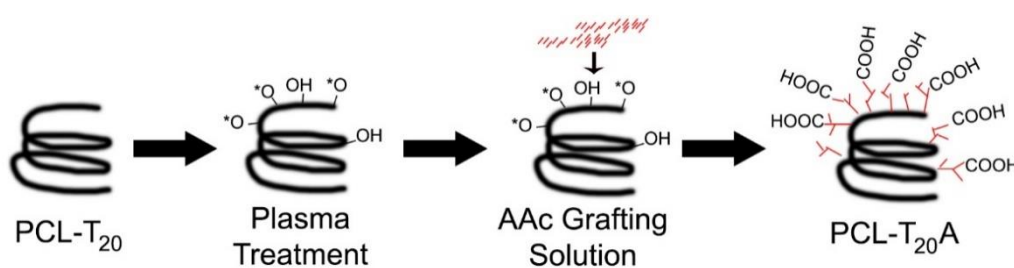


Figure 2.4. Acrylic acid grafting procedure on PCL-T₂₀ scaffolds.

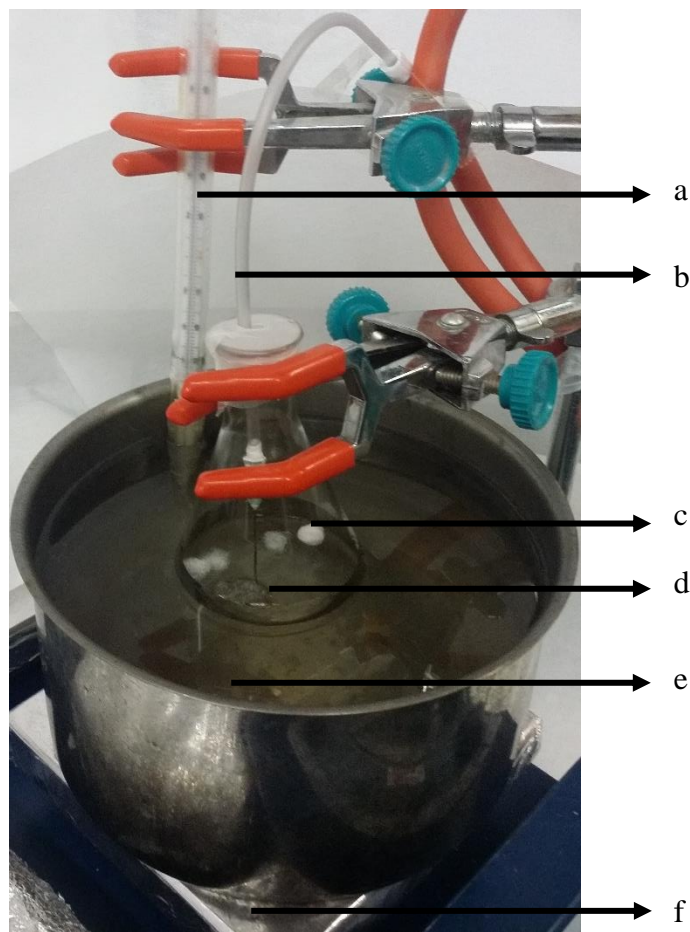


Figure 2.5. Acrylic acid grafting setup. (a) Thermometer, (b) tube for nitrogen gas purging, (c) samples in grafting solution, (d) nitrogen gas bubbles, (e) water bath, and (f) heater.

Degree of AAc grafting was determined by Toluidine Blue O (TBO) assay (Gupta et al., 2012). For this purpose, the scaffolds were treated with TBO (Sigma Aldrich, USA) solution (1 mL; 0.5 mM TBO prepared in deionized water (DI H₂O)), pH 10 was adjusted with NaOH (0.1 M), and scaffolds were kept in this solution for 4 h at 50 °C. Then, the scaffolds were removed, washed with NaOH solution (1 mL; 0.1 M NaOH prepared in DI H₂O; pH=9) to remove unbound TBO. Later on, scaffolds were treated with 1 mL 50% v/v acetic acid solution in order to remove the grafted acrylic

acid from the scaffolds, and the absorbance of this solution was measured at $\lambda=624$ nm with UV-Vis Spectrophotometer (Agilent, Germany). Grafting degree was calculated by referring to the constructed calibration curve.

Calibration curve was constructed by firstly preparing 50 mM TBO in DI H₂O (pH=9 adjusted by NaOH) at 50 °C. After that, the solution was diluted to several different concentrations as 2.5 mM, 5 mM, 10 mM and 20 mM TBO in DI H₂O. Then, the absorbance of the solutions was measured at $\lambda=624$ nm with UV-Vis Spectrophotometer. After constructing curve, the slope of the curve was calculated by creating a trendline over the curve. The equation of the curve was used for calculation of molarity of TBO in the samples (APPENDIX C, Figure C.1).

2.4.2. Surface Modification with Gelatin

Gelatin immobilization was applied only to PCL-T₂₀A scaffolds following the procedure described earlier by Krishnanand et al (Krishnanand et al., 2013) (Figure 2.6). Briefly, scaffolds were immersed into citrate buffer (CB; 1 mL; pH=4.8) solution having EDAC (1% w/v) and NHS (1% w/v) for 24 h at 4 °C. Then they were removed, rinsed with distilled water, and incubated in gelatin solution (1 mL; 0.3% w/v) prepared in phosphate buffer (PBS, 0.01 M, pH=7.4) for 24 h. Later on, scaffolds were removed, rinsed with distilled water and dried in vacuum oven at RT. These gelatin immobilized scaffolds were labelled as PCL-T₂₀G.

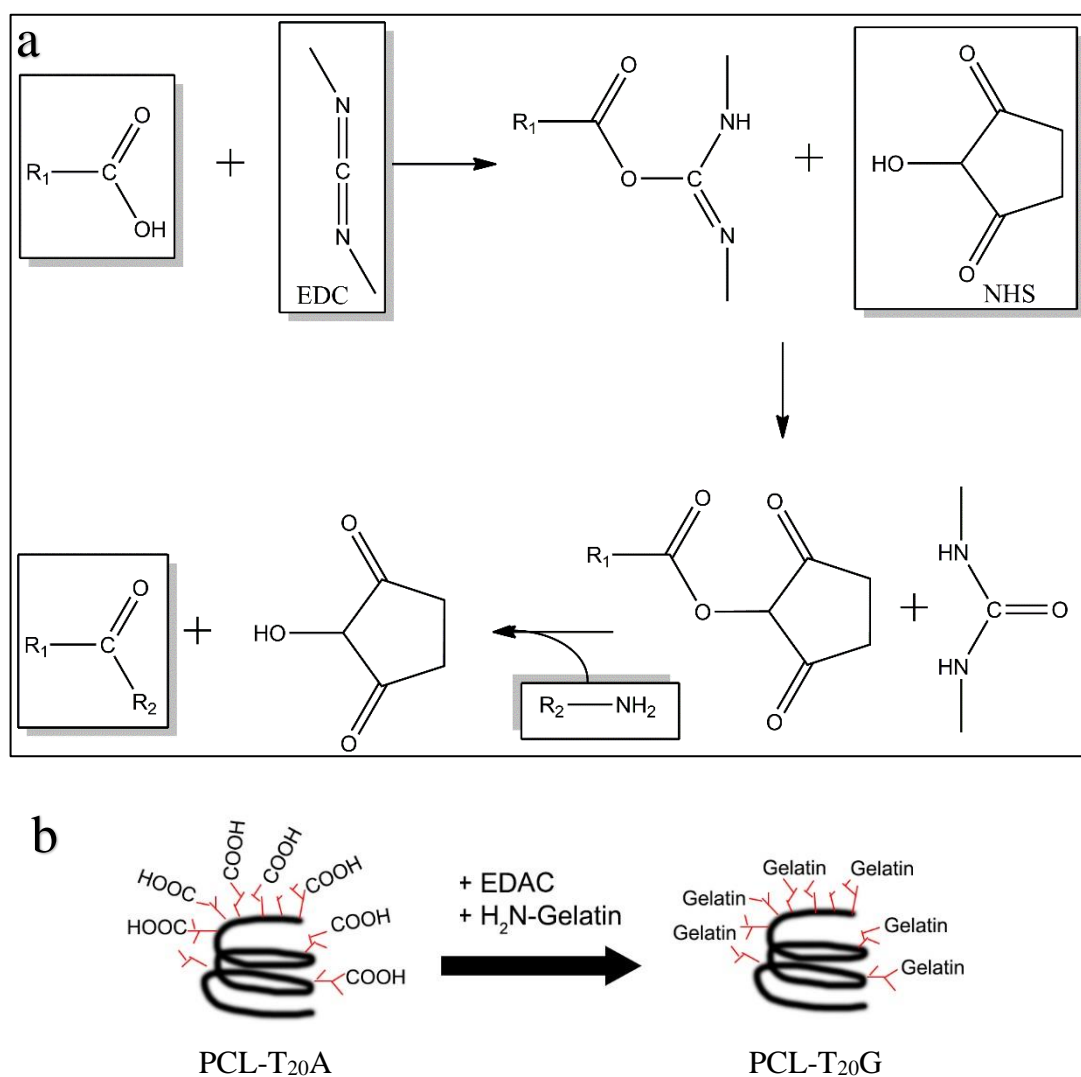


Figure 2.6. Gelatin immobilization. (a) Illustration of EDAC/NCS coupling and (b) scheme of gelatin coupling onto PCL-T₂₀A scaffolds.

2.4.3. XPS Analysis

X-Ray Photoelectron Spectroscopy (XPS, PHI 5000 VersaProbe; Chigasaki, Japan) was used to determine the presence of nitrogen due to gelatin immobilization on the scaffolds. After the survey analysis of 1 cps/eV, regional scanning with 10 cps/eV was applied. Carbon (C1s) and Oxygen (O1s) peak fitting was performed on regionally scanned XPS spectra by using XPSPEAK 4.1 software (Informer Technologies) and corrected with respect to aliphatic carbon levels at 285 eV.

2.4.4. Porosity of Wet Spun Scaffolds

For calculation of porosity of the scaffolds two different approaches were used; (a) using Mercury Intrusion Porosimetry (Quartachrome Poremaster 60; Florida, USA) and Helium Pycnometer (Quantochrome Ultrapycnometer 1000; Florida, USA), (b) using Micro-CT (micro-Computed Tomography) (Bruker microCT, SkyScan 1172; Belgium).

Since direct porosity calculation of soft samples is not possible using mercury intrusion porosimetry, a formula estimating the percent porosity was applied in approach (a). For this approach, first the ‘actual density’ (AD; in g/cm³) of the sample was obtained from helium pycnometer, and then ‘visible density’ (VD) was evaluated from mercury intrusion porosimetry data. Percent porosity of the sample was calculated by using the following formulas 2 and 3:

$$VD \text{ (g/cm}^3\text{)} = \frac{\text{sample weight (g)}}{\text{Volume of mercury in the sample (cm}^3\text{)}} \dots\dots\dots [2]$$

$$\text{Porosity (\%)} = \left[1 - \left(\frac{VD}{AD} \right) \right] \times 100 \dots\dots\dots [3]$$

For approach (b), microCT (Bruker microCT, SkyScan 1172; Belgium) evaluation was achieved by calculating porosity of 250 μm sections obtained from top, center and bottom of the scaffolds and combining them in one average porosity value. Porosity values were determined by the device for each section by calculating the void areas inside scaffold.

2.4.5. Preparation of Gelatin Microspheres (GM) and GM Containing Scaffolds

Gelatin microspheres (GM) were prepared by following the procedure reported previously by our group (Ulubayram et al., 2005; Sezer et al., 2013, 2014b). Shortly, aqueous gelatin solution (1 mL; 10% w/v) was added dropwise into corn oil (60 mL) with continuous mechanical stirring (2200 rpm) for 30 min. Then, glutaraldehyde (2 mL, 2% v/v) was added dropwise as crosslinker agent, mixed for further 20 min, cooled to 4 °C, washed with acetone, filtered and the obtained microspheres were dried at RT. For the preparation of Ceftriaxone sodium (CS) containing microsphere, CS was added into the gelatin solution to get the final drug concentration of 80 mM.

Three values as; (a) Percent yield , (b) Percent drug loading and (c) Percent entrapment efficiency were calculated for the drug loaded microspheres from the following formulas 4, 5 and 6 (Ding et al., 2010; Petkar, 2013):

$$\text{a) Yield (\%)} = \frac{\text{Weight of microspheres recovered}}{\text{Weight of drug + polymer added initially}} \times 100 \dots \dots [4]$$

$$\text{b) Drug Loading (\%)} = \frac{\text{Weight of drug in microspheres}}{\text{Weight of microspheres}} \times 100 \dots \dots [5]$$

$$\text{c) Entrapment Efficiency (\%)} = \frac{\text{Weight of drug in microspheres}}{\text{Weight of drug fed initially}} \times 100 \dots [6]$$

Afterwards, particles were examined with SEM (FEI Quanta 400F; Holland), light microscopy (Zeiss Axio Imager M2, Germany) and particle size analyser (Malvern Mastersizer 2000, UK).

For the preparation of GM containing scaffolds, 10 mg of these microspheres were dispersed in pure ethanol and added dropwise on PCL-T₂₀G scaffolds with

application of vacuum-pressure cycle after each drop. Scaffolds having gelatin microspheres are labelled as PCL-T₂₀GM (Figure 2.7):

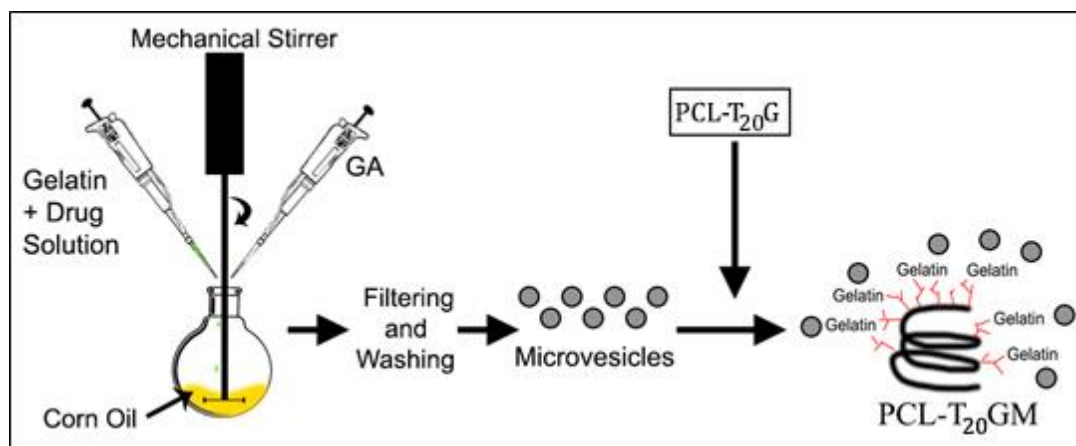


Figure 2.7. Microsphere preparation, loading and adsorption on the scaffolds.

Percent attachment efficiency (AE, %) of microspheres on to scaffolds was calculated from the released CS amounts. For this purpose, ratio of released CS values from 10 mg of drug loaded gelatin microspheres (GM) and PCL-T₂₀GM scaffolds treated with 10 mg of microspheres were considered in the equation 7 given below:

$$AE (\%) = \{ [\text{Release from PCL-T}_{20}\text{GM}] / [\text{Release from GM}] \} \times 100 \dots [7]$$

2.4.6. *In vitro* Drug Release

Amount of the Ceftriaxone sodium (CS) released from microspheres was determined by UV-Visible Spectrophotometer (Agilent, Germany). For release experiments, CS-loaded microspheres (10 g) and PCL-T₂₀GM (scaffolds carrying 10 g CS-loaded microspheres) were put in separate dialysis bags (dialysis tubing, 8.000 MWCO; Thermo scientific, USA) and immersed in 5 mL of PBS (0.01 M, pH=7.4) solution. The overall setup was placed in a water bath at 37 °C. At certain time points, the

dialysis bags were removed and immersed in 5 mL of fresh PBS medium. The released amount of drug was determined by measuring the absorbance of the solution at 270 nm (calibration curve of Ceftriaxone Sodium can be found in APPENDIX D, Figure D.1). Percent release values were calculated by assuming the maximum released amount as the total drug amount. Drug release studies were carried out as triplicates for each group.

For constructing calibration curve, 50 mg/mL CS solutions was prepared in PBS solution. After dissolution, different concentrations of CS solutions were prepared as 1 mg/mL, 2.5 mg/mL, 5 mg/mL, 10 mg/mL, 20 mg/mL and 25 mg/mL. Then, the absorbance of these solutions were measured using UV-Vis Spectrophotometer at $\lambda=270$ nm. After constructing a curve, its trendline was found and equation of trendline was used to find out amount of CS in sample solutions.

2.4.7. Antibacterial Test

To evaluate the antibacterial efficacy of the drug released from scaffolds, disc diffusion method was conducted as explained in our previous studies (Ucar et al., 2013, 2016). For this test, ceftriaxone sodium (CS), a potent gram-negative antibacterial agent, was used and its antibacterial efficiency on *E. coli*, model gram-negative bacteria, was determined. For this test, first, *E. coli* was spread on culture plates by cotton swabs and the prepared scaffolds (10 mm in diameter) were placed onto the plates as shown in Figure 2.8. The antibacterial efficiency was estimated by the diameter of the area of inhibition of bacterial growth around samples. As positive control, standard CS susceptibility discs (6 mm in diameter); as negative control, PCL-T₂₀ scaffolds (having no microspheres and drug) were used.

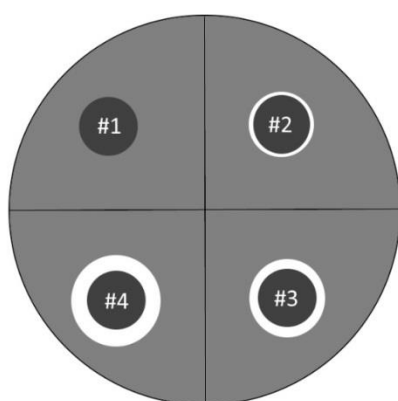


Figure 2.8. An example of disk diffusion result. Here, we can see #1: negative control (without drug), #4: positive control (antibiotic susceptibility disc), #2 and #3: samples loaded with different amount of antibiotics.

2.5. *In vitro* Cell Culture Tests

Scaffolds (h: 4 mm, d: 10 mm) were placed in 24-well plates and 70% ethanol was added. They were kept in 70% ethanol for 2 h for disinfection and then washed 3 times with PBS and left to dry under laminar flow. Two cell culture mediums were prepared, as (i) proliferative cell culture medium; containing McCoy's 5A medium (89%) supplemented with fetal calf serum (10%) and 100 U/mL penicillin and 100 µg/mL streptomycin (1%), and (ii) osteogenic cell culture medium; having additional β-glycerophosphate (2.16 g/L), dexamethasone (10 nM) and L-ascorbic acid (50 mg/L). Saos-2 cells (p.23) at confluence were harvested from tissue culture flasks with 0.1% trypsin / 10 mM EDTA, centrifuged, and resuspended in medium prior to cell seeding. After counting cells (cell number/mL) by nucleocounter, a cell suspension containing 2.5×10^5 cells were seeded on each sample and incubated for 30 min at 37 °C to allow cell attachment. Then, after 30 min, 50 µL of proliferative cell culture medium was added on each well. This was repeated 5 more times for each 30 min after seeding. After 3 h, cell culture medium was completed to 1 mL by addition of 700 µL proliferative cell culture medium. After 3 days of incubation, medium was changed to osteogenic cell culture medium and the cells were incubated for another 25 days in osteogenic cell culture medium (cell culture mediums were

changed every 2 days). Cells attached on scaffolds were evaluated by SEM analysis and Confocal Laser Scanning Microscopy (CLSM) (Leica DM2500, Germany).

2.5.1. Cell Viability

Cell proliferation efficiency was determined by AlamarBlue® assay using Elisa Plate Reader (Molecular Devices, USA). When entering cells, active part of Alamar Blue dye, resazurin, is getting reduced inside the cells to resorufin (Figure 2.9.a), due to the redox chain in oxidative phosphorylation cascade in mitochondria of cells (Markaki, 2009). AlamarBlue® does not harm cells, because it does not stop the electron transport chain as shown in Figure 2.9.b.

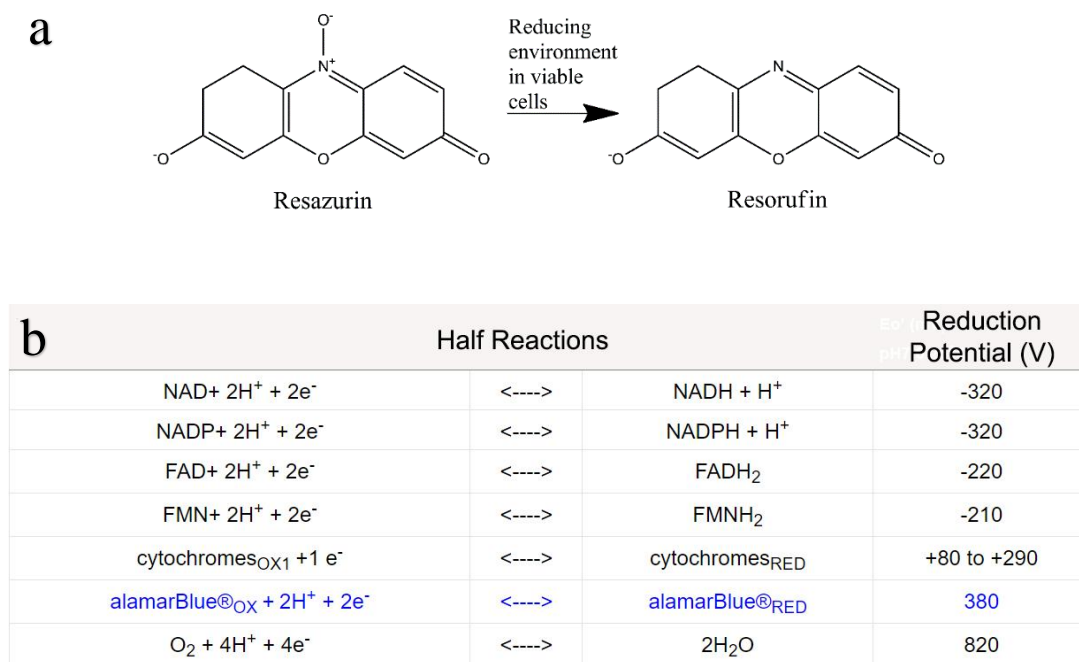


Figure 2.9. AlamarBlue® mechanism. (a) AlamarBlue® reduction inside cell, (b) reduction potential of alamarBlue® and other steps in oxidative phosphorylation.

To be able to correlate the absorbance values to the cell number on the scaffolds, firstly a calibration curve was constructed. Calibration curve of Saos-2 cells was conducted by treating the seeded cells 10.000 to 120.000 with Alamar Blue solution (1% pen-strep, 10% Alamar Blue, 89% colorless DMEM high modified medium). The solutions were left in CO₂ incubator at 37 °C for 1 h. After 1 h of incubation, 200 μL of solution from each well was transferred to 96 well plate in dark environment and immediately the well plate was transferred to Elisa Plate Reader. The percent reduction of resazurin was calculated from the absorbance values at 570 nm (λ_1) for resazurin and 595 nm (λ_2) for resorufin and putting the results into the equation 8 shown below:

$$\text{Reduced \%} = \frac{((\epsilon_{\text{ox}})_{\lambda_2} * A_{\lambda_1}) - ((\epsilon_{\text{ox}})_{\lambda_1} * A_{\lambda_2})}{((\epsilon_{\text{red}})_{\lambda_1} * A'_{\lambda_2}) - ((\epsilon_{\text{red}})_{\lambda_2} * A'_{\lambda_1})} * 100 \dots \dots \dots [8]$$

Where;

A → Absorbance of the sample solution

A' → Absorbance of negative control well solution (blank)

ϵ_{ox} → Molar extinction coefficient of oxidized Alamar Blue

ϵ_{red} → Molar extinction coefficient of reduced Alamar Blue

After getting the percent reduced Alamar Blue for the groups, the calibration curve was constructed (APPENDIX E, Figure E.1), and its slope was calculated from trendline for measuring cell number.

Same Alamar reduction test was conducted for the samples. For this purpose, scaffolds were treated with Alamar Blue solution for 1 h in a CO₂ incubator at 37 °C and then the same procedure given for calibration groups were followed. After calculating the percent reduced Alamar Blue, cell number was quantified from the slope value attained from the calibration curve.

2.5.2. Morphological Characterization of *In vitro* Cell Culture Tests

To examine the morphology of the cells on the scaffolds, SEM images were obtained from the fixated scaffold samples. To find out the cytoskeletal state and nuclear location of attached cells, also CLSM imaging was done.

2.5.2.1. SEM Imaging

Cells attached on scaffolds were evaluated by SEM analysis. For this purpose, scaffolds were removed from the cell growth culture media after 28 days of incubation, washed once with PBS and once with cacodylate buffer (0.1 M sodium cacodylate, pH 7.4) and cell fixation was performed by treating the samples with GA (0.5 mL, 2.5% v/v in cacodylate buffer) for 45 min. Later on, the scaffolds were left in -80 °C freezer overnight and then lyophilized by freeze dryer (Labconco, USA) the next day and the dry scaffolds were coated with gold/palladium prior to SEM analysis.

2.5.2.2. Confocal Laser Scanning Microscopy

Scaffolds were examined by confocal laser scanning microscopy (CLSM; Leica TCS SPE, Turkey) to detect cells' conformation using Alexa Fluor 532-phalloidin (for cytoskeleton) and DRAQ5 (for nucleus) dyes. For these studies, scaffolds were firstly washed with PBS (0.01 M, pH = 7.4) twice and fixed with PFA (4% w/v in dH₂O) for 30 min at RT. Then, scaffolds were washed again with PBS. To permeabilize cells, samples were treated with Triton X-100 solution (0.5 mL; 1% v/v in dH₂O) for 5 min at RT. Then, scaffolds were again washed with PBS, and treated with 1 mL of 1% w/v BSA: PBS solution for 30 min at 37 °C, to block non-specific binding of phalloidin (added in next step). Scaffolds were then put in 1 mL of 1:100 Alexa-labeled phalloidin solution and kept in the solution for 1 h at 37 °C. Then, scaffolds were washed with 1 mL PBS twice and treated with 0.5 mL of 1:1000 DRAQ5 solution for 30 min at 37 °C. Later on, the samples were washed with 1 mL PBS twice

again, and put into 0.5 mL of 1:5000 DAPI: BSA solution (prepared in PBS) and left at RT for 5 min. DAPI was used to color the nuclei and to detect it with fluorescent microscopy. Afterwards, scaffolds were washed with 1 mL PBS twice again and kept in 0.5 mL of PBS solution (to keep the scaffolds moist before proceeding to confocal microscopy). Excitation wavelengths of 350, 532 and 633 nm were used for DAPI, Alexa, and DRAQ5 dyes, respectively. Auto fluorescence signals caused by gelatin were gathered with the one coming from Alexa in two separate channels and overlaid with LAS AF software.

2.6. Statistical Analysis

The quantitative results throughout the study were expressed as mean and standard deviation from at least three repetitions. Statistical analysis of data was performed with significant values defined as $p < 0.05$, based on one-way analysis of variance (ANOVA) followed by Tukey's post-hoc HSD test for determination of the significance of difference between the groups examined.

CHAPTER 3

RESULTS and DISCUSSION

3.1. Optimization of Wet Spinning Process

In the preparation of wet spun scaffolds, several parameters such as different polymer concentrations, molecular weights of PCL, temperature, solvent/non-solvent pair were tested. Output was evaluated by the gross morphology, uniformity and elasticity of the extruded fibers. Two poly(ϵ -caprolactone) (PCL) were used with different molecular weights, $M_n=60.000$ and $M_n=80.000$. Many solvent/non-solvent pairs were tested. As plasticizer, to increase the solubility and homogeneity of polymer solution, three different polymers were tested: poly(ethylene glycol), poly(L-lactic-co-glycolic acid) and chitosan. Two ambient temperature for coagulation bath was tested, room temperature and in ice bath (at 4 °C). Different flow rates were tested to get long and smooth fibers. All these optimization studies of wet spinning process are given in APPENDIX A, Table A.1. At the end of all these studies, PCL ($M_n=80.000$), acetone, ethanol, 4 °C and 0.8 mL/h were chosen as the polymer, solvent, non-solvent, ambient temperature and flow rate, respectively.

3.2. Characterization of Scaffolds

In this study, PCL based wet spun fibrous scaffolds were prepared by using either PCL solution, or PCL solution containing β -TCP particles (10% and 20% w/w). Properties such as morphological, physical, chemical, mechanical, degradation and porosity were determined by using SEM, XPS, mechanical tester and micro-CT.

3.2.1. Morphological Analysis

β -TCP particles obtained from Riedel-de-Haen were ground and sieved while their size decreased from millimeters to nanometers (Figure 3.1). Nano size particles mixed with polymer homogenously and extruded easily through needle used in injection of the polymer solution. β -TCP was chosen since this mineral would provide an osteoinduction activation in the scaffolds (Albrektsson and Johansson, 2001). The osteoinduction of β -TCP particles was observed and reported by several researchers (Choi and Kim, 2012; Polo-Corrales et al., 2014; Metoki et al., 2016). This shows that as the amount of calcium phosphate mineral increases, osteoinduction effect also increases. In order to examine the effect of β -TCP on fiber structure and on mechanical properties, scaffolds were prepared as follows: (a) no β -TCP (control group), (b) maximum amount of β -TCP possible for extrusion (20% w/w), and (c) moderate amount of β -TCP (10% w/w, having half the concentration of that of maximum possible).

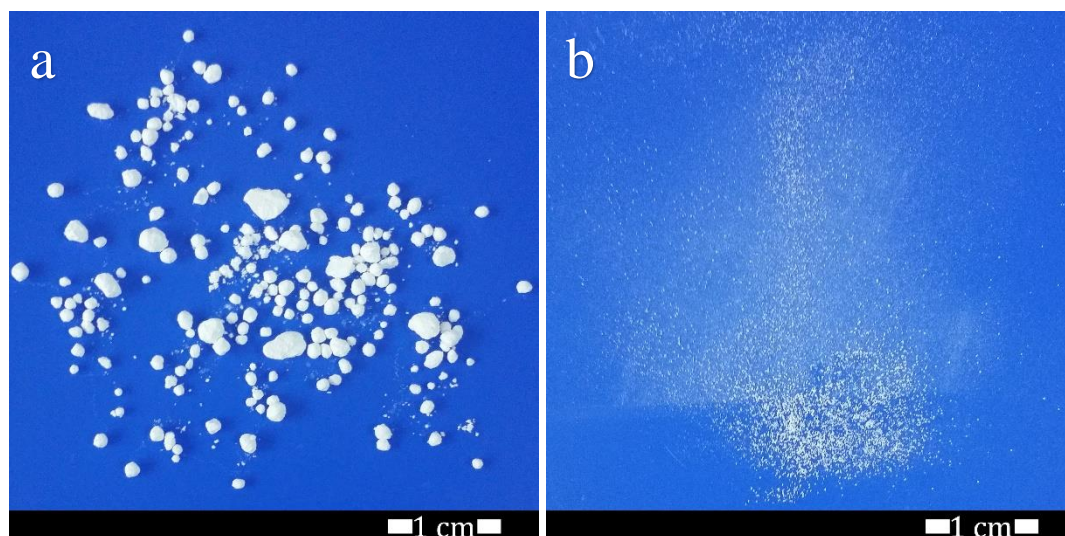


Figure 3.1. Morphology of β -TCP particles. (a) Before and (b) after grinding and sieving procedure.

The average size of grinded and sieved β -TCP particles was found to be $4.95 \mu\text{m}$ when measured by particle size analyser on aqueous media. Particle size analysis results of ground and sieved β -TCP particles are shown in APPENDIX B (Figure B.1). Before grinding it by pestle and mortar, sizes of β -TCP particles were in millimeter scale. After grinding and eliminating big particles by sieving through $125 \mu\text{m}$ sieve and then a $53 \mu\text{m}$ sieve, the β -TCP particles were in several μm scale. Due to their small size, they would distribute homogeneously through wet-spun fibers, and would not be entrapped in the nozzle of needle, thus providing a smooth drop of the fiber into the coagulation bath.

Wet spun scaffolds (PCL, PCL-T₁₀ and PCL-T₂₀) and β -TCP particles were examined by SEM and EDX. Scaffolds had proper accumulation of fibers with smooth surfaces as shown in Figure 3.2, where photograph (Figure 3.2.a) and SEM images (Figure 3.2.c) are given. Average diameter of wet spun fibers were $200 \pm 15 \mu\text{m}$ (n=40) obtained by application of ImageJ analysis. Meanwhile, the average size of β -TCP particles obtained from SEM images (using ImageJ, n=120) was found to be $145 \pm 26 \text{ nm}$ (Figure 3.2.b). On the other hand, the average size (D[4,3]; volume-weighted average size) was found as $4.95 \mu\text{m}$ when measured by particle sizer (Malvern Mastersizer 2000, UK) using the aqueous dispersion of the particles. This high value (about 34 fold increase) is most probably due to aggregation of the particles in aqueous medium. As it can be seen clearly in SEM image, the particles were much smaller than micron size and they were in nano size.

Fibers of β -TCP containing PCL scaffolds also had very smooth surfaces and presence of nanometer size β -TCP particles did not cause significant roughness on the surfaces (Figure 3.2.d-e). EDX analysis showed that calcium ions, which proves the existence of β -TCP particles in the scaffolds, were not present in PCL scaffolds (Figure 3.2.f), but detected in PCL-T₁₀ and PCL-T₂₀ scaffolds, as expected (Figure 3.2.g-h).

The diameter of the fibers were found to be around 200 μm (n=40) for wet spun scaffolds. In literature, diameters in the range of 100-350 μm were reported for wet spun fibers of PCL, starch-PCL, and PCL-HAp (Tuzlakoglu et al., 2010; Puppi et al., 2011a, 2011b) depending on the composition as well as the preparation process.

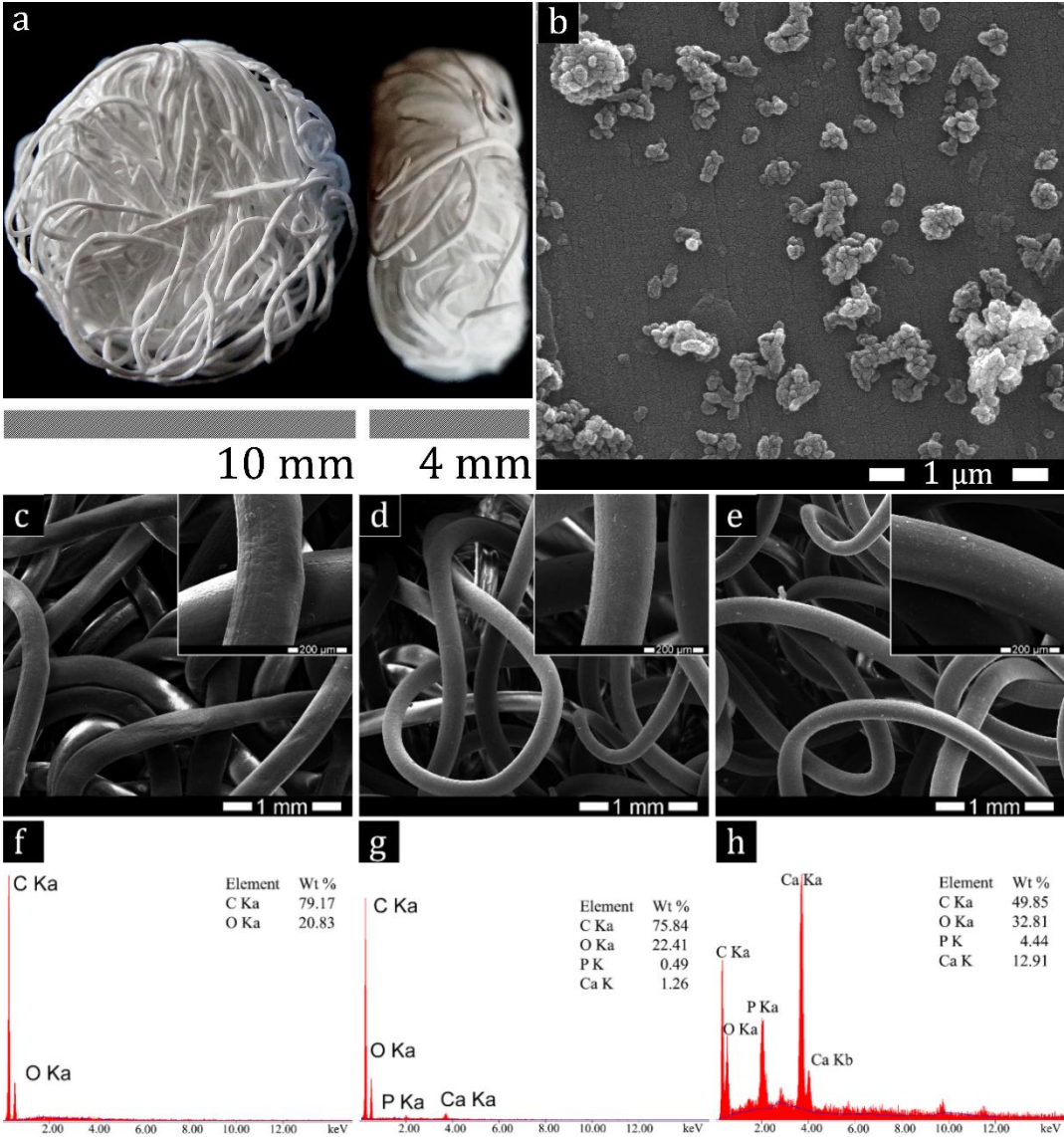


Figure 3.2. Images and elemental compositions of scaffolds. (a) Photograph of wet spun scaffolds. SEM images of (b) β -TCP (100000x), (c) PCL (100x, inset 500x), (d) PCL-T₁₀ (100x, inset 500x), (e) PCL-T₂₀ (100x, inset 500x) scaffolds. EDX analysis of (f) PCL, (g) PCL-T₁₀ and (h) PCL-T₂₀ scaffolds (scale bar for insets is 200 μm).

3.2.2. Mechanical Analysis

For bone tissue engineering applications, mechanical properties of the implant has utmost importance, since any inconsistency in this issue and in the pressure that the implant creates on the bone results in break of implant, necrosis and loss of tissue. Therefore, addition of inorganic materials as hydroxyapatite (HAp) or β -tricalcium phosphate (β -TCP) into the polymeric structures is commonly applied to enhance mechanical properties as well as affinity for the cells.

In this study, incorporation of β -TCP particles into the PCL solution increased mechanical strength and modulus of elasticity of PCL scaffolds obtained by wet spinning process (Figure 3.3.a). Compression tests were carried out for PCL scaffolds, and compressive strength at 50% strain (CS_{50}) and modulus of elasticity (M_E) values were found as 360 ± 40 kPa and 205 ± 40 kPa, respectively. These values increased about 1.2 fold (~20%) for PCL-T₁₀ (440 ± 60 kPa and 250 ± 15 kPa, respectively) and about 1.5 fold (~50%) for PCL-T₂₀ (485 ± 60 kPa and 355 ± 10 kPa, respectively) scaffolds as shown in Figure 3.3.b and Table 3.1.

Statistical analysis showed that PCL-T₂₀ scaffolds had significantly higher M_E than both PCL-T₁₀ and pure PCL scaffolds ($p < 0.05$ for both), whereas the increase in M_E for PCL-T₁₀ scaffolds was not significantly higher than that of pure PCL ($p > 0.05$). PCL-T₂₀ scaffolds also had significantly higher CS_{50} than pure PCL scaffolds ($p < 0.05$), whereas that difference was not significant between PCL-T₁₀ and pure PCL or PCL-T₁₀ and PCL-T₂₀ scaffolds ($p > 0.05$ for both).

Table 3.1. Mechanical test results.

Sample	Compressive Strength at 50% Strain (CS_{50}) (kPa)	Modulus of Elasticity (M_E) (kPa)
PCL	360 ± 40	205 ± 40
PCL-T ₁₀	440 ± 60	250 ± 15
PCL-T ₂₀	485 ± 60	355 ± 10

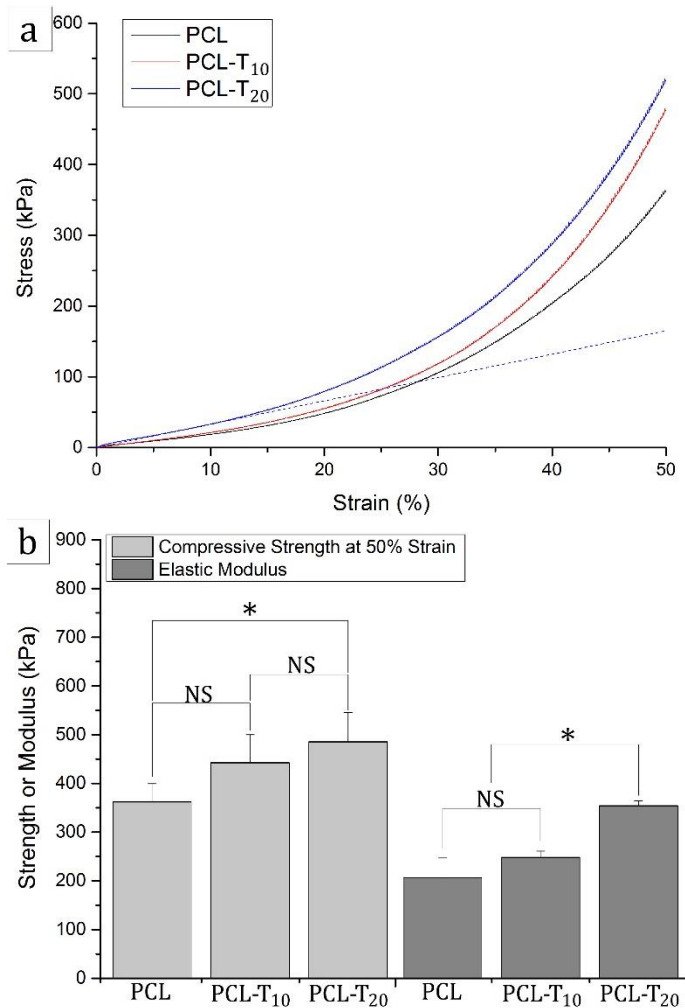


Figure 3.3. Mechanical test results. (a) Representative mechanical curves (dotted line is a representative slope of PCL-T₂₀) and (b) Compressive mechanical properties of PCL, PCL-T₁₀ and PCL-T₂₀ scaffolds (NS means ‘not significant’, $p > 0.05$; * means $p < 0.05$).

In literature it was reported that addition of 10% and 20% β -TCP into PCL scaffolds prepared by solid freeform fabrication, increased M_E value 1.1 and 1.3 fold, respectively, compared to pure PCL scaffolds (Mondrinos et al., 2006). Similarly, these values were reported as 2.1 and 2.6 folds for 3D printed PCL scaffolds (Lu et al., 2012). The increase in M_E values by addition of β -TCP in our study was not as high as it was reported for 3D printed scaffolds (Lu et al., 2012). This can be explained by the less ordered organization of wet spun fibers compared to highly

organized 3D printed ones. Meanwhile, the increase in M_E values in our study was higher than solid freeform fabricated scaffolds, due to more integrated structures compared to freeform fabricated scaffolds. Mechanical moduli of scaffolds applied for bone healing purposes were proposed to have values at least in 100-500 kPa range (Murphy et al., 2013; Polo-Corrales et al., 2014), for cells to differentiate towards osteogenic lineage due to effect of mechanical stimulation. Thus, the PCL (205 kPa), PCL-T₁₀ (250 kPa) and PCL-T₂₀ (355 kPa) samples prepared in this study match the required moduli for mechanical stimulation. Compressive strength of scaffolds at 50% strain was in the range of 360-485 kPa, which shows higher values than previously reported freeze dried PCL scaffolds (Sezer et al., 2013) and coincides with the ones for additive manufacturing-wet spun PCL scaffolds, which were found to be in the range of 260-470 kPa (Puppi et al., 2012). For insignificant difference in mechanical properties between PCL-T₁₀ and the control group PCL, further experiments (as surface modification, gelatin immobilization and microsphere addition) were performed with PCL-T₂₀ scaffolds.

3.2.3. *In vitro* Degradation Results

PCL is quite stable in aqueous media but degrades slowly in biological media. The enzyme, which is effective in biodegradation of PCL, is Lipase. Lipase is an abundant enzyme present in tissue fluids that cleaves ester bonds of PCL. After 30 days of incubation in lipase solution (0.18 U/mL), loss of weight was determined as 2.5 ± 0.7 % and 1.3 ± 0.4 % for PCL and PCL-T₂₀ scaffolds, respectively (Figure 3.4.a). Meanwhile, there was not a significant difference in the morphology of PCL and β -TCP containing fibers before (Figure 3.2.c and Figure 3.2.e) and after (Figure 3.4.b and Figure 3.4.c) the degradation due to enzyme effect. After degradation, EDX analysis showed a decrease in weight percent ratio of Ca/P, from 2.91 (Figure 3.2.h) to 1.41 (Figure 3.4.e). Our results indicated that incorporation of β -TCP into PCL scaffolds caused a delay in degradation of PCL fibers. Degradation kinetics depend on the scaffold chemistry and shape as well as the incubation media. Enzyme concentration in this study was derived from its serum concentration which is given

in literature as 0.03-0.19 U/mL (Tietz and Shuey, 1993; Frydrych et al., 2015). In literature it is also given that PCL-starch fibers with 200 μ m diameters lost about 5% weight after 30 days of incubation when the enzyme concentration was 0.18 U/mL (Martins et al., 2009). Faster degradations as 50% - 90% loss in one day were reported for freeze-dried PCL scaffolds when 0.1 mg/mL lipase was used (Sezer et al., 2014b). Similarly, when 1 mg/mL lipase was used, 40% weight loss was reported in 7 days for 3D printed PCL scaffolds (Seyednejad et al., 2012). Depending on the preparation technique and the organization of fibers in PCL scaffolds, the time required for complete degradation may take place years in biological media.

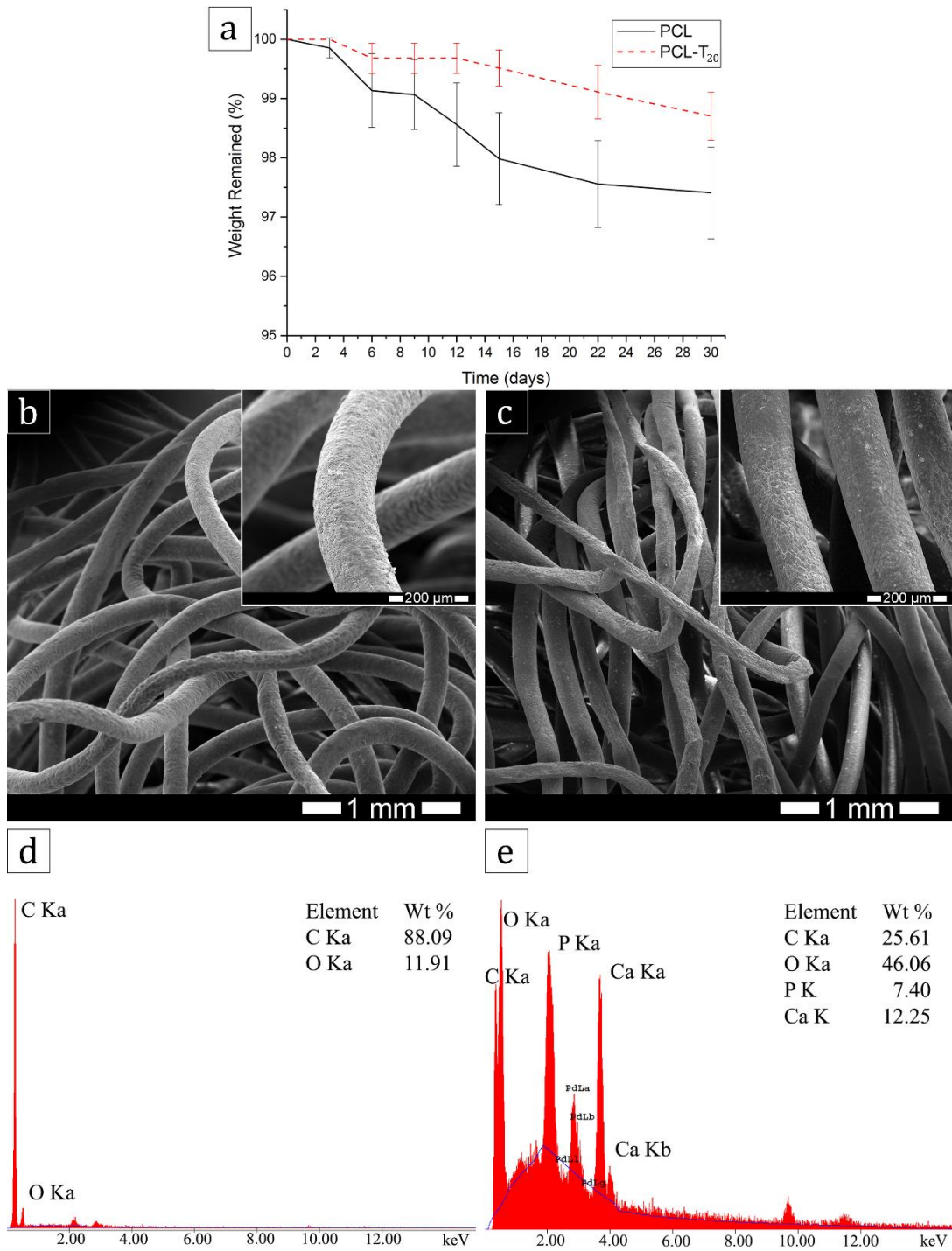


Figure 3.4. Degradation results. (a) Mass loss graph of PCL and PCL-T₂₀ in Lipase solution. SEM images of (b) PCL (100x, inset 500x) and (c) PCL-T₂₀ (100x, inset 500x) and EDX analysis of (d) PCL and (e) PCL-T₂₀ scaffolds after 30 days of incubation in Lipase solution (scale bar for insets is 200 μ m).

3.3. Surface Modification of Wet Spun Scaffolds

Surfaces of the scaffolds were modified by immobilizing gelatin after the surface activation with acrylic acid (AAc) grafting. AAc is one of the chemicals used for biofunctionalization of synthetic materials, such as methacrylate (Yue et al., 2015) or amine (Kim et al., 2014), which results in formation of free carboxyl (COO^-) end groups (Gupta et al., 2012). The amount of available free carboxyl groups shows the maximum possible functional points available for immobilization of gelatin via EDAC/NHS coupling reactions.

The degree of grafting on these scaffolds was determined by Toluidine Blue analysis and found to be $110 \pm 4 \mu\text{g}/\text{cc}$ (calibration curve of Toluidine Blue can be found in APPENDIX C, Figure C.1). In literature for PCL films, the values of $20 \mu\text{g}/\text{cm}^2$ and $6\text{--}18 \mu\text{g}/\text{cm}^2$ were reported (Gupta et al., 2012; Krishnanand et al., 2013). The AAc-grafted scaffolds were labelled as PCL-T₂₀A. XPS analysis confirmed AAc grafting on PCL-T₂₀A scaffolds upon administration of peak fitting on bonds of O atom. After the treatment of scaffolds with gelatin solution, presence of gelatin immobilized on the surface was detected by observing nitrogen and carbon peaks on XPS data.

3.3.1. XPS Analysis

Chemical structures of PCL, PCL-T₂₀, PCL-T₂₀A and PCL-T₂₀G scaffolds were examined by XPS (Figure 3.5). Figure 3.5.a shows the modification steps and functionalization of the surfaces of the scaffolds. In general XPS survey (Figure 3.5.b), an expected change of C/O ratio after AAc grafting and after gelatin immobilization was obtained. Presence of calcium ions was observed in the general survey but phosphate ions were not, most probably due to the steric hindrance created on these groups. Peak fitting and deconvolution of XPS data are also presented in Figure 3.5.c-j. For C1s fitting, the bonds observed were aliphatic carbon ($\text{C}-\underline{\text{C}}-\text{C}$ at 285 eV) (used as reference for curve fitting of XPS data), aliphatic ether ($\text{C}-\underline{\text{C}}-\text{O}$ at 286.35 eV), and aliphatic ester ($\text{O}=\underline{\text{C}}-\text{O}$ at 288.96 eV) (Louette et al., 2006). Amide

carbon ($O=C-N$ at 287.8 eV) was observed only in PCL-T₂₀G scaffolds indicating presence of nitrogen due to the presence of gelatin (de Luca et al., 2013). Oxygen atoms were observed for all samples as seen in O1s fitting curves as carbonyl oxygen ($C=O$, at 532 eV) and as ether oxygen ($C-O$, at 533.3 eV). Carboxyl oxygen ($O=C-OH$ at 534.5 eV) was present in PCL-T₂₀A (free acrylic acid groups) and PCL-T₂₀G (free 5'COOH ends and acidic R groups of amino acids) (Chen et al., 2012; Li, 2012; Yu et al., 2014). Presence of carboxyl in PCL-T₂₀A shows proper incorporation of acid groups needed for gelatin immobilization.

Table 3.2. Electron binding energy values (in eV) of atoms present in structure.

Atom		Electron Binding Energy (eV)
Carbon (C)	Aliphatic	285
	Aliphatic Ether	286.35
	Aliphatic Ester	288.96
	Amide	287.8
Oxygen (O)	Carbonyl	532
	Ether	533.3
	Carboxyl	534.5

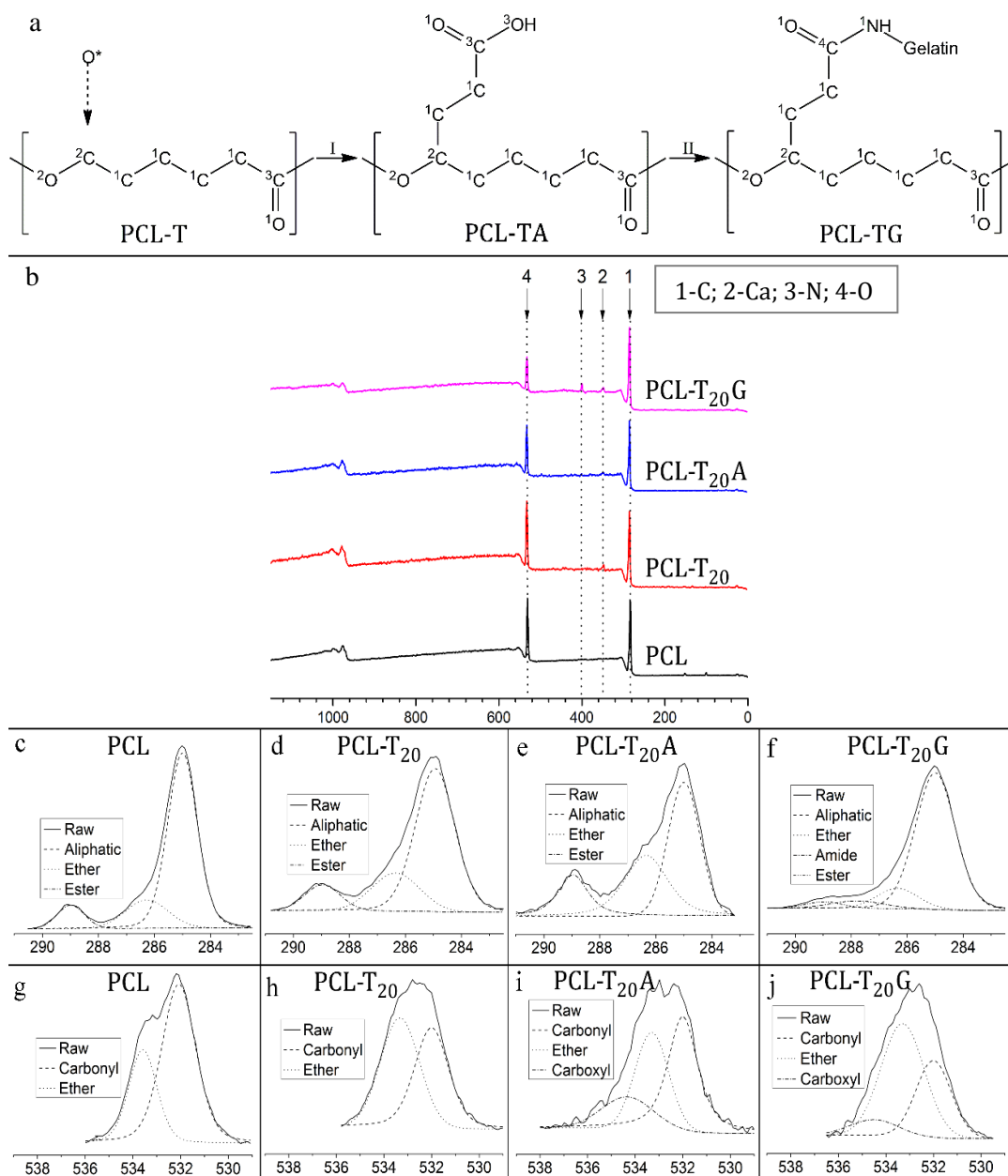


Figure 3.5. Surface modification steps and XPS results. (a) Surface modification steps; I–AAc grafting after oxygen plasma, II–gelatin immobilization. The numbers on the atoms define; ¹C–aliphatic, ²C–Ether, ³C–Ester, ⁴C–Amide, ¹O–carbonyl, ²O–ether, ³O–carboxyl. (b) XPS general survey results of PCL, PCL-T₂₀, PCL-T₂₀A and PCL-T₂₀G scaffolds. (c–f) C1s fitting of (c) PCL, (d) PCL-T₂₀, (e) PCL-T₂₀A, (f) PCL-T₂₀G. (g–j) O1s fitting of (g) PCL, (h) PCL-T₂₀, (i) PCL-T₂₀A and (j) PCL-T₂₀G.

3.4. Characterization of Activated and Modified Scaffolds

3.4.1. Morphological Analysis

Surface modifications by AAc grafting (Figure 3.6.a) and gelatin immobilization (Figure 3.6.b) created micron-level roughness on the surface of the fibers. After these steps, gelatin microspheres containing ceftriaxone sodium (CS) inside were added and attached on to the gelatin immobilized fibers. Gelatin microspheres were about $40.2 \pm 6.4 \mu\text{m}$ in diameter (Figure 3.6.c) determined from the SEM images (ImageJ, $n=250$). Microspheres affect two parameters; (i) increase possibility of cell attachment onto fibers, (ii) provide high surface area-to-volume ratio for prolonged drug release. In this study, gelatin microspheres were attached onto the gelatin immobilized fiber surfaces without using a crosslinker to avoid adverse effects of crosslinkers (Gendler et al., 1984). Presence of drug containing microspheres can be observed on the fibers (Figure 3.6.d).

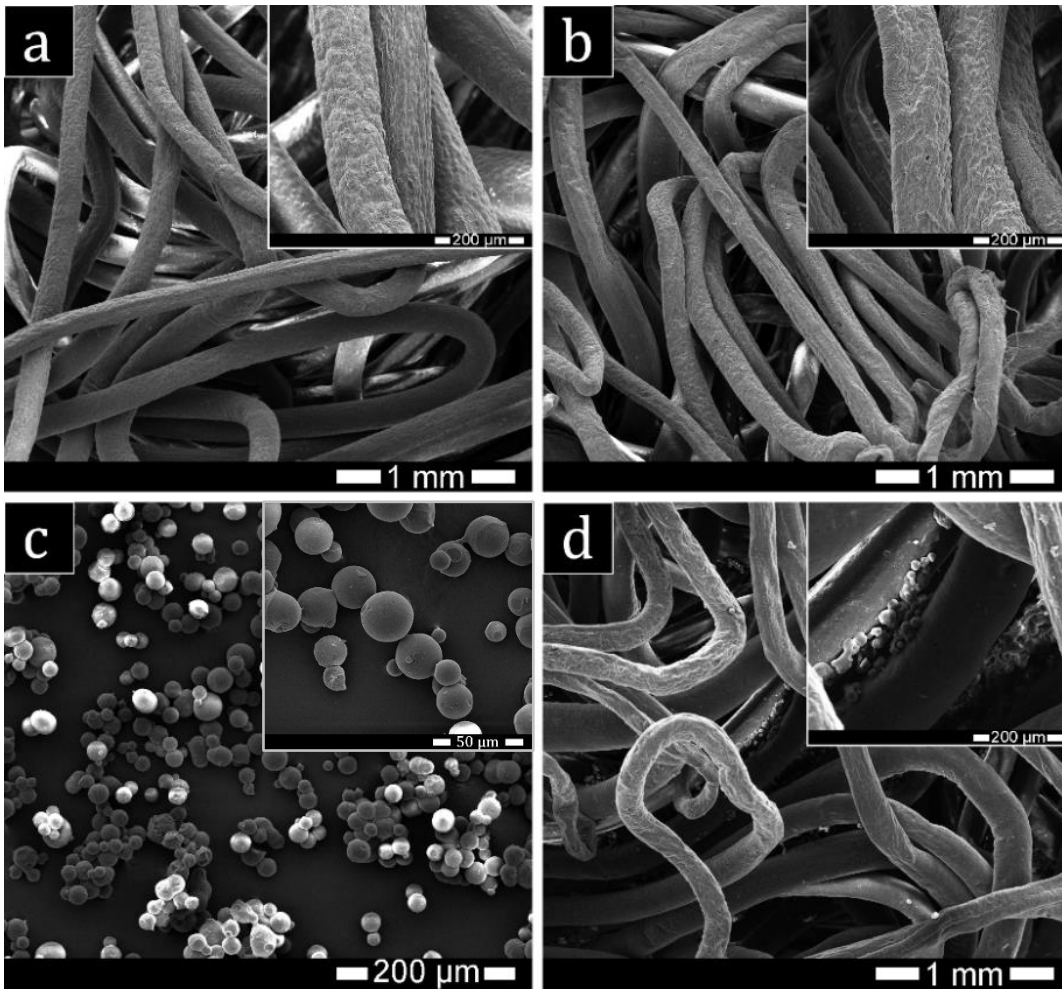


Figure 3.6. SEM Images of surface modified scaffolds. (a) PCL-T₂₀A (100x, inset 500x), (b) PCL-T₂₀G (100x, inset 500x), (c) gelatin microspheres (500x, inset 2000x) and (d) PCL-T₂₀GM (100x, inset 500x) (scale bar for insets is 200 μ m; scale bar for c part is 50 μ m).

3.4.2. Porosity Analysis

Porosity of scaffolds was measured by two techniques, using 1) Mercury Intrusion Porosimeter and Helium Pycnometer, and 2) micro-CT analysis. Mercury Intrusion Porosimeter and Helium Pycnometer calculations (as described in section 2.3.4) resulted in 68%, 65% and 69% porosity for PCL, PCL-T₂₀ and PCL-T₂₀G, respectively. Meanwhile, evaluation of porosity using micro-CT resulted in 72 ± 3 ,

70±1 and 75±1 percent porosity for the same samples, respectively. Micro-CT sections obtained from the scaffolds demonstrate high amount of void spaces, which can be filled with cells and the ECM (Figure 3.7.a-c). 3D images of micro-CT scan results of the scaffolds are also given in Figure 3.7 (d-f). The optimum porosity of the scaffolds for bone tissue engineering are estimated to be about 70%, even though lower or higher porosities have also been reported in literature (Ghanaati et al., 2010; Tang et al., 2016). Fibrous nature of the scaffolds enables fluid, nutrient and metabolite transfer owing to the presence of interconnected voids, as can be observed from SEM and μ CT images (Baker and Chen, 2012). Interconnected pores ensure the improved cell-to-cell interaction in scaffold for better communication and increased fluid and gas flow inside the scaffold for nutrient delivery, waste disposal and gas exchange (Hutmacher, 2000; Polo-Corrales et al., 2014).

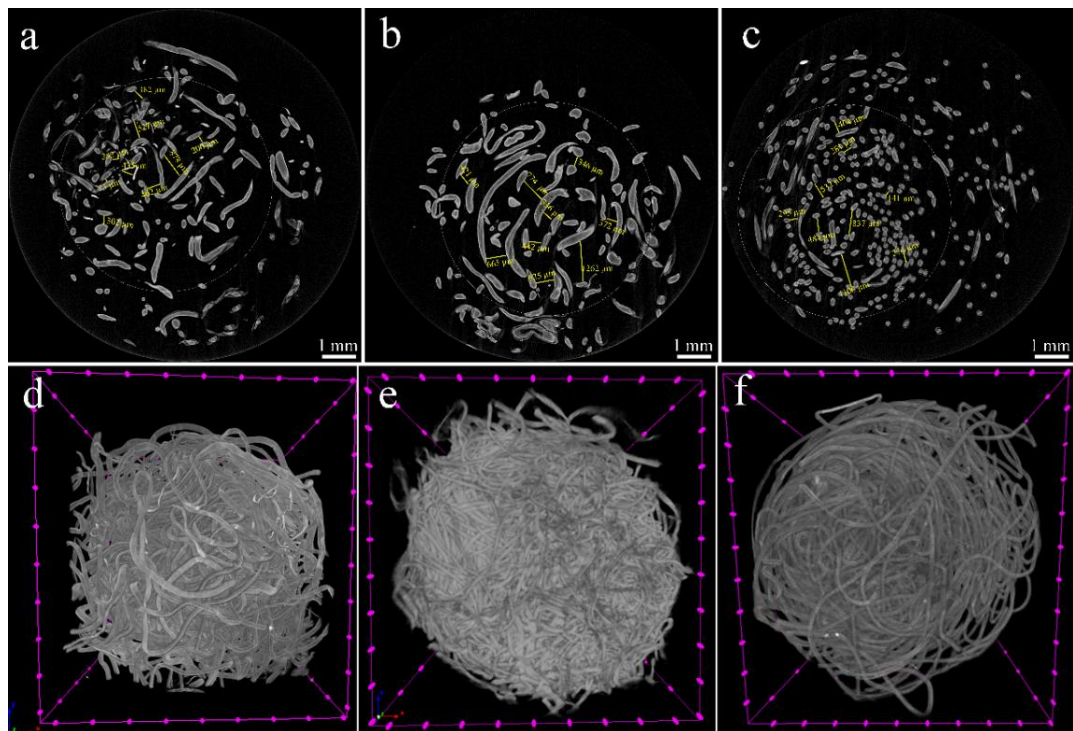


Figure 3.7. μ CT analysis results of the scaffolds. (a,b,c) Sections obtained from the middle point of the PCL, PCL-T₂₀ and PCL-T₂₀G scaffolds and (d,e,f) total images of the scaffolds.

3.4.3. *In vitro* Drug Release and Antibacterial Efficacy

Gelatin microspheres were prepared by water-oil dispersion method. The aqueous gelatin solution was poured into corn oil with vigorous spinning. Then the crosslinker was added to and solution was put into +4 °C for cooling. Afterwards, the solution was washed with acetone to remove oil from microvesicles whilst using filter to eliminate everything smaller than microvesicles. Figure 3.8.a,b shows the light microscopy images of the dry and the swollen microspheres. Due to the aqueous medium, gelatin microspheres were swollen significantly. The sizes were determined as 40 μm from SEM images (Figure 3.6.c) by applying ImageJ analysis (n=250), determined as 30 μm and 50 μm (n=8 for both) for dry and wet microspheres in light microscopy (Zeiss Axio Imager M2, Germany) (Figure 3.8.a,b) and determined as 85 μm (D[4,3]; volume-weighted average size) from particle size analyser (Malvern Mastersizer 2000, UK) when dispersed in water (Figure 3.8.c). The reason for almost doubling in size between SEM and particle size analysis results is due to swelling and coagulation of the particles in aqueous media as explained above. The differences in light microscopy results with respect to others is most probably because of small sample size.

Yield, drug loading and entrapment efficiency percentage values of microspheres were calculated to be 52%, 37% and 80%, respectively as explained in section 2.4.5. Attachment efficiency of microspheres onto the scaffolds was calculated as ~77%. Release graphs of Ceftriaxone sodium (CS) from gelatin microspheres (GM) and GM containing scaffolds (PCL-T₂₀GM) demonstrated an initial burst release followed by limited delayed release up to 7 days (Figure 3.8.d). Release was consistent till the end of first week and ended in about 15 days (calibration curve of Ceftriaxone Sodium is given in APPENDIX D, Figure D.1).

For an effective application, it was shown that (Diaz and Newman, 2015), the release of antibiotics should have an initial burst effect with progressing slower but effective release into the host tissue. This factor enables the protection of the tissue at time

zero, with substantial prolonged effect for the time interval of possible bacterial manifestation (Diaz and Newman, 2015). The results of disk diffusion tests (t=24 h) showed a direct relevancy of antibacterial efficacy of drug loaded microspheres (Figure 3.8.e-g). The level of antibacterial efficacy was observed to be >30 mm, which is in the range of acceptable antibacterial effect (≥ 29 mm for *E. coli* (Benex Limited, 2011)). Meanwhile, this effect is a function of drug loaded into microspheres and the amount of microspheres attached on the scaffold. By changing these factors it would be possible to arrange antimicrobial efficiency of the scaffolds. It was also shown that release from gelatin microspheres was faster than that of the ones embedded in PCL matrix. This is due to direct interaction of microspheres with release medium (Sezer et al., 2013). Also, a delayed release for larger size of microspheres and a less water soluble drug was reported previously (Ulubayram et al., 2005). Meanwhile, entire drug release in 2-12 h from gelatin/starch microparticles with size of 60-100 μm (Phromsopha and Baimark, 2014), and effects of crosslinking type used for stabilization of gelatin microspheres on the release kinetics (García Cruz et al., 2013) were reported. Studies show that, chemistry and size of particles, as well as the types of drugs and crosslinkers are all effective in controlling the rate of release of the bioactive agents.

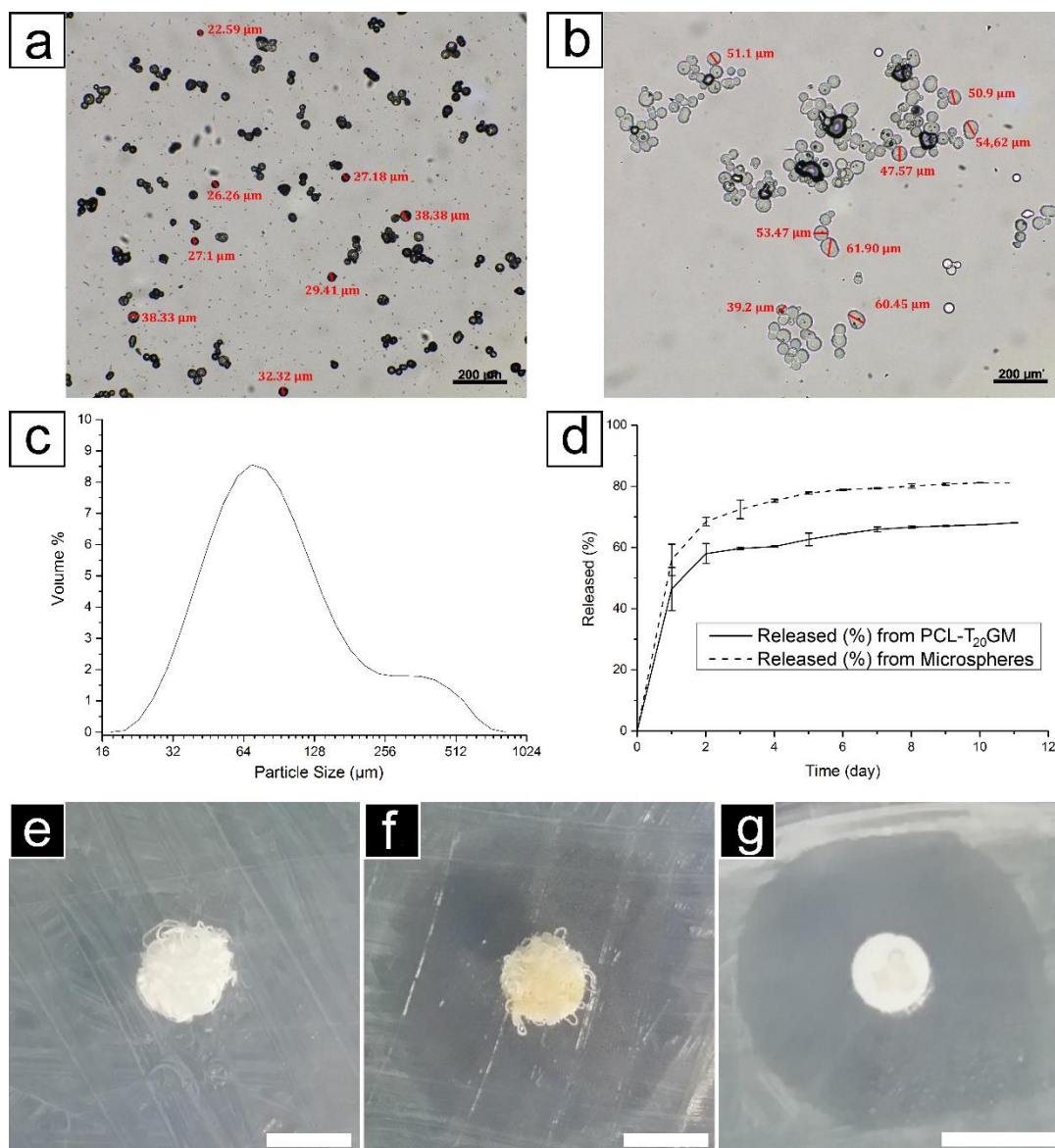


Figure 3.8. Gelatin microspheres and release results. (a and b) Dry and wet gelatin microsphere images obtained by light microscopy. (c) Particle size distribution of gelatin microspheres. (d) Release of CS from PCL-T₂₀GM scaffolds and microspheres alone. Antibacterial effect of (e) PCL-T₂₀, (f) PCL-T₂₀GM and (g) CS control discs. Scale bars for e-g are 10 mm.

3.4.4. *In vitro* Cell Culture Tests

Saos-2 cells were used for the cell attachment studies. Cell viability tests, which were carried out by AlamarBlue® assay, showed that the number of cells on the scaffolds having gelatin microspheres (PCL-T₂₀GM) were significantly higher (63%) than PCL-T₂₀ group ($p < 0.05$) in the first day. However, for the proceeding time points there were no significant difference among the scaffolds and they demonstrated almost similar cell attachment behavior (Figure 3.9). From day 1 to day 14, cells have almost doubled in number in a week period, but starting from day 14, they did not show a significant increase. One reason for it might be the confluency and missing interconnectivity between PCL fibers, which prevents migration of cells towards unpopulated spots in the scaffold.

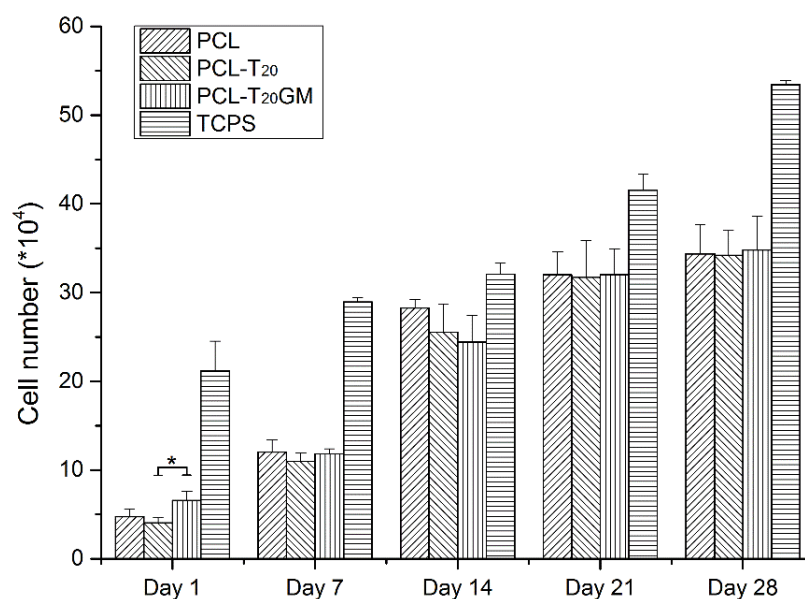


Figure 3.9. Cell viability of PCL, PCL-T₂₀ and PCL-T₂₀GM scaffolds (* $p < 0.05$).

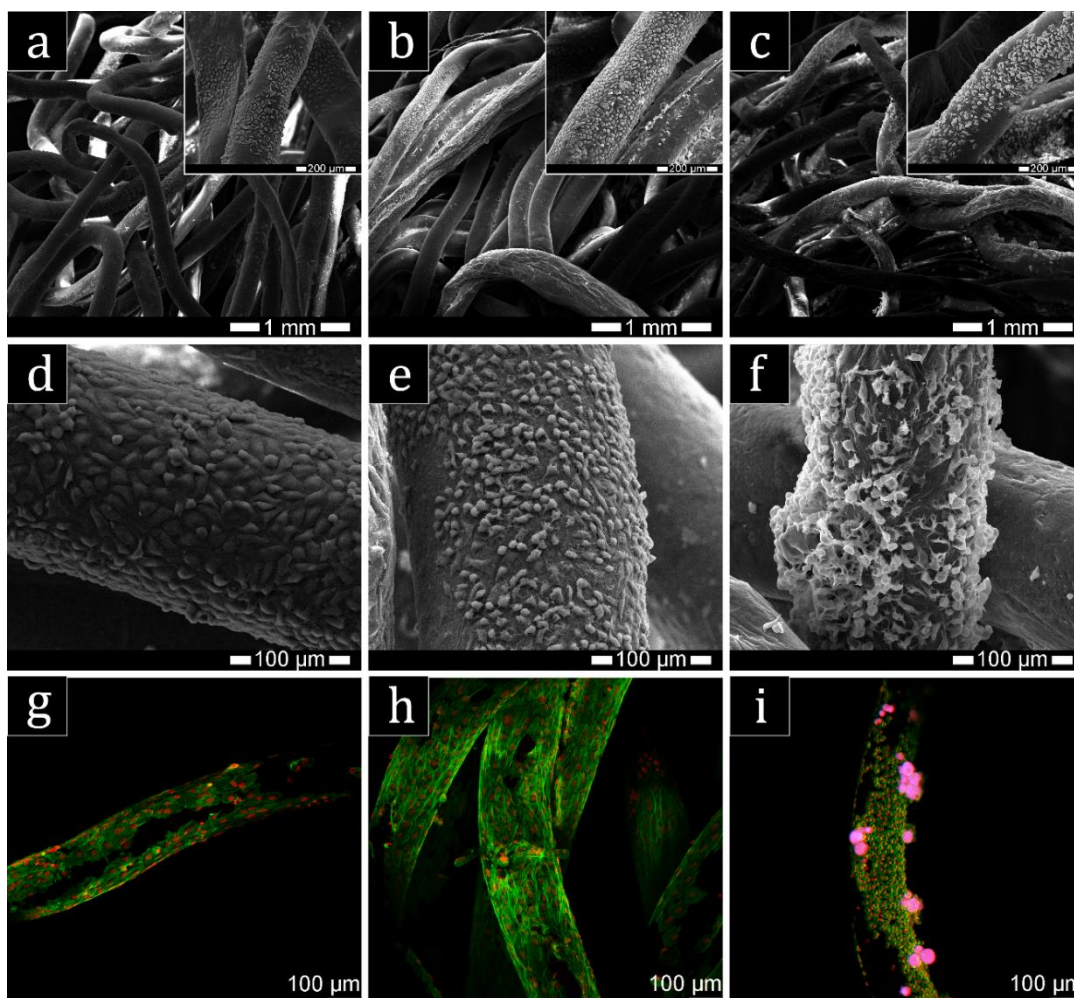


Figure 3.10. Characterization of Saos-2 seeded scaffolds at the end of day 28. (a) PCL, (b) PCL-T₂₀, (c) PCL-T₂₀GM; (d-f) SEM results (1000x), (d) PCL, (e) PCL-T₂₀, (f) PCL-T₂₀GM. (g-i) CLSM results, (g) PCL, (h) PCL-T₂₀, (i) PCL-T₂₀GM (red: nuclei, green: cytoskeleton, pink (overlap of red and green): microspheres).

Cells attached and spread on fibers of all scaffold groups can be observed on the SEM micrographs (Figure 3.10.a-f). Confocal images also showed that cells were spread and proliferated on the surfaces of the fibers (Figure 3.10.g-i). It can be concluded that the presence of gelatin microspheres enhanced the cell attachment and did not cause any toxic effect on the cells, as it was observed from SEM and confocal images. This also proves that glutaraldehyde used in crosslinking of gelatin did not

demonstrate any toxicity on the cells. In literature it is also given that gelatin microspheres in PCL structure have no toxic effect both *in vitro* (Sezer et al., 2014b) and *in vivo* (Sezer et al., 2014a) applications. Cell spreading is important for the formation of extracellular matrix (ECM) and for the migration and proliferation of the cells leading to tissue regeneration. In our case, in *in vitro* experiments, cells were proliferated on the fibers and the number of cells attached on the scaffolds significantly increased in two weeks.

Due to the absence of bridges among fibers, cells could not easily move from one fiber to another. They could only move between adjacent fibers. Filopodia extensions from one fiber to another can occur at the points where the fibers are quite close to each other (Figure 3.11). Because they could not move freely between the fibers apart from each other and therefore cells could not fill the void volume of the scaffold. Colonization of the cells were observed on the fibers at their attachment points (Harley et al., 2008).

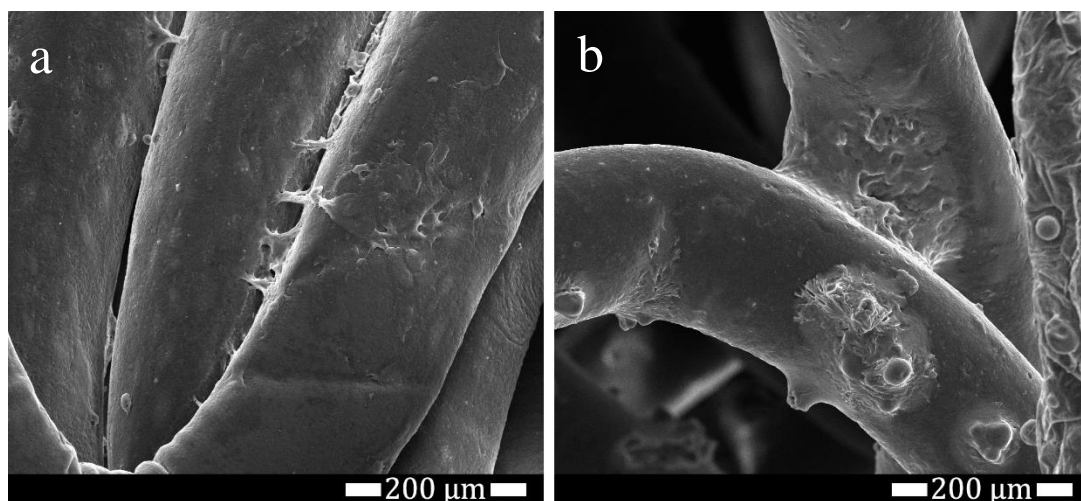


Figure 3.11. Movements of cells between fibers. (a) Without and (b) with the presence of microspheres.

One solution to this may be to create extra interconnection between the fibers so cells could migrate throughout the scaffold. A similar result was obtained by wet spun three-arm star branched PCL scaffolds, which exhibited an increase in cell number of pre-osteoblast cells till 14 days and cells mostly covered the outer layer of scaffolds (Puppi et al., 2011a). Calcified wet spun chitosan fibers were tested for viability of Saos-2 cells and the results suggested that fibers with diameter of about 100 μm can provide environment for migration of cells and formation of ECM between fibers (Ucar et al., 2016). It is also important that, gelatin microspheres attached strongly on the fibers and they demonstrate two functions as; 1) carrier for the antibiotic (or any drug loaded in); and 2) points for the cells to attach (since they have protein structure simulating the attachment and proliferation of the cells).

CHAPTER 4

CONCLUSION

Bone tissue damages get slower healing than other regions in the body due to the hard structure of bone with less amount of blood circulation. In the treatment of bone defects, one promising way is application of tissue engineering technique and support the defected area. Scaffolds are one of the essential parts of tissue engineered constructs. They provide the environment for cells to colonize, proliferate and form the required matrix. Scaffolds of different forms obtained by using various methods have been introduced into tissue engineering studies. Wet spinning is one of those methods, which produces fibrous scaffolds with interconnected porosity. The material of scaffold is also very important and the ones having high biocompatibility, low batch-to-batch variation and easy modification make them preferable materials. Some synthetic polymers have fulfilled these requirements and therefore have shown their superiority. Meanwhile, in order to prevent any possibility of surgical site infections, a drug release regimen can be introduced to the prepared scaffolds.

In this study, wet spun PCL and PCL-TCP scaffolds were prepared. To decide on whether to use 10% w/w (PCL-T₁₀) or 20% w/w (PCL-T₂₀) β -TCP, mechanical tests with application of compression force were carried out. Based on the results of these compression tests, we eliminated PCL-T₁₀ scaffolds from the proceeding modifications due to their inferior mechanical properties with respect to PCL-T₂₀. Further experiments were carried out on PCL and PCL-T₂₀ scaffolds. Both PCL and PCL-T₂₀ scaffolds exhibited enzymatic degradation in the media containing lipase enzyme. The rate of degradation of PCL-T₂₀ was significantly slower than that of PCL group, which is favorable in case of bone tissue engineering.

PCL-T₂₀ scaffolds were treated further by surface modification and by grafting of acrylic acid groups onto fiber surfaces (PCL-T₂₀A) to make them functionalized for gelatin binding. After acrylic acid grafting, the scaffolds were treated with gelatin and gelatin was immobilized onto fibers of the scaffolds (PCL-T₂₀G). XPS studies proved the existence of calcium phosphate ions in PCL-T₂₀ scaffolds, acrylic acid in PCL-T₂₀A scaffolds and gelatin in PCL-T₂₀G scaffolds after introducing peak fitting into XPS graphs. PCL, PCL-T₂₀ and PCL-T₂₀G had around 70% interconnected porosity. Analyses, which were achieved by micro-computed tomography, also proved that the interconnected porosity was present throughout the scaffold.

Meanwhile, gelatin microspheres were prepared and loaded with Ceftriaxone sodium (CS). The size of these microspheres were found to be 40 μm by SEM images, 30 μm and 50 μm for dry and wet microspheres by light microscopy and 85 μm by particle size analyser. Gelatin microspheres loaded with CS were attached onto PCL-T₂₀G scaffolds, forming (PCL-T₂₀GM). Release of CS was observed from both drug-loaded GM and PCL-T₂₀GM scaffolds where they demonstrated an initial burst release followed by a limited delayed release for up to 7 days. Antibacterial efficacy of these scaffolds was tested against a model gram negative bacterium, *E. coli* and effective results were obtained in the disk diffusion tests.

In order to examine the material-cell interactions, PCL, PCL-T₂₀ and PCL-T₂₀GM scaffolds were put through *in vitro* cell culture tests with human osteosarcoma cell line (Saos-2). In first day, cell viability of PCL-T₂₀GM scaffolds were significantly higher than that of PCL-T₂₀ group due to immobilized gelatin and attached gelatin microspheres. For upcoming days, no significant differences were observed on cell viability among PCL, PCL-T₂₀ and PCL-T₂₀GM scaffolds. Significant increase in the cell population up to 2 weeks indicates sufficiency of porosity providing metabolite/nutrient transfer throughout the scaffold. As can be observed from SEM and confocal microscopy images, cells populated on the surfaces of the fibers and also in the vicinity of the microspheres.

These results demonstrate that these wet spun scaffolds prepared in this study can be good candidates for bone tissue engineering applications. Mechanical properties of scaffolds were complying with the requirements for bone tissue engineering constructs. The degradation profile of scaffolds also showed that the scaffolds are quite stable and degrade slowly in the presence of lipase enzyme. This slow degradation is preferable for healing of bone tissue. Lastly, release of antibacterial drug releasing from the microspheres can provide the required protection against surgical site infections.

For future studies, a modification will be introduced to scaffolds that can form bridges between fibers. This would enhance cell migration and distribute cells all over the scaffold. Increase in cell number will also provide a faster ECM formation, which in place will improve healing process of scaffold.

REFERENCES

- Abedalwafa, M.; Wang, F.; Wang, L.; Li, C. Biodegradable Poly-Epsilon-Caprolactone (PCL) for Tissue Engineering Applications: A Review. *Rev Adv Mater Sci* **2013**, *34* (2), 123–140.
- Albrektsson, T.; Johansson, C. Osteoinduction, Osteoconduction and Osseointegration. *Eur Spine J* **2001**, *10* (SUPPL. 2), 96–101.
- Alexandru, D. A. Early Transition Metal Catalyzed Living Radical and Ring Opening Polymerizations for Complex Copolymer Architectures. *56th Annu Rep Res 2011* **2011**, AC7.
- Algul, D.; Sipahi, H.; Aydin, A.; Kelleci, F.; Ozdatli, S.; Yener, F. G. Biocompatibility of Biomimetic Multilayered Alginate–chitosan/ β -TCP Scaffold for Osteochondral Tissue. *Int J Biol Macromol* **2015**, *79*, 363–369.
- Aragon, J.; Navascues, N.; Mendoza, G.; Irusta, S. Laser-Treated Electrospun Fibers Loaded with Nano-Hydroxyapatite for Bone Tissue Engineering. *Int J Pharm* **2017**, *525* (1), 112–122.
- Arahira, T.; Maruta, M.; Matsuya, S.; Todo, M. Development and Characterization of a Novel Porous β -TCP Scaffold with a Three-Dimensional PLLA Network Structure for Use in Bone Tissue Engineering. *Mater Lett* **2015**, *152*, 148–150.
- Ashbaugh, A. G.; Jiang, X.; Zheng, J.; Tsai, A. S.; Kim, W.-S.; Thompson, J. M.; Miller, R. J.; Shahbazian, J. H.; Wang, Y.; Dillen, C. A.; et al. Polymeric Nanofiber Coating with Tunable Combinatorial Antibiotic Delivery Prevents Biofilm-Associated Infection in Vivo. *Proc Natl Acad Sci* **2016**, E6919–E6928.

Azimi, B.; Nourpanah, P.; Rabiee, M.; Arbab, S. Poly (ϵ -Caprolactone) Fiber: An Overview. *J Eng Fiber Fabr* **2014**, *9* (3), 74–90.

Bajpai, S. K.; Chand, N.; Soni, S. Controlled Release of Anti-Diabetic Drug Gliclazide from Poly(caprolactone)/poly(acrylic Acid) Hydrogels. *J Biomater Sci Polym Ed* **2015**, *26* (14), 947–962.

Baker, B. M.; Chen, C. S. Deconstructing the Third Dimension - How 3D Culture Microenvironments Alter Cellular Cues. *J Cell Sci* **2012**, *125* (13), 3015–3024.

Benex Limited. *BBL Sensi-Disc Antimicrobial Susceptibility Test Discs*; Shannon, Ireland, **2011**.

Bhattacharjee, P.; Naskar, D.; Kim, H.-W.; Maiti, T. K.; Bhattacharya, D.; Kundu, S. C. Non-Mulberry Silk Fibroin Grafted PCL Nanofibrous Scaffold: Promising ECM for Bone Tissue Engineering. *Eur Polym J* **2015**, *71*, 490–509.

Billiet, T.; Vandenhoute, M.; Schelfhout, J.; Van Vlierberghe, S.; Dubruel, P. A Review of Trends and Limitations in Hydrogel-Rapid Prototyping for Tissue Engineering. *Biomaterials* **2012**, *33* (26), 6020–6041.

Buchanan, F. Hydrolytic Degradation of Polycaprolactone. In *Degradation Rate of Bioresorbable Materials: Prediction and Evaluation*; Buchanan, F., Ed.; Woodhead Publishing: Cambridge, **2008**, 357–392.

Cañas, A. I.; Delgado, J. P.; Gartner, C. Biocompatible Scaffolds Composed of Chemically Crosslinked Chitosan and Gelatin for Tissue Engineering. *J Appl Polym Sci* **2016**, *133* (33), 1–10.

Chandy, T.; Wilson, R. F.; Rao, G. H. R.; Das, G. S. Changes in Cisplatin Delivery due to Surface-Coated Poly(lactic Acid)-Poly(ϵ -Caprolactone) Microspheres. *J Biomater Appl* **2002**, *16* (4), 275–291.

Chaudhuri, B.; Mondal, B.; Kumar, S.; Sarkar, S. C. Myoblast Differentiation and Protein Expression in Electrospun Graphene Oxide (GO)-Poly (ϵ -Caprolactone, PCL) Composite Meshes. *Mater Lett* **2016**, *182*, 194–197.

Chen, C. M.; Huang, J. Q.; Zhang, Q.; Gong, W. Z.; Yang, Q. H.; Wang, M. Z.; Yang, Y. G. Annealing a Graphene Oxide Film to Produce a Free Standing High Conductive Graphene Film. *Carbon N Y* **2012**, *50* (2), 659–667.

Chi, Y.; Zhu, S.; Wang, C.; Zhou, L.; Zhang, L.; Li, Z.; Dai, Y. Glioma Homing Peptide-Modified PEG-PCL Nanoparticles for Enhanced Anti-Glioma Therapy. *J Drug Target* **2016**, *24* (3), 224–232.

Choi, M. O.; Kim, Y. J. Fabrication of Gelatin/calcium Phosphate Composite Nanofibrous Membranes by Biomimetic Mineralization. *Int J Biol Macromol* **2012**, *50* (5), 1188–1194.

Cooper, A.; Bhattarai, N.; Zhang, M. Fabrication and Cellular Compatibility of Aligned Chitosan-PCL Fibers for Nerve Tissue Regeneration. *Carbohydr Polym* **2011**, *85* (1), 149–156.

Correia, T. R.; Ferreira, P.; Vaz, R.; Alves, P.; Figueiredo, M. M.; Correia, I. J.; Coimbra, P. Development of UV Cross-Linked Gelatin Coated Electrospun Poly(caprolactone) Fibrous Scaffolds for Tissue Engineering. *Int J Biol Macromol* **2016**, *93*, 1539–1548.

Costa, N. M. F.; Yassuda, D. H.; Sader, M. S.; Fernandes, G. V. O.; Soares, G. D. A.; Granjeiro, J. M. Osteogenic Effect of Tricalcium Phosphate Substituted by Magnesium Associated with Genderm® Membrane in Rat Calvarial Defect Model. *Mater Sci Eng C* **2016**, *61*, 63–71.

Cui, L.; Zhang, N.; Cui, W.; Zhang, P.; Chen, X. A Novel Nano/micro-Fibrous Scaffold by Melt-Spinning Method for Bone Tissue Engineering. *J Bionic Eng* **2015**, *12* (1), 117–128.

Darouiche, R. O. Treatment of Infections Associated with Surgical Implants. *N Engl J Med* **2004**, *350*, 1422–1429.

Derakhshan, Z. H.; Shaghghi, B.; Asl, M. P.; Majidi, M.; Ghazizadeh, L.; Chegini, A.; Bonakdar, S. In Situ Forming Hydrogel Based on Chondroitin Sulfate–Hydroxyapatite for Bone Tissue Engineering. *Int J Polym Mater Polym Biomater* **2015**, *64* (17), 919–926.

Díaz, E.; Sandonis, I.; Valle, M. B. In Vitro Degradation of Poly(ϵ -caprolactone)/nHA Composites. *J Nanomater* **2014**, *2014*, 1–8.

Diaz, V.; Newman, J. Surgical Site Infection and Prevention Guidelines: A Primer for Certified Registered Nurse Anesthetists. *Am Assoc Nurse Anesth* **2015**, *83* (1), 63–68.

Ding, M.; Zhou, L.; Fu, X.; Tan, H.; Li, J.; Fu, Q. Biodegradable Gemini Multiblock Poly(ϵ -Caprolactone Urethane)s toward Controllable Micellization: Supplementary Data. *Soft Matter* **2010**, *6* (9), 2087.

Dini, F.; Barsotti, G.; Puppi, D.; Coli, A.; Briganti, A.; Giannesi, E.; Miragliotta, V.; Mota, C.; Piroso, A.; Stornelli, M. R.; et al. Tailored Star Poly (ϵ -Caprolactone) Wet-Spun Scaffolds for in Vivo Regeneration of Long Bone Critical Size Defects. *J Bioact Compat Polym* **2015**, *31* (1), 15–30.

Dong, C. M.; Guo, Y. Z.; Qiu, K. Y.; Gu, Z. W.; Feng, X. De. In Vitro Degradation and Controlled Release Behavior of D,L-PLGA50 and PCL-B-D,L-PLGA50 Copolymer Microspheres. *J Control Release* **2005**, *107* (1), 53–64.

Edlund, U.; Albertsson, A.-C. Degradable Polymer Microspheres for Controlled Drug Delivery. *Degrad Aliphatic Polyesters* **2002**, *157*, 67–112.

Elomaa, L.; Kokkari, A.; Närhi, T.; Seppälä, J. V. Porous 3D Modeled Scaffolds of Bioactive Glass and Photocrosslinkable Poly(ϵ -Caprolactone) by Stereolithography. *Compos Sci Technol* **2013**, *74*, 99–106.

Endogan, T.; Kiziltay, A.; Hasirci, V.; Hasirci, N. Modification of Acrylic Bone Cements with Oxygen Plasma and Additives. *J Biomater Tissue Eng* **2012**, *2* (3), 236–243.

Fayyazbakhsh, F.; Solati-Hashjin, M.; Keshtkar, A.; Shokrgozar, M. A.; Dehghan, M. M.; Larijani, B. Novel Layered Double Hydroxides-Hydroxyapatite/gelatin Bone Tissue Engineering Scaffolds: Fabrication, Characterization, and in Vivo Study. *Mater Sci Eng C* **2017**, *76*, 701–714.

Felfel, R. M. M.; Pooza, L.; Gimeno-Fabra, M.; Milde, T.; Hildebrand, G.; Ahmed, I.; Scotchford, C.; Sottile, V.; Grant, D. M. D. M.; Liefeth, K. In Vitro Degradation and Mechanical Properties of PLA-PCL Copolymer Unit Cell Scaffolds Generated by Two-Photon Polymerization. *Biomed Mater* **2016**, *11* (1), 1–14.

Feng, S.; Chen, Y.; Meng, C.; Mai, B. Y.; Wu, Q.; Gao, H. Y.; Liang, G. D.; Zhu, F. M. Study on the Condensed State Physics of Poly(ϵ -Caprolactone) Nano-Aggregates in Aqueous Dispersions. *J Colloid Interface Sci* **2015**, *450*, 264–271.

Frese, L.; Dijkman, P. E.; Hoerstrup, S. P. Adipose Tissue-Derived Stem Cells in Regenerative Medicine. *Transfus Med Hemotherapy* **2016**, *43* (4), 268–274.

Frydrych, M.; Román, S.; Macneil, S.; Chen, B. Biomimetic Poly(glycerol Sebacate)/poly(L-Lactic Acid) Blend Scaffolds for Adipose Tissue Engineering. *Acta Biomater* **2015**, *18*, 40–49.

Fuse, M.; Hayakawa, T.; Hashizume-takizawa, T.; Takeuchi, R.; Kurita-ochiai, T. Original MC3T3-E1 Cell Assay on Collagen or Fibronectin Immobilized Poly(lactic Acid- ϵ -Caprolactone) Film. *J Hard Tissue Biol* **2015**, *24* (3), 249–256.

García Cruz, D. M.; Sardinha, V.; Escobar Ivirico, J. L.; Mano, J. F.; Gómez Ribelles, J. L. Gelatin Microparticles Aggregates as Three-Dimensional Scaffolding System in Cartilage Engineering. *J Mater Sci Mater Med* **2013**, *24* (2), 503–513.

Gendler, E.; Gendler, S.; Nimni, M. E. Toxic Reactions Evoked by Glutaraldehyde-Fixed Pericardium and Cardiac Valve Tissue Bioprosthesis. *J Biomed Mater Res* **1984**, *18*, 727–736.

Gentile, P.; Nandagiri, V. K.; Pabari, R.; Daly, J.; Tonda-Turo, C.; Ciardelli, G.; Ramtoola, Z. Influence of Parathyroid Hormone-Loaded PLGA Nanoparticles in Porous Scaffolds for Bone Regeneration. *Int J Mol Sci* **2015**, *16* (9), 20492–20510.

Gentile, P.; Nandagiri, V. K.; Daly, J.; Chiono, V.; Mattu, C.; Tonda-Turo, C.; Ciardelli, G.; Ramtoola, Z. Localised Controlled Release of Simvastatin from Porous Chitosan-Gelatin Scaffolds Engrafted with Simvastatin Loaded PLGA-Microparticles for Bone Tissue Engineering Application. *Mater Sci Eng C* **2016**, *59*, 249–257.

Ghanaati, S.; Barbeck, M.; Orth, C.; Willershausen, I.; Thimm, B. W.; Hoffmann, C.; Rasic, A.; Sader, R. A.; Unger, R. E.; Peters, F.; et al. Influence of β -Tricalcium Phosphate Granule Size and Morphology on Tissue Reaction in Vivo. *Acta Biomater* **2010**, *6* (12), 4476–4487.

Gleadall, A.; Pan, J.; Kruft, M. A.; Kellomäki, M. Degradation Mechanisms of Bioresorbable Polyesters. Part 1. Effects of Random Scission, End Scission and Autocatalysis. *Acta Biomater* **2014a**, *10* (5), 2223–2232.

Gleadall, A.; Pan, J.; Kruft, M. A.; Kellomäki, M. Degradation Mechanisms of Bioresorbable Polyesters. Part 2. Effects of Initial Molecular Weight and Residual Monomer. *Acta Biomater* **2014b**, *10* (5), 2233–2240.

Goyanes, A.; Det-Amornrat, U.; Wang, J.; Basit, A. W.; Gaisford, S. 3D Scanning and 3D Printing as Innovative Technologies for Fabricating Personalized Topical Drug Delivery Systems. *J Control Release* **2016**, *234*, 41–48.

Gozutok, M.; Baitukha, A.; Arefi-Khonsari, F.; Turkoglu Sasmazel, H. Novel Thin Films Deposited on Electrospun PCL Scaffolds by Atmospheric Pressure Plasma Jet for L929 Fibroblast Cell Cultivation. *J Phys D Appl Phys* **2016**, *49* (47), 474002.

Guo, B.; Ma, P. X. Synthetic Biodegradable Functional Polymers for Tissue Engineering: A Brief Review. *Sci China Chem* **2014**, *57* (4), 490–500.

Gupta, B.; Krishnanand, K.; Deopura, B. L. Oxygen Plasma-Induced Graft Polymerization of Acrylic Acid on Polycaprolactone Monofilament. *Eur Polym J* **2012**, *48* (11), 1940–1948.

Harley, B. A. C.; Kim, H.-D.; Zaman, M. H.; Yannas, I. V.; Lauffenburger, D. A.; Gibson, L. J. Microarchitecture of Three-Dimensional Scaffolds Influences Cell Migration Behavior via Junction Interactions. *Biophys J* **2008**, *95* (8), 4013–4024.

Herman, M. F. Tissue Engineering. In *Encyclopedia of Polymer Science and Technology*; John Wiley & Sons, Inc.: New Jersey, **2007**, 1259-1289.

Hernández, A. R.; Contreras, O. C.; Acevedo, J. C.; Moreno, L. G. N. Poly(ϵ -Caprolactone) Degradation under Acidic and Alkaline Conditions. *Am J Polym Sci* **2013**, *3* (4), 70–75.

Hiramatsu, H.; Hori, A.; Yajima, Y.; Yamada, M.; Seki, M. Microfluidics-Based Wet Spinning of Protein Microfibers as Solid Scaffolds for 3D Cell Cultivation. In *2016 International Symposium on Micro-NanoMechatronics and Human Science (MHS)*; IEEE, **2016**, 1–4.

Hissink, E. C.; Steendam, R.; Meyboom, R.; Flipsen, T. A. C. Biogradable Multi-Block Co-Polymers. Patent No: WO2005068533, **2005**.

Hong, S.; Kim, G. Fabrication of Electrospun Polycaprolactone Biocomposites Reinforced with Chitosan for the Proliferation of Mesenchymal Stem Cells. *Carbohydr Polym* **2011**, *83* (2), 940–946.

Hoskins, J. N.; Grayson, S. M. Synthesis and Degradation Behavior of Cyclic Poly(ϵ -Caprolactone). *Macromolecules* **2009**, *42* (17), 6406–6413.

Hou, Q.; Grijpma, D. W.; Feijen, J. Porous Polymeric Structures for Tissue Engineering Prepared by a Coagulation, Compression Moulding and Salt Leaching Technique. *Biomaterials* **2003**, *24* (11), 1937–1947.

Hsieh, F. Y.; Lin, H. H.; Hsu, S. hui. 3D Bioprinting of Neural Stem Cell-Laden Thermoresponsive Biodegradable Polyurethane Hydrogel and Potential in Central Nervous System Repair. *Biomaterials* **2015**, *71*, 48–57.

Huang, Y.-T.; Wang, W.-C.; Hsu, C.-P.; Lu, W.-Y.; Chuang, W.-J.; Chiang, M. Y.; Lai, Y.-C.; Chen, H.-Y. The Ring-Opening Polymerization of ϵ -Caprolactone and L-Lactide Using Aluminum Complexes Bearing Benzothiazole Ligands as Catalysts. *Polym. Chem.* **2016**, *7* (26), 4367–4377.

Huang, Y.; Xu, X.; Luo, X.; Ma, D. Molecular Weight Dependence of the Melting Behavior of Poly(ϵ -Caprolactone). *Chinese J Polym Sci* **2002**, *20*, 45–51.

Hutmacher, D. W. Scaffolds in Tissue Engineering Bone and Cartilage. *Biomaterials* **2000**, *21* (24), 2529–2543.

Isikli, C.; Hasirci, N. Surface and Cell Affinity Properties of Chitosan-Gelatin-Hydroxyapatite Composite Films. *Key Eng Mater* **2012**, *493–494*, 337–342.

Johnson, C. T.; García, A. J. Scaffold-Based Anti-Infection Strategies in Bone Repair. *Ann Biomed Eng* **2015**, *43* (3), 515–528.

Kara, F.; Aksoy, E. A.; Yuksekdag, Z.; Hasirci, N.; Aksoy, S. Synthesis and Surface Modification of Polyurethanes with Chitosan for Antibacterial Properties. *Carbohydr Polym* **2014**, *112*, 39–47.

Khan, G.; Yadav, S. K.; Patel, R. R.; Kumar, N.; Bansal, M.; Mishra, B. Tinidazole Functionalized Homogeneous Electrospun Chitosan/poly (ϵ -Caprolactone) Hybrid Nanofiber Membrane: Development, Optimization and Its Clinical Implications. *Int J Biol Macromol* **2017**, *103*, 1311–1326.

Kim, M. S.; Kim, G. Three-Dimensional Electrospun Polycaprolactone (PCL)/alginate Hybrid Composite Scaffolds. *Carbohydr Polym* **2014**, *114*, 213–221.

Kim, Y. H.; Jyoti, M. A.; Song, H. Y. Immobilization of Cross Linked Col-I-OPN Bone Matrix Protein on Aminolysed PCL Surfaces Enhances Initial Biocompatibility of Human Adipogenic Mesenchymal Stem Cells (hADMSC). *Appl Surf Sci* **2014**, *303*, 97–106.

Kiziltay, A.; Marcos-Fernandez, A.; San Roman, J.; Sousa, R. A.; Reis, R. L.; Hasirci, V.; Hasirci, N. Poly(ester-Urethane) Scaffolds: Effect of Structure on Properties and Osteogenic Activity of Stem Cells. *J Tissue Eng Regen Med* **2015**, *9* (8), 930–942.

Koupaei, N.; Karkhaneh, A.; Daliri Joupari, M. Preparation and Characterization of (PCL-Crosslinked-PEG)/hydroxyapatite as Bone Tissue Engineering Scaffolds. *J Biomed Mater Res - Part A* **2015**, *103* (12), 3919–3926.

Krishnanand, K.; Lal Deopura, B.; Mishra, A.; Gupta, B. Immobilization of Gelatin onto Acrylic Acid Grafted Polycaprolactone Monofilament. *J Biomater Tissue Eng* **2013**, *3* (2), 233–239.

Kulanthaivel, S.; Roy, B.; Agarwal, T.; Giri, S.; Pramanik, K.; Pal, K.; Ray, S. S.; Maiti, T. K.; Banerjee, I. Cobalt Doped Proangiogenic Hydroxyapatite for Bone Tissue Engineering Application. *Mater Sci Eng C* **2016**, *58*, 648–658.

Lam, C. X. F.; Hutmacher, D. W.; Schantz, J.-T.; Woodruff, M. A.; Teoh, S. H. Evaluation of Polycaprolactone Scaffold Degradation for 6 Months in Vitro and in Vivo. *J Biomed Mater Res A* **2009**, *90* (3), 906–919.

Lange, J. R.; Fabry, B. Cell and Tissue Mechanics in Cell Migration. *Exp Cell Res* **2013**, *319* (16), 2418–2423.

Lanza, R.; Langer, R.; Vacanti, J. The Challenge of Imitating Nature. In *Principles of Tissue Engineering*; Lanza, R., Langer, R., Vacanti, J., Eds.; Elsevier Academic Press: Burlington, **2007**, 7–14.

Lee, H.; Kim, G. Biocomposites Electrospun with Poly(ϵ -Caprolactone) and Silk Fibroin Powder for Biomedical Applications. *J Biomater Sci Polym Ed* **2010**, *21* (13), 1687–1699.

Lee, J. B.; Kim, J. E.; Bae, M. S.; Park, S. A.; Balikov, D. A.; Sung, H. J.; Jeon, H. B.; Park, H. K.; Um, S. H.; Lee, K. S.; et al. Development of Poly(ϵ -Caprolactone) Scaffold Loaded with Simvastatin and Beta-Cyclodextrin Modified Hydroxyapatite Inclusion Complex for Bone Tissue Engineering. *Polymers (Basel)* **2016**, *8* (2), 1–9.

Li, B.; Liu, Z.; Yang, J.; Yi, Z.; Xiao, W.; Liu, X.; Yang, X.; Xu, W.; Liao, X. Preparation of Bioactive β -Tricalcium Phosphate Microspheres as Bone Graft Substitute Materials. *Mater Sci Eng C* **2017a**, *70*, 1200–1205.

Li, H. PhD Thesis. Determination of Oxygen Functionality on Highly Oriented Pyrolytic Graphite (HOPG), Free University of Berlin, **2012**.

Li, J.; Liu, D.; Hu, C.; Sun, F.; Gustave, W.; Tian, H.; Yang, S. Flexible Fibers Wet-Spun from Formic Acid Modified Chitosan. *Carbohydr Polym* **2016**, *136*, 1137–1143.

Li, X.; Zhang, Q.; Ye, D.; Zhang, J.; Guo, Y.; You, R.; Yan, S.; Li, M.; Qu, J. Fabrication and Characterization of Electrospun PCL/ Antheraea Pernyi Silk Fibroin Nanofibrous Scaffolds. *Polym Eng Sci* **2017b**, *57* (2), 206–213.

Liao, N.; Rajan, A.; Kumar, M.; Prasad, A.; Tshool, S.; Park, C.; Sang, C. Electrospun Bioactive Poly(ϵ -Caprolactone)-Cellulose Acetate-Dextran Antibacterial Composite Mats for Wound Dressing Applications. *Colloids Surfaces A Physicochem Eng Asp* **2015**, *469*, 194–201.

Lou, T.; Wang, X.; Song, G.; Gu, Z.; Yang, Z. Fabrication of PLLA/ β -TCP Nanocomposite Scaffolds with Hierarchical Porosity for Bone Tissue Engineering. *Int J Biol Macromol* **2014**, *69*, 464–470.

Louette, P.; Bodino, F.; Pireaux, J. Polycaprolactone (PCL) XPS Reference Core Level and Energy Loss Spectra. *Surf Sci* **2006**, *12*, 27–31.

Lu, L.; Zhang, Q.; Wootton, D.; Chiou, R.; Li, D.; Lu, B.; Lelkes, P.; Zhou, J. Biocompatibility and Biodegradation Studies of PCL/ β -TCP Bone Tissue Scaffold Fabricated by Structural Porogen Method. *J Mater Sci Mater Med* **2012**, *23* (9), 2217–2226.

de Luca, A. C.; Stevens, J. S.; Schroeder, S. L. M.; Guilbaud, J. B.; Saiani, A.; Downes, S.; Terenghi, G. Immobilization of Cell-Binding Peptides on Poly-E-Caprolactone Film Surface to Biomimic the Peripheral Nervous System. *J Biomed Mater Res - Part A* **2013**, *101* (2), 491–501.

Maquet, V.; Pagnouelle, C.; Evrard, B.; Jerome, R.; Foidart, J.-M.; Frankenne, F. Active Substance Delivery System Comprising a Hydrogel Matrix and Microcarriers. Patent No: WO2006053836, **2006**.

Markaki, E. A. Report. AlamarBlue[®] Assay for Assessment of Cell Proliferation Using the FLUOstar OPTIMA; Cambridge, **2009**.

Martins, A. M.; Pham, Q. P.; Malafaya, P. B.; Sousa, R. a; Gomes, M. E.; Raphael, R. M.; Kasper, F. K.; Reis, R. L.; Mikos, A. G. The Role of Lipase and Alpha-Amylase in the Degradation of Starch/poly(ϵ -Caprolactone) Fiber Meshes and the Osteogenic Differentiation of Cultured Marrow Stromal Cells. *Tissue Eng Part A* **2009**, *15* (2), 295–305.

Mehrasa, M.; Asadollahi, M. A.; Ghaedi, K.; Salehi, H.; Arpanaei, A. Electrospun Aligned PLGA and PLGA/gelatin Nanofibers Embedded with Silica Nanoparticles for Tissue Engineering. *Int J Biol Macromol* **2015**, *79*, 687–695.

Al Meslmani, B.; Mahmoud, G.; Strehlow, B.; Mohr, E.; Leichtweiß, T.; Bakowsky, U. Development of Thrombus-Resistant and Cell Compatible Crimped Polyethylene Terephthalate Cardiovascular Grafts Using Surface Co-Immobilized Heparin and Collagen. *Mater Sci Eng C* **2014**, *43*, 538–546.

Metoki, N.; Rosa, C. M. R.; Zanin, H.; Marciano, F. R.; Eliaz, N.; Lobo, A. O. Electrodeposition and Biomineralization of Nano- β -Tricalcium Phosphate on Graphenated Carbon Nanotubes. *Surf Coatings Technol* **2016**, *297*, 51–57.

Migonney, V. Synthetic and Natural Degradable Polymers. In *Biomaterials*; Migonney, V., Ed.; Hoboken, NJ, **2014**, 59.

Mitsak, A. G.; Kemppainen, J. M.; Harris, M. T.; Hollister, S. J. Effect of Polycaprolactone Scaffold Permeability on Bone Regeneration in Vivo. *Tissue Eng - Part A* **2011**, *17* (13–14), 1831–1839.

Mondrinos, M. J.; Dembzyński, R.; Lu, L.; Byrapogu, V. K. C.; Wootton, D. M.; Lelkes, P. I.; Zhou, J. Porogen-Based Solid Freeform Fabrication of Polycaprolactone-Calcium Phosphate Scaffolds for Tissue Engineering. *Biomaterials* **2006**, *27* (25), 4399–4408.

Mun, C. H.; Hwang, J. Y.; Lee, S. H. Microfluidic Spinning of the Fibrous Alginate Scaffolds for Modulation of the Degradation Profile. *Tissue Eng Regen Med* **2016**, *13* (2), 140–148.

Münchow, E. A.; Pankajakshan, D.; Albuquerque, M. T. P.; Kamocki, K.; Piva, E.; Gregory, R. L.; Bottino, M. C. Synthesis and Characterization of CaO-Loaded Electrospun Matrices for Bone Tissue Engineering. *Clin Oral Investig* **2016**, *20* (8), 1921–1933.

Murdock, M. H.; Badylak, S. F. Biomaterials-Based In Situ Tissue Engineering. *Curr Opin Biomed Eng* **2017**, *1*, 4–7.

Murphy, C. M.; O'Brien, F. J.; Little, D. G.; Schindeler, A. Cell Scaffold Interactions in the Bone Tissue Engineering Triad. *Eur Cell Mater* **2013**, *26*, 120–132.

Murphy, S. MSc Thesis. Melting Point Depression in Biodegradable Polyesters, The University of Birmingham, **2011**.

Narayanan, G.; Gupta, B. S.; Tonelli, A. E. Enhanced Mechanical Properties of Poly (ϵ -Caprolactone) Nanofibers Produced by the Addition of Non-Stoichiometric Inclusion Complexes of Poly (ϵ -Caprolactone) and α -Cyclodextrin. *Polymer* **2015**, *76*, 321–330.

Ossa, H. P. de la D.; Ligresti, A.; Gil-Alegre, M. E.; Aberturas, M. R.; Molpeceres, J.; Di Marzo, V.; Torres Suárez, A. I. Poly- ϵ -Caprolactone Microspheres as a Drug Delivery System for Cannabinoid Administration: Development, Characterization and in Vitro Evaluation of Their Antitumoral Efficacy. *J Control Release* **2012**, *161* (3), 927–932.

Ozcan, C.; Zorlutuna, P.; Hasirci, V.; Hasirci, N. Influence of Oxygen Plasma Modification on Surface Free Energy of PMMA Films and Cell Attachment. *Macromol Symp* **2008**, *269* (1), 128–137.

Patrício, T.; Glória, A.; Bártolo, P. Mechanical and Biological Behaviour of PCL and PCL/PLA Scaffolds for Tissue Engineering Applications. *Chem Eng Trans* **2013**, *32*, 1645–1650.

Paulson, J. Monocryl (Poliglecaprone 25) Suture, Undyed. Patent No: K964072, **1996**.

Petisco-Ferrero, S.; Sánchez-Ilárduya, M. B.; Díez, A.; Martín, L.; Meaurio Arrate, E.; Sarasua, J. R. Surface Functionalization of an Osteoconductive Filler by Plasma Polymerization of Poly(ϵ -Caprolactone) and Poly(acrylic Acid) Films. *Appl Surf Sci* **2016**, *386*, 327–336.

Petkar, K. C. PhD Thesis. Nanotechnology for Drug and Vaccine Delivery: Formulation and Biopharmaceutical Characterization of Mucosal Tuberculosis Drug and Vaccine Delivery Systems, The Maharaja Sayajirao University of Baroda, **2013**.

Phromsopha, T.; Baimark, Y. Preparation of Starch/gelatin Blend Microparticles by a Water-in-Oil Emulsion Method for Controlled Release Drug Delivery. *Int J Biomater* **2014**, *2014*, 1–7.

Plant, A. L.; Bhadriraju, K.; Spurlin, T. A.; Elliott, J. T. Cell Response to Matrix Mechanics: Focus on Collagen. *Biochim Biophys Acta - Mol Cell Res* **2009**, *1793* (5), 893–902.

Polo-Corrales, L.; Latorre-Esteves, M.; Ramirez-Vick, J. E. Scaffold Design for Bone Regeneration. *J Nanosci Nanotechnol* **2014**, *14* (1), 15–56.

Prabhakar, A.; Lynch, A. P.; Ahearne, M. Self-Assembled Infrapatellar Fat-Pad Progenitor Cells on a Poly- ϵ -Caprolactone Film for Cartilage Regeneration. *Artif Organs* **2016**, *40* (4), 376–384.

Puppi, D.; Chiellini, F. Wet-Spinning of Biomedical Polymers: From Single-Fibre Production to Additive Manufacturing of Three-Dimensional Scaffolds. *Polym Int* **2017**, doi: 10.1002/pi.5332

Puppi, D.; Dinucci, D.; Bartoli, C.; Mota, C.; Migone, C.; Dini, F.; Barsotti, G.; Carlucci, F.; Chiellini, F. Development of 3D Wet-Spun Polymeric Scaffolds Loaded with Antimicrobial Agents for Bone Engineering. *J Bioact Compat Polym* **2011a**, *26*, 478–492.

Puppi, D.; Piras, A. M.; Chiellini, F.; Chiellini, E.; Martins, A.; Leonor, I. B.; Neves, N.; Reis, R. L. Optimized Electro- and Wet-Spinning Techniques for the Production of Polymeric Fibrous Scaffolds Loaded with Bisphosphonate and Hydroxyapatite. *J Tissue Eng Regen Med* **2011b**, *5*, 253–263.

Puppi, D.; Mota, C.; Gazzarri, M.; Dinucci, D.; Gloria, A.; Myrzabekova, M.; Ambrosio, L.; Chiellini, F. Additive Manufacturing of Wet-Spun Polymeric Scaffolds for Bone Tissue Engineering. *Biomed Microdevices* **2012**, *14* (6), 1115–1127.

Puppi, D.; Migone, C.; Morelli, A.; Bartoli, C.; Gazzarri, M.; Pasini, D.; Chiellini, F. Microstructured Chitosan/ Poly(γ -Glutamic Acid) Polyelectrolyte Complex Hydrogels by Computer-Aided Wet-Spinning for Biomedical Three-Dimensional Scaffolds. *J Bioact Compat Polym* **2016**, *31* (5), 531–549.

Qu, X.; Xia, P.; He, J.; Li, D. Microscale Electrohydrodynamic Printing of Biomimetic PCL/nHA Composite Scaffolds for Bone Tissue Engineering. *Mater Lett* **2016**, *185*, 554–557.

Rajzer, I.; Menaszek, E.; Kwiatkowski, R.; Planell, J. A.; Castano, O. Electrospun Gelatin/poly(ϵ -Caprolactone) Fibrous Scaffold Modified with Calcium Phosphate for Bone Tissue Engineering. *Mater Sci Eng C Mater Biol Appl* **2014**, *44*, 183–190.

Russo, V.; Tamaro, L.; Di Marcantonio, L.; Sorrentino, A.; Ancora, M.; Valbonetti, L.; Turriani, M.; Martelli, A.; Cammà, C.; Barboni, B. Amniotic Epithelial Stem Cell Biocompatibility for Electrospun Poly(lactide-Co-Glycolide), Poly(ϵ -Caprolactone), Poly(lactic Acid) Scaffolds. *Mater Sci Eng C* **2016**, *69*, 321–329.

Sabbatier, G.; Larranaga, A.; Guay-Begin, A. A.; Fernandez, J.; Dieval, F.; Durand, B.; Sarasua, J. R.; Laroche, G. Design, Degradation Mechanism and Long-Term Cytotoxicity of Poly(l-Lactide) and Poly(lactide-Co- ϵ -Caprolactone) Terpolymer Film and Air-Spun Nanofiber Scaffold. *Macromol Biosci* **2015**, *15* (10), 1392–1410.

Sabzi, F.; Boushehri, A. Sorption Phenomena of Organic Solvents in Polymers: Part II. *Eur Polym J* **2005**, *41* (9), 2067–2087.

Savelyeva, M. S.; Abalymov, A. A.; Lyubun, G. P.; Vidyasheva, I. V.; Yashchenok, A. M.; Douglas, T. E. L.; Gorin, D. A.; Parakhonskiy, B. V. Vaterite Coatings on Electrospun Polymeric Fibers for Biomedical Applications. *J Biomed Mater Res - Part A* **2017**, *105* (1), 94–103.

Schäler, K.; Achilles, A.; Bärenwald, R.; Hackel, C.; Saalwächter, K. Dynamics in Crystallites of Poly(ϵ -Caprolactone) as Investigated by Solid-State NMR. *Macromolecules* **2013**, *46*, 7818–7825.

Serra, I. R.; Fradique, R.; Vallejo, M. C. S.; Correia, T. R.; Miguel, S. P.; Correia, I. J. Production and Characterization of Chitosan/gelatin/ β -TCP Scaffolds for Improved Bone Tissue Regeneration. *Mater Sci Eng C* **2015**, *55*, 592–604.

Seyednejad, H.; Ghassemi, A. H.; Van Nostrum, C. F.; Vermonden, T.; Hennink, W. E. Functional Aliphatic Polyesters for Biomedical and Pharmaceutical Applications. *J Control Release* **2011**, *152* (1), 168–176.

Seyednejad, H.; Gawlitta, D.; Kuiper, R. V.; Bruin, A. De; Nostrum, C. F. Van; Vermonden, T.; Dhert, W. J. A.; Hennink, W. E. In Vivo Biocompatibility and Biodegradation of 3D-Printed Porous Scaffolds Based on a Hydroxyl-Functionalized Poly(ϵ -Caprolactone). *Biomaterials* **2012**, *33* (17), 4309–4318.

Sezer, U. A.; Aksoy, E. A.; Hasirci, V.; Hasirci, N. Poly(ϵ -Caprolactone) Composites Containing Gentamicin-Loaded β -Tricalcium Phosphate/gelatin Microspheres as Bone Tissue Supports. *J Appl Polym Sci* **2013**, *127* (3), 2132–2139.

Sezer, U. A.; Billur, D.; Huri, G.; Huri, P. Y.; Aksoy, E. A.; Terzioglu, H.; Konukseven, E.; Hasirci, V.; Hasirci, N. In Vivo Performance of Poly(ϵ -Caprolactone) Constructs Loaded with Gentamicin Releasing Composite Microspheres for Use in Bone Regeneration. *J Biomater Tissue Eng* **2014a**, *4* (10), 786–795.

Sezer, U. A.; Arslantunali, D.; Aksoy, E. A.; Hasirci, V.; Hasirci, N. Poly(ϵ -Caprolactone) Composite Scaffolds Loaded with Gentamicin-Containing β -Tricalcium Phosphate/gelatin Microspheres for Bone Tissue Engineering Applications. *J Appl Polym Sci* **2014b**, *131* (8), 1–11.

Shah, L. K.; Amiji, M. M. Intracellular Delivery of Saquinavir in Biodegradable Polymeric Nanoparticles for HIV/AIDS. *Pharm Res* **2006**, *23* (11), 2638–2645.

Shalumon, K. T.; Anulekha, K. H.; Girish, C. M.; Prasanth, R.; Nair, S. V.; Jayakumar, R. Single Step Electrospinning of Chitosan/poly(caprolactone) Nanofibers Using Formic Acid/acetone Solvent Mixture. *Carbohydr Polym* **2010**, *80* (2), 414–420.

Sharma, C.; Dinda, A. K.; Potdar, P. D.; Chou, C.-F.; Mishra, N. C. Fabrication and Characterization of Novel Nano-Biocomposite Scaffold of Chitosan–gelatin–alginate–hydroxyapatite for Bone Tissue Engineering. *Mater Sci Eng C* **2016**, *64*, 416–427.

Smith, L.; Cho, S.; Discher, D. E. Mechanosensing of Matrix by Stem Cells: From Matrix Heterogeneity, Contractility, and the Nucleus in Pore-Migration to Cardiogenesis and Muscle Stem Cells in Vivo. *Semin Cell Dev Biol* **2017**, 1–15, doi: 10.1016/j.semcdb.2017.05.025

Takahashi, K.; Yamanaka, S. Induction of Pluripotent Stem Cells from Mouse Embryonic and Adult Fibroblast Cultures by Defined Factors. *Cell* **2006**, *126* (4), 663–676.

Tang, D.; Tare, R. S.; Yang, L.-Y.; Williams, D. F.; Ou, K.-L.; Oreffo, R. O. C. Biofabrication of Bone Tissue: Approaches, Challenges and Translation for Bone Regeneration. *Biomaterials* **2016**, *83*, 363–382.

Tevlin, R.; Walmsley, G. G.; Marecic, O.; Hu, M. S.; Wan, D. C.; Longaker, M. T. Stem and Progenitor Cells: Advancing Bone Tissue Engineering. *Drug Deliv Transl Res* **2016**, *6* (2), 159–173.

Tietz, N. W.; Shuey, D. F. Lipase in Serum - The Elusive Enzyme: An Overview. *Clin Chem* **1993**, *39* (5), 746–756.

Tong, S. Y.; Wang, Z.; Lim, P. N.; Wang, W.; Thian, E. S. Uniformly-Dispersed Nanohydroxapatite-Reinforced Poly(ϵ -Caprolactone) Composite Films for Tendon Tissue Engineering Application. *Mater Sci Eng C* **2016**, *70*, 1149–1155.

Trampuz, A.; Widmer, A. F. Infections Associated with Orthopedic Implants. *Curr.Opin.Infect.Dis.* **2006**, *19*, 349–356.

Tuzlakoglu, K.; Pashkuleva, I.; Rodrigues, M. T.; Gomes, M. E.; Van Lenthe, G. H.; Müller, R.; Reis, R. L. A New Route to Produce Starch-Based Fiber Mesh Scaffolds by Wet Spinning and Subsequent Surface Modification as a Way to Improve Cell Attachment and Proliferation. *J Biomed Mater Res - Part A* **2010**, *92* (1), 369–377.

Ucar, S. MSc Thesis. Polymeric Scaffolds for Bioactive Agent Delivery in Bone Tissue Engineering, Middle East Technical University, **2012**.

Ucar, S.; Yilgor, P.; Hasirci, V.; Hasirci, N. Chitosan-Based Wet-Spun Scaffolds for Bioactive Agent Delivery. *J Appl Polym Sci* **2013**, *130* (5), 3759–3769.

Ucar, S.; Ermis, M.; Hasirci, N. Modified Chitosan Scaffolds: Proliferative, Cytotoxic, Apoptotic, and Necrotic Effects on Saos-2 Cells and Antimicrobial Effect on Escherichia Coli. *J Bioact Compat Polym* **2016**, 1–16.

Ulubayram, K.; Kiziltay, A.; Yilmaz, E.; Hasirci, N. Desferrioxamine Release from Gelatin-Based Systems. *Biotechnol Appl Biochem* **2005**, *42* (Pt 3), 237–245.

Vashaghian, M.; Zandieh, B.; Roovers, J. P.; Smit, T. H. Electrospun Matrices for Pelvic Floor Repair: Effect of Fiber Diameter on Mechanical Properties and Cell Behavior. *Tissue Eng Part A* **2016**, *22*, 1305–1316.

Woodruff, M. A.; Hutmacher, D. W. The Return of a Forgotten Polymer - Polycaprolactone in the 21st Century. *Prog Polym Sci* **2010**, *35* (10), 1217–1256.

Wu, T.; Zheng, H.; Chen, J.; Wang, Y.; Sun, B.; Morsi, Y.; El-Hamshary, H.; Al-Deyab, S. S.; Chen, C.; Mo, X.; et al. Application of a Bilayer Tubular Scaffold Based on Electrospun poly(L-Lactide-Co-Caprolactone)/collagen Fibers and Yarns for Tracheal Tissue Engineering. *J Mater Chem B* **2017**, *5* (1), 139–150.

Xu, B.; Du, L.; Zhang, J.; Zhu, M.; Ji, S.; Zhang, Y.; Kong, D.; Ma, X.; Yang, Q.; Wang, L. Circumferentially Oriented Microfiber Scaffold Prepared by Wet-Spinning for Tissue Engineering of Annulus Fibrosus. *RSC Adv* **2015**, *5* (53), 42705–42713.

Xu, F. J.; Wang, Z. H.; Yang, W. T. Surface Functionalization of Polycaprolactone Films via Surface-Initiated Atom Transfer Radical Polymerization for Covalently Coupling Cell-Adhesive Biomolecules. *Biomaterials* **2010**, *31* (12), 3139–3147.

Yao, R.; He, J.; Meng, G.; Jiang, B.; Wu, F. Electrospun PCL/Gelatin Composite Fibrous Scaffolds: Mechanical Properties and Cellular Responses. *J Biomater Sci Polym Ed* **2016**, *27* (9), 824–838.

Yi, H.; Choi, Y.; Shin, K.; Min, J.; Gupta, R.; Nyeo, M.; Kyong, I.; Mi, C.; Cheol, S.; Cho, D. A 3D-Printed Local Drug Delivery Patch for Pancreatic Cancer Growth Suppression. *J Control Release* **2016**, *238*, 231–241.

Yildirim, M. S.; Hasanreisoglu, U.; Hasirci, N.; Sultan, N. Adherence of Candida Albicam to Glow-Discharge Modified Acrylic Denture Base Polymers. *J Oral Rehabil* **2005**, *32* (7), 518–525.

Yildirimer, L.; Seifalian, A. M. Three-Dimensional Biomaterial Degradation - Material Choice, Design and Extrinsic Factor Considerations. *Biotechnol Adv* **2014**, *32* (5), 984–999.

Yilgor, P.; Sousa, R. A.; Reis, R. L.; Hasirci, N.; Hasirci, V. 3D Plotted PCL Scaffolds for Stem Cell Based Bone Tissue Engineering. *Macromol Symp* **2008**, *269* (1), 92–99.

Yilgor, P.; Tuzlakoglu, K.; Reis, R. L.; Hasirci, N.; Hasirci, V. Incorporation of a Sequential BMP-2/BMP-7 Delivery System into Chitosan-Based Scaffolds for Bone Tissue Engineering. *Biomaterials* **2009**, *30* (21), 3551–3559.

Yu, B.; Wang, X.; Qian, X.; Xing, W.; Yang, H.; Ma, L.; Lin, Y.; Jiang, S.; Song, L.; Hu, Y.; et al. Functionalized Graphene Oxide/phosphoramidate Oligomer Hybrids Flame Retardant Prepared via in Situ Polymerization for Improving the Fire Safety of Polypropylene: Supplementary Information. *RSC Advance* **2014**, *4* (60), 31782–31794.

Yue, K.; Trujillo-de Santiago, G.; Alvarez, M. M.; Tamayol, A.; Annabi, N.; Khademhosseini, A. Synthesis, Properties, and Biomedical Applications of Gelatin Methacryloyl (GelMA) Hydrogels. *Biomaterials* **2015**, *73*, 254–271.

Zhang, D.; Wei, G.; Li, P.; Zhou, X.; Zhang, Y. Urine-Derived Stem Cells: A Novel and Versatile Progenitor Source for Cell-Based Therapy and Regenerative Medicine. *Genes Dis* **2014**, *1* (1), 8–17.

Zhang, K.; Huang, D.; Yan, Z.; Wang, C. Heparin/collagen Encapsulating Nerve Growth Factor Multilayers Coated Aligned PLLA Nanofibrous Scaffolds for Nerve Tissue Engineering. *J Biomed Mater Res - Part A* **2017**, *105* (7), 1900–1910.

Zhang, Q.; Wang, N.; Hu, R.; Pi, Y.; Feng, J.; Wang, H.; Zhuang, Y.; Xu, W.; Yang, H. Wet Spinning of Bletilla Striata Polysaccharide/silk Fibroin Hybrid Fibers. *Mater Lett* **2015**, *161*, 576–579.

APPENDIX A

Optimization of Wet Spinning

Table A.1. Optimization of wet spinning setup.

No	Polymer Solution	Non-solvent Solution	Setup (Syringe and needle - FR)	Results
1	PCL (60k) in CHCl ₃ :EtOH (9:1) 15% w/v	dH ₂ O:MetOH (1:5)	Plastic - 5 mL/h	No polymer hardening
2	PCL (60k) in CHCl ₃ :EtOH (9:1) 25% w/v	dH ₂ O:MetOH (1:5)	Plastic - 5 mL/h	No polymer hardening
3	PCL (60k) in CHCl ₃ :EtOH (9:1) 15% w/v	dH ₂ O:MetOH (1:5)	Plastic - 10 mL/h	No polymer hardening
4	PCL (60k) in CHCl ₃ :EtOH (9:1) 20% w/v	dH ₂ O:MetOH (1:4)	Plastic - 10 mL/h	No polymer hardening
5	PCL (60k) in CHCl ₃ :EtOH (9:1) 25% w/v	dH ₂ O:MetOH (1:4)	Plastic - 10 mL/h	No polymer hardening
6	PCL (60k) in CHCl ₃ :EtOH (9:1) 40% w/v			Polymer did not dissolve in 40% w/v
7	PCL (60k) in DMAC 10% w/v	dH ₂ O	Plastic - 10 mL/h	No polymer hardening
8	PCL (60k) in DMAC 10% w/v	EtOH	Plastic - 10 mL/h	No polymer hardening
9	PCL (60k) in acetone 6% w/v	EtOH	Plastic - 10 mL/h	No polymer hardening
10	PCL (60k) in acetone 15% w/v	EtOH:dH ₂ O (1:4)	Plastic - 10 mL/h	Polymer gets hardened. No fiber formation
11	PCL (60k) in acetone 15% w/v	MetOH:dH ₂ O (1:4)	Plastic - 10 mL/h	Hardened polymer. No fiber formation
12	PCL (60k) in acetone 15% w/v	MetOH	Plastic - 10 mL/h	No polymer hardening

Table A.1. (continued)

No	Polymer Solution	Non-solvent Solution	Setup (Syringe and needle - FR)	Results
13	PCL (60k) in acetone 15% w/v	dH ₂ O	Plastic - 10 mL/h	No polymer hardening
14	PCL (60k) in acetone 15% w/v	EtOH:dH ₂ O (1:4)	Plastic - 10 mL/h	No polymer hardening
15	PCL (60k) in acetone 10% w/v	MetOH	Plastic - 10 mL/h	No polymer hardening
16	PCL (60k) in acetone 10% w/v	dH ₂ O	Plastic - 10 mL/h	No polymer hardening
17	PCL (60k) in acetone 10% w/v	EtOH:dH ₂ O (1:4)	Plastic - 10 mL/h	No polymer hardening
18	PCL (60k) in acetone 10% w/v	EtOH	Plastic - 10 mL/h	Immiscible cloud in beaker
19	PCL (60k) in acetone 15% w/v (heated for homogeneity)	EtOH (cold)	Plastic - 10 mL/h	Short, thick fibers formed. Cluttered needle. Fibers were not hard.
20	PCL (60k) in acetone 10% w/v (heated for homogeneity)	EtOH (cold)	Plastic - 10 mL/h	Short, thick fibers formed. Cluttered needle. Fibers were not hard.
21	PCL (60k) in acetone 6% w/v (heated for homogeneity)	EtOH (cold)	Plastic - 1 mL/h	Long, thin, beady fibers. Cluttered needle. Fibers were not hard.
22	PCL (60k) in acetone 9% w/v (heated for homogeneity)	EtOH (cold)	Plastic - 1 mL/h	Long, thin, beady fibers. Cluttered needle. Fibers were not hard.
23	PCL (60k) in acetone 15% w/v (heated for homogeneity)	EtOH (cold)	Plastic - 3 mL/h	Long, thin, beady fibers. Cluttered needle. Fibers were not hard.
24	PCL (60k) in acetone 15% w/v (heated for homogeneity)	EtOH (cold)	Glass - 99 mL/h	Long, thin, beady fibers. Cluttered needle. Fibers were not hard.
25	PCL (60k) in acetone 15% w/v (heated for homogeneity)	EtOH (cold)	Plastic - 1 mL/h	Long, thin, beady fibers. Cluttered needle. Fibers were not hard.
26	PCL (60k) in acetone 15% w/v (heated for homogeneity)	EtOH (cold)	Glass - 50 mL/h	Long, thin, beady fibers. Cluttered needle. Fibers were not hard.
27	PCL (60k) in acetone 15% w/v (heated for homogeneity)	EtOH (cold)	Glass - 60 mL/h	Long, thin, beady fibers. Cluttered needle. Fibers were not hard.

Table A.1. (continued)

No	Polymer Solution	Non-solvent Solution	Setup (Syringe and needle - FR)	Results
28	PCL (60k) in acetone 15% w/v (heated for homogeneity)	EtOH (cold)	Glass - 70 mL/h	Long, thin, beady fibers. Cluttered needle. Fibers were not hard.
29	PCL (60k) in acetone 15% w/v (heated for homogeneity)	EtOH (cold)	Glass - 80 mL/h	Long, thin, beady fibers. Cluttered needle. Fibers were not hard.
30	PCL (60k) in acetone 15% w/v (heated for homogeneity)	EtOH (cold)	Glass - 90 mL/h	Long, thin, beady fibers. Cluttered needle. Fibers were not hard.
31	PCL (60k) in acetone 15% w/v + β -TCP 12% w/w (heated for homogeneity)	EtOH (cold)	Glass - 20 mL/h	Long, thin, beady fibers. Cluttered needle. Fibers were not hard.
32	PCL (60k) 10% w/v + PLGA (50:50) 10% w/v in acetone (heated for homogeneity)	EtOH (cold)	Glass - 20 mL/h	Short, thin, beady fibers. Cluttered needle. Fibers were not hard.
33	PCL (60k) in acetone 15% w/v (heated for homogeneity)	EtOH (cold)	Glass - 20 mL/h	Long, thin, beady fibers. Cluttered needle. Fibers were not hard.
34	PCL (60k) in acetone 15% w/v (heated for homogeneity)	MetOH (cold)	Glass - 20 mL/h	No polymer hardening
35	PCL (60k) in CHCl_3 15% w/v	EtOH (cold)	Glass - 20 mL/h	No polymer hardening
36	PCL (60k) in CHCl_3 15% w/v	MetOH (cold)	Glass - 20 mL/h	No polymer hardening
37	PCL (60k) in acetone 15% w/v + β -TCP 12% w/w (heated for homogeneity)	EtOH (cold)	Glass - 20 mL/h	Long, thin, beady fibers. Cluttered needle. Fibers were not hard.
38	PCL (60k) in acetone 15% w/v + β -TCP 36% w/w (heated for homogeneity)	EtOH (cold)	Glass - 20 mL/h	Long, thin, beady fibers. Cluttered needle. Fibers were not hard.
39	PCL (60k) in acetone 15% w/v + β -TCP 36% w/w (heated for homogeneity)	EtOH (cold)	Glass - 20 mL/h	Long, thin, beady fibers. Cluttered needle. Fibers were not hard.
40	PCL (60k) 15% w/v + Chitosan 1.5% w/v in acetone (heated for homogeneity)	EtOH (cold)	Glass - 5 mL/h	Long, thin, beady fibers. Cluttered needle. Fibers were not hard.

Table A.1. (continued)

No	Polymer Solution	Non-solvent Solution	Setup (Syringe and needle - FR)	Results
41	PCL (60k) 15% w/v + Chitosan 1.5% w/v in acetone (heated for homogeneity)	MeOH (cold)	Glass - 5 mL/h	Short, thin, beady fibers. Cluttered needle. Fibers were not hard.
42	PCL (60k) in acetone 20% w/v (heated for homogeneity)	EtOH (cold)	Glass - 5 mL/h	Long, thin, beady fibers. Cluttered needle. Fibers were not hard.
43	PCL (60k) 25% w/v + PEG 2.5% w/v in DCM	EtOH (cold)	Glass - 5 mL/h	No polymer hardening
44	PCL (80k) in acetone 6% w/v (heated for homogeneity)	EtOH (cold)	Glass - 5 mL/h	Long thin smooth fibers. Less cluttered needle. Durable fibers
45	PCL (80k) in acetone 8% w/v (heated for homogeneity)	EtOH (cold)	Glass - 5 mL/h	Long thin smooth fibers. Less cluttered needle. Durable fibers
46	PCL (80k) in acetone 10% w/v (heated for homogeneity)	EtOH (cold)	Glass - 5 mL/h	Long thin smooth fibers. Less cluttered needle. Durable fibers
47	PCL (80k) in acetone 20% w/v (heated for homogeneity)	EtOH (cold)	Glass - 5 mL/h	Long thin smooth fibers. Cluttered needle. Durable fibers
48	PCL (80k) in acetone 20% w/v (heated for homogeneity)	EtOH (cold)	Glass - 0.8 mL/h	Long thin smooth fibers. No clutters in needle. Durable fibers
49	PCL (80k) in acetone 20% w/v + β -TCP 10% w/w (heated for homogeneity)	EtOH (cold)	Glass - 0.8 mL/h	Long thin smooth fibers. No clutters in needle. Durable fibers
50	PCL (80k) in acetone 20% w/v + β -TCP 20% w/w (heated for homogeneity)	EtOH (cold)	Glass - 0.8 mL/h	Long thin smooth fibers. No clutters in needle. Durable fibers
51	PCL (80k) in acetone 20% w/v + β -TCP 25% w/w (heated for homogeneity)	EtOH (cold)	Glass - 0.8 mL/h	Long thin smooth fibers. Less cluttered needle. Durable fibers
52	PCL (80k) in acetone 25% w/v + β -TCP 20% w/w (heated for homogeneity)	EtOH (cold)	Glass - 0.8 mL/h	Long thin smooth fibers. Less cluttered needle. Durable fibers

APPENDIX B

Particle Size Analysis Results of β -TCP

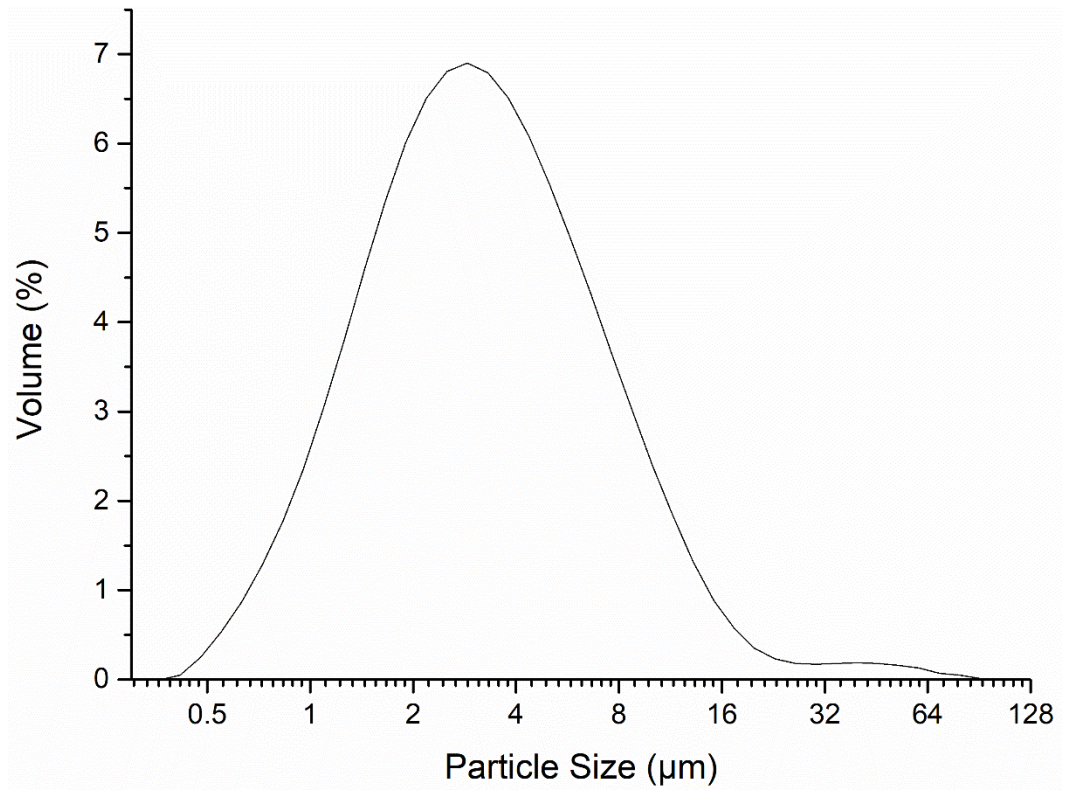


Figure B.1. Particle size analysis of β -TCP after grinding and sieving.

APPENDIX C

Calibration curve of Toluidine Blue

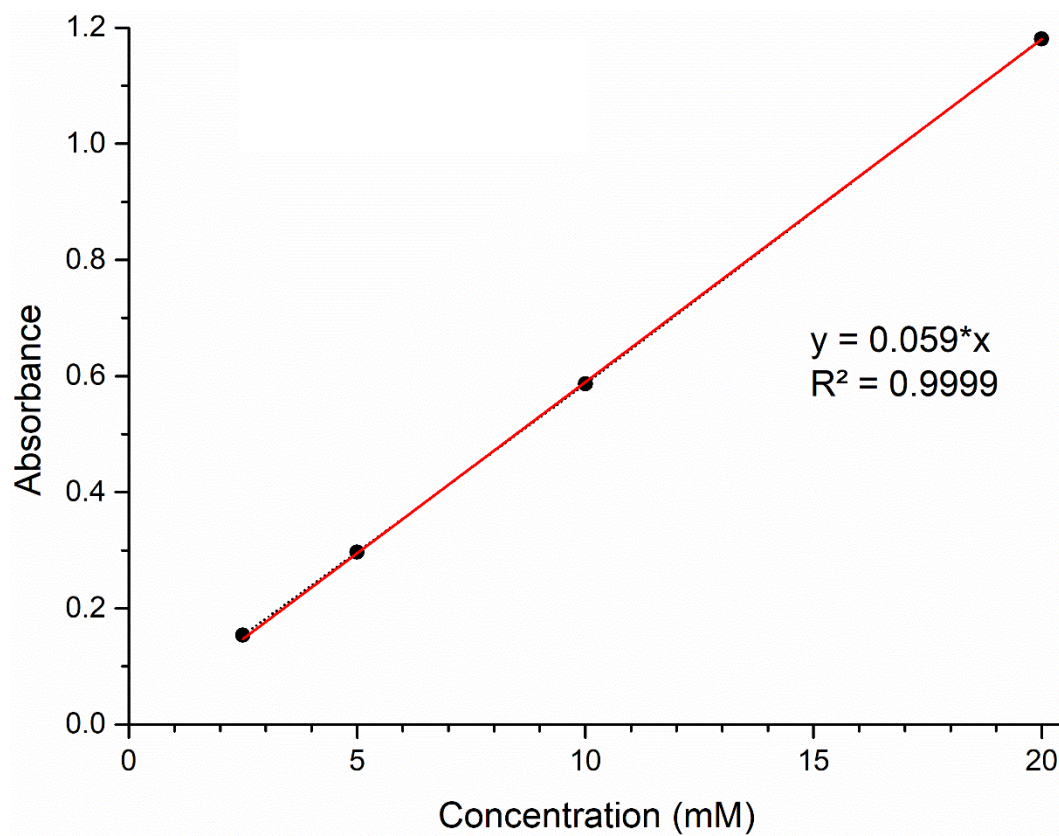


Figure C.1. Calibration curve of Toluidine Blue (at 624 nm).

APPENDIX D

Calibration curve of Ceftriaxone Sodium

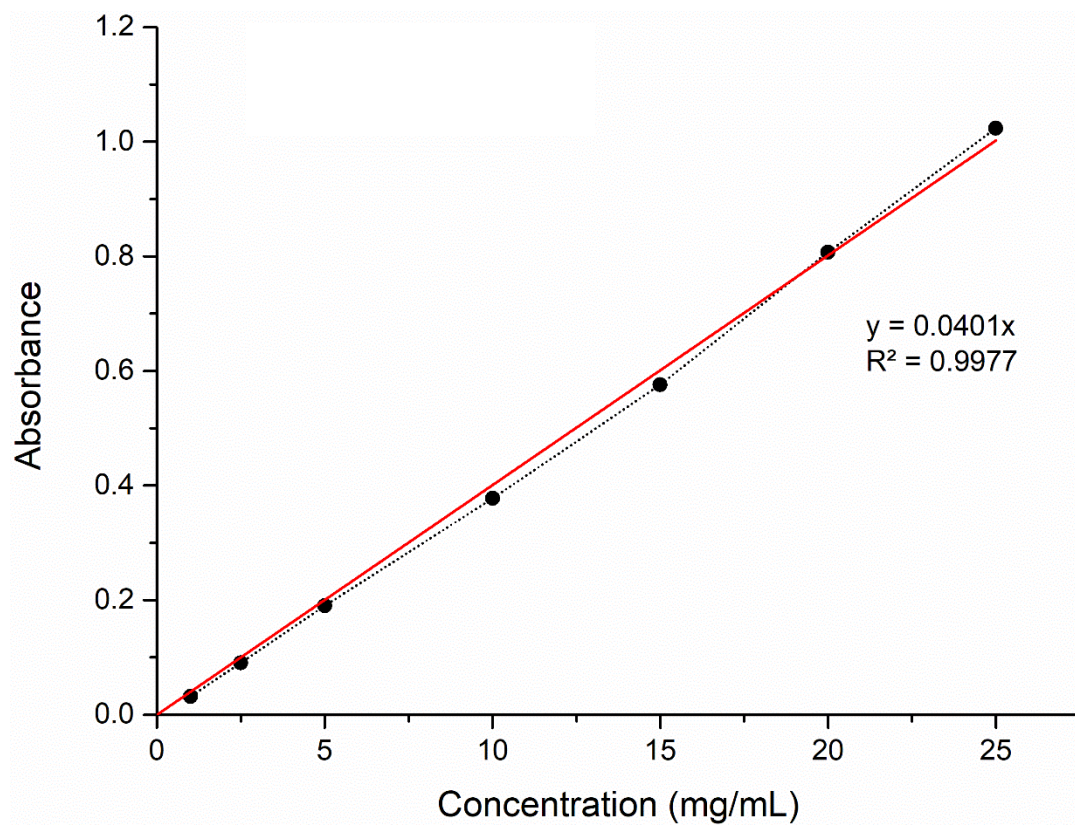


Figure D.1. Calibration curve of Ceftriaxone Sodium (at 270 nm).

APPENDIX E

Calibration curve of Saos-2 cells

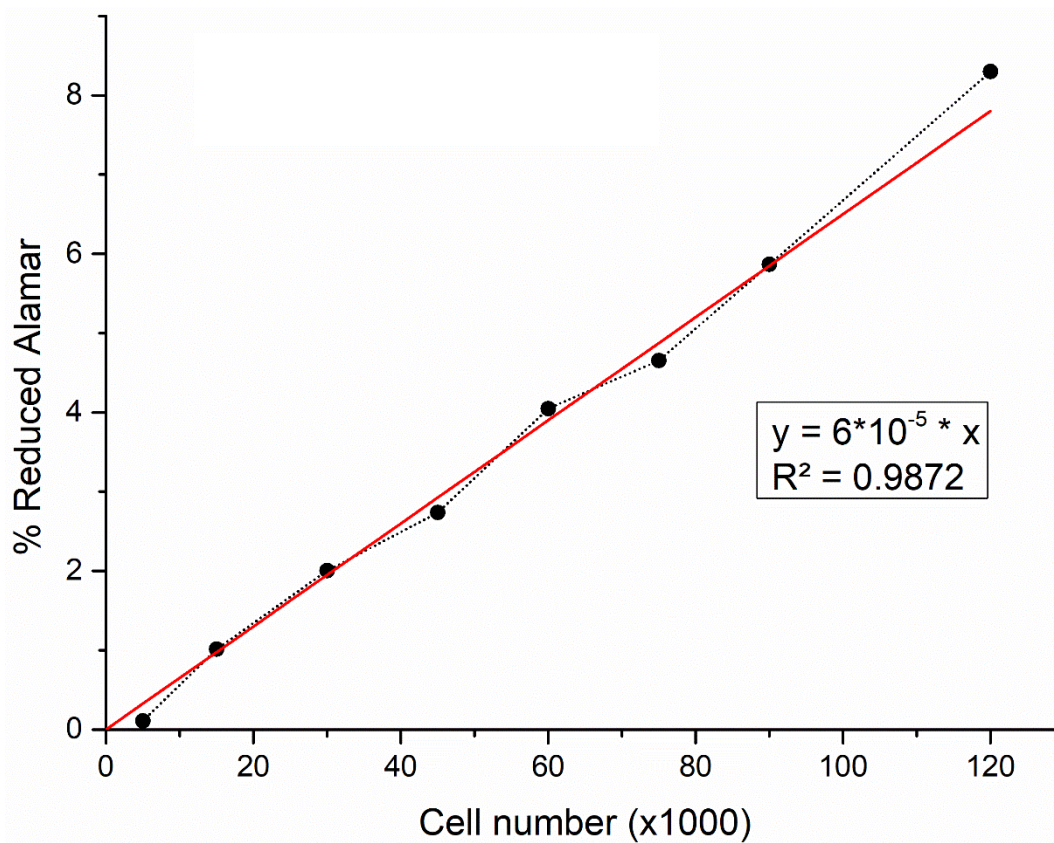


Figure E.1. Calibration curve of Saos-2 cells with AlamarBlue® analysis (at 570 and 595 nm).

APPENDIX F

Curriculum Vitae

PERSONAL INFORMATION

Surname, Name: Malikmammadov, Elbay

Nationality: Azerbaijan (AZ)

Date and Place of Birth: 01 December, Baku

Marital Status: Single

Phone: +90 312 210 51 63

E-mail: elbay.malikmammadov@metu.edu.tr

EDUCATION

<u>Degree</u>	<u>Institution</u>	<u>Year of Graduation</u>
BS	METU Biology Department	2013
High School	Baku Private Turkish Highschool	2007

ACADEMIC EXPERIENCE

<u>Year</u>	<u>Place</u>	<u>Enrollment</u>
2013 -	METU – Biomaterials and Tissue Engineering Laboratory (BIOMATEN)	Full Time Researcher

FOREIGN LANGUAGES: English, Russian, Turkish

PUBLICATIONS:

1. Malikmammadov E, Endogan TT, Kiziltay A, Hasirci V and Hasirci N, “PCL and PCL-Based Materials in Biomedical Applications”. Submitted to Journal of Biomaterials Science, Polymer Edition.
2. Malikmammadov E, Endogan TT, Kiziltay A, Hasirci V and Hasirci N, “PCL-TCP wet spun scaffolds carrying antibiotic-loaded microspheres for bone tissue engineering”. *Journal of Biomaterials Science, Polymer Edition*. Accepted. doi: 10.1080/09205063.2017.1354671.

ORAL PRESENTATIONS:

1. Malikmammadov E, Endogan TT, Kiziltay A, Hasirci V and Hasirci N (2016). Surface modified multi-functional PCL/TCP fibrous scaffolds. *Front. Bioeng. Biotechnol. Conference Abstract: 10th World Biomaterials Congress*. doi: 10.3389/conf.FBIOE.2016.01.01555.

POSTER PRESENTATIONS:

1. E. Malikmammadov, T. Endogan, A. Kiziltay, V. Hasirci and N. Hasirci, “PCL-Fibrin Scaffolds for Tissue Engineering”, 22nd International Biomedical Science and Technology Symposium, Ankara, Turkey, 12-14 May, 2017.
2. E. Ergene, E. Malikmammadov, P. Yilgor-Huri and V. Hasirci, “Cellular alignment enhance the mechanical properties of ASC laden fibrin”, 22nd International Biomedical Science and Technology Symposium, Ankara, Turkey, 12-14 May, 2017.
3. E. Malikmammadov, T. Endogan, A. Kiziltay, V. Hasirci and N. Hasirci, “Functional PCL Scaffolds: Local Antibiotic Delivery in Bone Tissue Engineering Applications”, 21st International Biomedical Science and Technology Symposium, Antalya, Turkey, 22-24 October, 2015.
4. E. Malikmammadov, T. Endogan, A. Kiziltay, V. Hasirci and N. Hasirci, “PCL Wet Spun Scaffolds for Antibiotic Delivery”, 11th International Symposium on Frontiers In Biomedical Polymers, Riva Del Garda, Italy, 8-11 July, 2015.